

Characterization and contextualization of problematic substrates for Endoplasmic Reticulum Associated Degradation

by

Grant Joseph Daskivich

Bachelor of Science, University of Pittsburgh, 2015

Submitted to the Graduate Faculty of the
Dietrich School of Arts and Sciences in partial fulfillment
of the requirements for the degree of
Doctor of Philosophy

University of Pittsburgh

2023

UNIVERSITY OF PITTSBURGH
DIETRICH SCHOOL OF ARTS AND SCIENCES

This dissertation was presented

by

Grant Joseph Daskivich

It was defended on

September 19, 2023

and approved by

Kirill Kiselyov, Ph.D, Associate Professor, Department of Biological Sciences

Anne E. Carlson, Ph.D., Associate Professor, Department of Biological Sciences

Allyson F. O'Donnell., Ph.D, Assistant Professor, Department of Biological Sciences

Alexander Sorkin, Ph.D, Professor, Department of Cell Biology

Dissertation Advisor: Jeffrey L. Brodsky, Ph.D., Professor, Department of Biological Sciences

Copyright © by Grant Joseph Daskivich

2023

Characterization and contextualization of problematic substrates for Endoplasmic Reticulum Associated Degradation

Grant Joseph Daskivich, PhD

University of Pittsburgh, 2023

Proteostasis, the finely tuned system that ensures proper protein folding, trafficking, and clearance, is a fundamental process in all living organisms. This dynamic network of cellular pathways regulates the quality and quantity of proteins within the cell. It is crucial for maintaining cellular homeostasis and preventing the accumulation of aberrant proteins, which can lead to cellular dysfunction and disease. Specifically, highly stable protein aggregates irreversibly disrupt proteostasis and trigger disease onset. Therefore, for my research, I constructed TM-Ubc9ts, a temperature-sensitive membrane protein degraded by ER-associated degradation (ERAD) in yeast, to study how endoplasmic reticulum tethered, aggregation-prone proteins impact proteostasis. I hypothesized that TM-Ubc9ts would be an ERAD substrate in mammalian cells and aggregate at elevated temperatures.

In this document, I first review the proteostasis network, beginning with protein folding, followed by protein aggregation and finally protein quality control. I then explain how I tested the above hypothesis via cycloheximide chase and detergent solubility assays respectively. Degradation of TM-Ubc9ts was largely dependent on the proteasome, especially at elevated temperatures. Solubility did not change significantly, but I observed the evolution of distinct clipped forms of TM-Ubc9ts that were stabilized when the proteasome was inhibited. Subsequently, I ask if TM-Ubc9ts was a substrate of the intramembrane protease RHBDL4, which clips ER membrane proteins in preparation for retrotranslocation. Though I found TM-Ubc9ts clipping to be independent of RHBDL4 function, I established a pipeline by which ER membrane

proteins can be characterized at specific stages of ERAD. Finally, I describe the rationale and construction of another set of aggregation-prone ERAD substrates, Sec62-A β 42 and Sec62-A β 40. These substrates were analyzed through the same experimental pipeline and found to be remarkably stable compared to TM-Ubc9ts, highlighting the complex relationship between hypotheses and experimental results. Future work can utilize this streamlined set of experiments to quickly and precisely identify the point at which aggregation prone proteins in the ER disrupt proteostasis.

Table of Contents

Preface.....	xiii
1.0 Introduction.....	1
1.1 Protein Folding	1
1.1.1 Structure-Driven Protein Folding	2
1.1.2 Chaperone-Dependent Protein Folding	3
1.2 Protein Aggregation	8
1.2.1 Mechanism.....	8
1.2.2 Beneficial Effects of Inclusions	9
1.2.3 Harmful Effects of Protein Inclusions/Aggregates.....	11
1.2.3.1 Proteinopathies	11
1.2.3.1.1 Alzheimer’s Disease.....	12
1.2.3.1.2 Huntington’s Disease.....	14
1.2.3.1.3 Parkinson’s Disease.....	15
1.2.3.1.4 Prion-related Diseases	17
1.3 Protein Disaggregation.....	19
1.3.1 Mechanism	19
1.3.2 Bacterial and Yeast Disaggregases	20
1.3.2.1 ClpB	20
1.3.2.2 Hsp104	21
1.3.3 Mammalian disaggregases	23
1.3.3.1 Hsp70	23

1.3.3.2 Hsp40	24
1.3.3.3 Hsp70-40-110 complex.....	24
1.3.3.4 sHsps	26
1.4 Protein Quality Control	27
1.4.1 Ubiquitin Proteasome System	27
1.4.2 Cytoplasmic Quality Control	29
1.4.3 Unfolded Protein Response	30
1.4.4 Endoplasmic Reticulum Associated Degradation	31
1.4.4.1 Substrate Recognition	32
1.4.4.2 Ubiquitination	33
1.4.4.3 Retrotranslocation	34
1.4.4.4 Degradation	36
1.4.5 Decision between ER retention and ERAD vs. ER exit	38
1.5 Summary of Goals and Discoveries	41
2.0 Differential handling of an aggregation-prone integral membrane ERAD	
substrate in yeast and a human cell line	43
2.1 Introduction	43
2.2 Results.....	47
2.2.1 TM-Ubc9ts undergoes ERAD in mammalian cells, as in yeast.....	47
2.2.2 TM-Ubc9ts is both more insoluble and clipped at higher temperatures	51
2.2.3 TM-Ubc9ts degradation is consistent between transient and stable expression	
systems.....	54
2.2.4 Intramembrane protease RHBDL4 does not cleave TM-Ubc9ts.....	63

2.3 Discussion	67
2.4 Materials and Methods	71
2.4.1 Molecular Methods	71
2.4.2 Human cell culture protocols	72
2.4.3 siRNA-mediated knockdown and RT-qPCR.....	73
2.4.4 Protein solubility assays.....	74
2.4.5 Protein stability assays.....	75
2.4.6 Carbonate Extraction	76
2.4.7 Statistical methods	76
3.0 Conclusions and Future Directions	78
3.1 A characterization pipeline for both endogenous and chimeric aggregation-prone ER membrane proteins	78
3.2 Manipulating substrate structure to answer questions of membrane insertion and topology	80
3.3 Unbiased screening of the substrate “proximity proteome”	81
3.4 Limitations of this study	83
3.5 Concluding remarks.....	85
Appendix A Characterization of a pair of disease-relevant aggregation prone substrates: Sec62-Aβ42 and Sec62-Aβ40	86
Appendix A.1 Introduction.....	86
Appendix A.2 Materials and Methods	87
Appendix A.3 Results and Discussion	87
Bibliography	91

List of Tables

Table 1. Protein chaperones categorized by location, function, and homology.....	7
Table 2 Major aggregation-prone proteins and their related proteases.....	19
Table 3 Degradation fates of chimeric ERAD substrates in yeast.....	40

List of Figures

Figure 1 Summary of ERAD with respect to several types of substrate proteins.	38
Figure 2 TM-Ubc9ts is a model aggregation-prone ERAD substrate.....	48
Figure 3 The ERAD of TM-Ubc9ts is magnified at elevated temperatures.	50
Figure 4. F508del CFTR is less soluble than WT at elevated temperatures	52
Figure 5. TM-Ubc9ts is clipped after incubation at elevated temperatures.....	53
Figure 6. Time dependent induction of TM-Ubc9ts in a tetracycline-inducible expression system.....	55
Figure 7 ERAD-dependent processing of TM-Ubc9ts is also temperature dependent in stable cells.	57
Figure 8. TM-Ubc9ts solubility and clipping in a stable expression system reflect the results after transient transfection.....	60
Figure 9 p97 inhibition liberates a proteolytic TM-Ubc9ts product.	62
Figure 10. TM-Ubc9ts cleavage is RHBDL4 independent	65
Figure 11 Proposed model for TM-Ubc9ts clipping during ERAD.	68
Figure 12 Sec62-Aβ42 and Sec62-Aβ40 undergo ERAD but are relatively stable.....	89
Figure 13. Sec62-Aβ42 and Sec62-Aβ40 solubility does not change under temperature or ERAD inhibition.....	90

LIST OF ABBREVIATIONS

(Sorted by alphabetical order)

AAA+: ATPases associated with diverse cellular activities

AD: Alzheimer's Disease

APP: Amyloid precursor protein

ATP: Adenosine triphosphate

AT-Z: α 1-antitrypsin Z

CFTR: Cystic fibrosis transmembrane regulator

CHIP: Carboxyl terminus of Hsc70 interacting protein

CME: Clathrin-mediated endocytosis

COP-I, COP-II: Coatamer complex 1 and 2

E1: Ubiquitin activating enzyme

E2: Ubiquitin conjugating enzyme

E3: Ubiquitin ligase

ER: Endoplasmic reticulum

ERAD: Endoplasmic reticulum-associated degradation

ER-phagy: ER autophagy

ESCRT: Endosomal sorting complex required for transport

GoF: Gain-of-function

HSC70: Heat shock cognate 70kDa protein

HSP: Heat shock protein

INQ: Intranuclear quality control site

IPOD: Insoluble protein deposit

JUNQ: Juxtannuclear quality control site

LoF: Loss-of-function

MVB: Multivesicular body

NEF: Nucleotide exchange factor

NFT: Neurofibrillary tangle

PD: Parkinson's Disease

PM: Plasma membrane

PMQC: Plasma membrane quality control

PolyQ: poly-glutamine

PrPc: Prion protein

PTM: Post translational modification

QC: Quality control

SDS-PAGE: Sodium dodecyl-sulfate polyacrylamide gel electrophoresis

SBD: Substrate binding domain

SRP: Signal recognition particle

TGN: Trans Golgi network

TMD: Transmembrane domain

Ub: Ubiquitin

UPR: Unfolded protein response

VCP: Valosin containing protein

Preface

It is hard to conceptualize the support and encouragement I have received over the years that has culminated in this dissertation. If you ask my parents, they'll tell you that from a very young age, when asked what I wanted to be when I grew up, I'd exuberantly answer "I'm going to be a doctor and cure cancer." I knew little of what it took to back up such a claim and my life has taken some slightly different trajectories, but I can still look back and tell my younger self proudly that I'm well on my way to achieving that goal. I'd like to dedicate this thesis to both my uncles Dr. Fredrick Crock and David Crock who passed away during my time as a graduate student. Together they taught me respect, humility, and passion. They represent to me what it means to be both a scholar and a gentleman in everyday life.

Throughout high school, my early love for science was fostered by a wonderful and talented group of instructors. I would like to give special thanks to William Waryck, my AP Biology teacher for encouraging to push forward with my biology education and stoking the fire that drives my sense of wonder and discovery. My undergraduate education at the University of Pittsburgh was even more full of memorable people. My freshman year I met both Dr. Nancy Kaufmann and Dr. Erica McGreevy who were invaluable both as instructors and mentors and I was fortunate enough to conduct undergraduate research projects with Dr. Elaine Fishilevich, Dr. Michael Tsang, and Dr. Divay Chandra.

As I look back on my career as a graduate student, I see behind me an endless line of support from faculty, friends, and family. I started my experience by rotating in the labs of Dr. Kirill Kiselyov and Dr. Anne Carlson. I fondly remember open and earnest discussions about science, life, and everything in between in Kirill's office as a nervous first year graduate student

and he did his utmost to make me feel welcome in the department. Anne made learning complex electrophysiology and patch clamping easy and showed me the diversity of disciplines within the department. Both were integral to welcoming me into the department and I continue to value their scientific and personal feedback as members of my committee. I must also thank Dr. Allyson O'Donnell for her dedicated mentorship, inspiration, feedback as a committee member, lab neighbor, and in our regular lab meetings. She manages an impressive number of projects while mentoring students and working tirelessly for the department, which inspires me daily. I'd also like to thank Dr. Laura Zapanta, Dr. Zusana Swigonova, and Dr. Valerie Oke for their teaching mentorship which has opened future career paths for me as an educator.

In the Brodsky lab, I feel as though I have a whole family surrounding me. Jeff is a thoughtful and considerate mentor, all while spinning countless other plates both in the department and throughout the scientific community. He has been my lighthouse through the storm, always guiding me back to land as I venture off course with a warm and comforting light. Jen is like our lab mother in that she makes sure I behave, listens to all of our woes, and makes us delicious treats to keep us happy. At the bench, Dr. Chris Guerrerio, Dr. Teresa Buck, and Dr. Sara Sannino have been extremely patient with all of my questions and tolerant of all of my mistakes while teaching me all of the biochemical tips and tricks to make my western blots, gels, and PCRs run just right. My fellow graduate students, both current (Katie Nguyen, Morgan Kok, Katherine Sharp, and Anu Iyer) and former (Dr. Sam Estabrooks, Dr. Deepa Kumari, Dr. Zhihao Sun, Dr. Michael Preston, Dr. Lynley Doonan), have commiserated and celebrated with me over the years as I navigated graduate school and everything that comes with it.

Finally, I'd like to thank my family and friends for their continual love and support. My aunts Susie, Kathy, Kathleen, and Chris keep me well-fed, happy and healthy with constant check-

ups and well wishes. My parents, Diane and Bruce have dedicated their lives to making sure I had everything I needed to succeed. I couldn't have made it this far without their constant support and unending love. I will leave you with this quote, which embodies my graduate experience:

“There's nothing that can't be overcome with Science!”

-Senku Ishigami, Dr. Stone

1.0 Introduction

The cellular factory relies on countless proteins to break down, build up, and maintain the complex machinery responsible for life's various functions. To carry out their specific tasks, protein biogenesis and activity are tightly regulated, and they have specific structures that determine their function. Because newly translated proteins are simply a string of amino acids, they require assistance to both fold properly and efficiently into their functional forms. This process, like many others in biology, is inherently error-prone, and so the cell also requires a system by which misfolded proteins may be either refolded or degraded. Proteins that escape this quality control system often accumulate into aggregates, some of which can cause disease if left unchecked.

In this Introduction, I will address how proteins fold with and without the help of molecular chaperones. I will discuss protein aggregation as it occurs (in some cases) when proteins misfold and how it can be either beneficial and harmful to the cell. Finally, I will define the protein quality control processes, specifically those that occur in the endoplasmic reticulum (ER) membrane, and highlight our current knowledge concerning the degradation and solubilization of harmful aggregates in mammalian cells.

1.1 Protein Folding

Much like how a sheet of paper can be folded in a complex manner to form an origami crane, a polypeptide must undergo a series of complex conformational changes to adopt a

functional shape. Left to purely sample all possible conformations, it would take an inordinate amount of time for a polypeptide to achieve a fully folded state. Therefore, molecular chaperones help ensure that newly translated polypeptides fold without accessing misfolded or aggregation-prone conformations.

1.1.1 Structure-Driven Protein Folding

Christian Anfinsen and colleagues coined the hypothesis of thermodynamically-driven folding. Still, I now appreciate that the route of folding reactions is not as crucial as the stable, native state that is ultimately reached [1]. Until the late 1980's, it was thought that protein folding proceeded in a stepwise manner, as hypothesized by Levinthal and colleagues [2], in which the primary structure determined secondary structure, and the tertiary structure depended on both the primary and secondary structure. It was subsequently suggested that hydrophobic forces dominate later steps in the protein folding pathway [3, 4]. This led to the construction of the modern “folding funnel” hypothesis [5]. I now know that polypeptides rely on a complex system of short-range intramolecular interactions within their local environment, such as hydrogen bonding, hydrophobic interactions, and electrostatic interactions, which guide them towards their native conformations [6-8]. Independent of these “built-in” factors, polypeptides also experience co-translational folding pressures based upon the rate of translation and the environment created by the ribosome itself [9-11]. Guided by these interactions, polypeptides achieve the correct orientation of hydrophobic regions towards the interior of the protein, the formation of secondary structures such as alpha-helices and beta-sheets, and the proper alignment of motifs that will be post-translationally modified. As the nascent protein adopts more ordered structures, it also resides in progressively lower free energy states, which provides the thermodynamic force driving protein

folding [12]. The relative low free energy of the native conformation when compared to various intermediates also ensures that proteins are more likely to remain folded [13]. Nevertheless, native proteins still sample, and may be held in, intermediate states in the folding pathway, some of which are required for protein function, as shown for androgen receptors [14]. Yet, partially folded proteins can alternatively aggregate. For example, prions and amyloids form when exposed hydrophobic motifs begin to clump, an event that leads to the generation of a non-native thermodynamically hyper stable state [15-17]. To help prevent this event, molecular chaperones both sequester these hydrophobic patches until the polypeptide accesses more energetically favorable steps in the folding pathway and prevent the formation of off-pathway intermediates. They also can assist in folding more directly through repeatedly changing a polypeptide's conformational so the lower free-energy state can ultimately be found.

1.1.2 Chaperone-Dependent Protein Folding

The term molecular chaperone was initially used to describe the protein machines responsible for the sequestration of histones from charged proteins in the nucleoplasm [18], but it was quickly adapted for those responsible for assembly of larger oligomeric complexes, such as RuBisCo [19]. It is now appreciated that molecular chaperones are responsible for the proper folding of polypeptides at various stages during their synthesis and processing [20, 21]. More specifically, different chaperones act on newly synthesized polypeptides [22], folding intermediates (as mentioned above) [23], and misfolded proteins targeted for recycling or degradation [24]. They are additionally responsible for linking together these three events, which are part of the protein homeostasis (proteostasis) network that oversees protein synthesis, maturation, transport, degradation, and functional maintenance. More specifically, their varied

functions include promoting polypeptide folding in cases where the lack of chaperones is insufficient to favor folding [25], aiding in the transport of nascent proteins into the ER [26] and mitochondria [27], sequestering misfolded proteins to prepare them for degradation [28, 29], and disaggregating protein aggregates—and in some cases amyloids and prions (see Section 1.1.1)—in an ATP-dependent manner [30, 31]. Notably, many chaperones exhibit substrate specificities that are re-modulated via interactions with co-chaperones [32, 33]. For instance, while ATP-dependent Hsp70 chaperones can bind a select number of protein substrates, they require the assistance of Hsp40 co-chaperones to diversify their functions (See Section 1.3.3.2) [34]. Even more intriguing, Hsp70s and Hsp40s, in concert with Hsp70 nucleotide exchange factors (NEFs), such as Hsp110, can form a mammalian disaggregation complex that strips polypeptides from aggregates so they can be degraded (see section 1.3.3.3) [35]. All these varied functions are carried out by protein chaperone networks (sometimes referred to as the “chaperome”) to maintain proteostasis [36].

Some of the first chaperones discovered were the chaperonins (also known as Hsp60s) that form large complexes to provide a specialized environment to facilitate protein folding. Approximately 10% of the proteins in the cell, particularly those that struggle to fold correctly without assistance from other chaperone systems and those with β -sheet dominant structure [37], require chaperonins to fold [38]. The first observations that protein chaperonins were required for protein maturation came from studies with *E. coli* mutants that were defective in the assembly of bacteriophage capsids and tails [39, 40].

The mutant protein responsible, bacterial chaperonin GroEL, consists of two rings of seven subunits each, creating a folding chamber. The folding process itself is regulated by ATP hydrolysis and the binding of another protein, called GroES, or Hsp10. GroEL captures non-native

proteins and, through ATP-dependent conformational changes and association with GroES, creates an enclosed cavity in which a nascent protein can fold. GroEL/ES accelerates the folding of its substrate proteins by 20- to 100-fold above their spontaneous folding rate by providing a favorable folding environment within the chaperonin and thus preventing the formation of kinetically trapped intermediates that could slow down or halt folding [41]. Substrates of GroEL/ES include, but are not limited to, metalloproteases, maltose-binding protein, and RuBisCo [42-44]. Interestingly, the GroEL rings function sequentially, with one ring encapsulating the protein for folding while the other undergoes ATP-dependent conformational changes [45]. The sequential action of the GroEL rings, ATP binding, and interaction with GroES facilitates protein encapsulation, while the unique structural features of GroEL/ES, such as steric confinement, the generation of hydrophobic interactions, and a partially negatively charged cavity, contribute to its catalytic function in protein folding. Interestingly, there are also cases in which GroEL/ES are able to mediate the folding of proteins too big to fully fit inside the complex [46], leading to evidence of GroEL-specific unfoldase activity [47]. It has been suggested that GroEL-dependent folding, either by encapsulation or unfolding of off-target substrate intermediates, indicates a coevolutionary optimization between the chaperonin and specific protein conformations [48].

Hsp90s are another class protein chaperones known as heat shock proteins, but in this case they appear to be involved in the late folding pathway [49, 50]. They can be found throughout the cellular milieu with Hsp90A/B native to the cytoplasm, GRP94 to the ER, and TRAP-1 to the mitochondria [49]. Structurally, Hsp90s consist of an N-terminal domain, a charged linker region, a middle domain, and a C-terminal domain. Each of these regions is responsible for an element of Hsp90 chaperone function, namely ATP binding, ATPase activity, and client binding, respectively [51]. The central dogma of Hsp90 chaperone activity consists of a cycle of opening and closing of

the Hsp90 homodimer via ATP hydrolysis [52], which requires an array of co-chaperones. Hop1/Sti1 are responsible for keeping Hsp90 open and accessible for ATP binding, while Aha1 promotes ATP hydrolysis by initializing the conversion to a closed conformation. Finally, Sba1 stabilizes the closed conformation to ensure that there is sufficient time for substrate binding and ATP hydrolysis before release [53]. Like the Hsp70 folding cycle (see section 1.3.3.1), repeated binding and release of client proteins results in protein folding and function.

Over time, organisms evolved methods for guiding misfolded proteins toward their native folded states, which resulted in the network of protein chaperones that have been characterized to date (**Table 1**). Still, chaperones are not always able to prevent misfolded proteins from forming harmful aggregates. In the next section, I will discuss the mechanisms of protein aggregation as well as its consequences, both beneficial and harmful.

Table 1. Protein chaperones categorized by location, function, and homology. ‡ cytosol includes nucleoplasm, * only select homologs denoted

Chaperone	Cellular Localization in Eukaryotes [‡]	<i>E. coli</i>	<i>S. cerevisiae</i>	<i>H. sapiens</i> *	Significance	Refs
Hsp70	ER Lumen	DnaK	Kar2	BiP	Protein folding, ERAD	[54]
	Cytosol		Ssa1-4	HSPA8, HSPA1A		
Chaperonin	Mitochondria	GroEL/ES	Hsp60/10	HSP60/10	Sequesters non-native proteins, protein folding	[41, 44]
Hsp40 (J-protein)	Cytosol	DnaJ	Ydj1, Sis1	DNAJ2, DNAJB1	Co-chaperone of Hsp70	[33]
	ER Lumen		Jem1, Scj1	Erdj3, Erdj4		
Hsp110	Cytosol	-	Sse1/2	HSPH1/2	Hsp70 nucleotide exchange factor	[55]
Hsp100	Cytosol	ClpB	Hsp104	-	Protein disaggregation	[31, 56, 57]
	Mitochondria		Hsp78	Skd3		
sHsps	Cytosol	IbpA, IbpB	Hsp26, Hsp42	HSPB1, B3, B4, B5	ATP-independent holdases	[28]
Bag6	Cytosol	-	-	BAG6	ATP-independent holdase, protein quality control	[58, 59]
RuvB	Nucleus	RuvA/B	Rvb1/2	RUVBL1/2	Protein disaggregation, chromatin remodeling	[60]

1.2 Protein Aggregation

Most nascently translated polypeptides fold efficiently and function properly as they adopt the lowest free energy conformation permitted by their sequence and their environment, but the reality is that occasionally aggregates form because of protein misfolding. While this is most often thought to give rise to toxic species, if protein condensate formation is regulated, this can provide a way to store or sequester cellular machinery [61-64]. Often, however, aggregates form due to genetic mutations, errors during transcription or translation, or under conditions of cellular stress. Regardless of the source, protein aggregates, as opposed to regulated condensates, disrupt cellular homeostasis and exert cytotoxic effects which are evident in several diseases (see section 1.2.3.1).

1.2.1 Mechanism

Proteins undergo conformational fluctuations and structural perturbations, which can expose aggregation-prone sequences or "hot spots". These changes may lead to the formation of non-native dimers and oligomers, a process known as nucleation, which represents the initial step of protein aggregation [65]. A non-optimal folding environment (or stressors) can induce structural perturbations, affecting the initiation of aggregate formation, also called the nucleation rate. In addition to illegitimate hydrophobic interactions and van der Waals forces [66, 67], electrostatic interactions represent another force driving protein self-association that result in the formation of reversible oligomers through long-range repulsions and short-range attractions [7, 68]; hydrogen bonds also contribute to this event [69]. In any of these cases, the dominant upstream driving force for aggregation depends on protein structure, solution composition, and experimental conditions, making it difficult to determine a single mechanism that defines the protein aggregation pathway.

Nevertheless, protein-protein interactions are clearly concentration-dependent, with increased concentration promoting monomer association into oligomers or clusters [70]. High protein concentration can also lead to more extensive and differently shaped clusters, and short-range interactions play a significant role at high concentrations. Protein crowding is particularly noteworthy since the protein concentration in the cell can be as high as ~300 mg/ml, though this value varies between cell types [71].

1.2.2 Beneficial Effects of Inclusions

Aggregation is an efficient and self-propagating process, so in cases in which the formation of cellular inclusions/condensates is beneficial, this event must be precisely regulated in order to ensure that cellular toxicity is absent. One mechanism of regulation is the presence of amino acid residues, such as lysine, arginine, and proline, which inhibit condensate formation [72, 73]. These residues prevent the aggregation-prone stretches of amino acids in proteins from forming condensates, thus modulating aggregation propensity and earning the moniker “gatekeeper” residues. Indeed, mutations in gatekeeper residues can lead to the disruption of regulated amyloid structure such as anti-parallel β -sheets [74], which is implicated in certain diseases, such as amyloidosis [73], highlighting the importance of their proper arrangement within protein structure.

The term amyloid was introduced in the 19th century to describe macroscopic tissue abnormalities that exhibited specific staining patterns [75]. Although not all amyloids show the same characteristics, the term is commonly used to describe ordered aggregates of single proteins, including toxic species such as those found in Alzheimer’s plaques, which are formed by the A β peptide [76]. In other cases, amyloids require specific partner proteins, which help form functional condensates. For example, the interaction between programmed cell death signaling proteins Rip1

and Rip3 leads to the formation of heteromeric amyloid fibers, which play a role in necroptosis, a type of programmed cell death [77]. In this example, the amyloid-like structures act as scaffolds to activate downstream pathways that trigger necroptosis. Additionally, environmental factors, such as pH and ion concentration, can control the formation and breakdown of condensates. This is evident in the pH-dependent regulation of Pmel17, a functional amyloidgenic protein that is responsible for the deposition of pigment in the eyes and skin via scaffolding and melanosome maturation [78]. Pmel17 itself must be cleaved into C and N terminal fragments that go on to form fibrils within the melanosome on which pigment can accumulate [79].

Many condensate-forming proteins are RNA-binding proteins, such as TDP43 [80], FXR1 [81], and SMAUG1 [82], and RNA can act as a co-condensate with proteins, thus influencing aggregation. RNA condensate formation is a complex process that can result from tandem repeats, protein:RNA ratio, and RNA secondary structure. The RNA may act as a scaffold, proteins may recognize only certain types of RNA (single stranded vs. double stranded), or conformational changes in the protein can result from RNA binding [83]. RNA helicases are frequently associated with condensates and can even regulate RNA structure and, in turn, protein binding [84]. Post-translational modifications (PTMs), such as phosphorylation, can further modulate protein aggregation behavior [85]. In fact, reversible PTMs provide a way to regulate protein aggregation [86], and dysregulation of PTM activities contributes to the formation of toxic aggregates and disease, as described below.

1.2.3 Harmful Effects of Protein Inclusions/Aggregates

1.2.3.1 Proteinopathies

Proteinopathies are diseases characterized by abnormal protein aggregation, which leads to changes in their conformation and function, and consequently compromise cell function. Although proteinopathies can affect various organs—and can be expressed simultaneously in all tissues—they are most commonly associated with the central nervous system [87]. Genetic factors play a significant role in these diseases, although age and traumatic brain injuries can also increase the risk of proteopathic inclusion formation [88]. The underlying reason for this is likely a combination of proteostasis failure, cellular senescence, telomere reduction, and/or general genomic instability [89]. Alzheimer’s disease (AD), Parkinson’s disease (PD), Lewy body disease, and prion diseases are some examples of proteinopathies with few treatment options and no known cures. These diseases can also be caused by the aggregation of multiple different proteins, such as tau tangles and amyloid plaques in Alzheimer’s disease [90], which increases the complexity of identifying a single treatment regimen.

Prion diseases were thought to be unique among proteinopathies because they involve infectious misfolded prions that can cross species barriers [91], but recent studies suggest that misfolded proteins may also exhibit neuron-to-neuron transmission in Alzheimer's and Parkinson's diseases, potentially contributing to pathology progression [92]. Experimental observations suggest that protein aggregates can move from affected to unaffected areas of the brain, similar to prion propagation, through the expression of viral ligands which predisposes cells to transmit proteopathic aggregates [92]. Nevertheless, different prions exhibit distinct levels of infectivity and irreversible aggregation. While evidence supporting prion-like transmission exists for transmissible prion encephalopathies, such as Creutzfeldt-Jakob disease [93], the case for

Alzheimer's and Parkinson's diseases is less conclusive. There is evidence of interaction between A β and tau, with overlapping but distinct patterns of pathology, where A β and tau aggregates can spread from cell to cell and between brain regions. Interestingly, injecting brain extracts containing A β or tau aggregates into animal models accelerates pathology in animals [94, 95]. Despite ongoing discussions, caution is advised when using the term "prion-like" for non-prion proteinopathies, as the mechanisms involved may differ.

1.2.3.1.1 Alzheimer's Disease

The main neuropathological features of Alzheimer's disease (AD) include gross brain atrophy, the presence of amyloid plaques, neurofibrillary tangles (NFTs), and extensive neuronal loss [96]. Patients exhibit memory loss, changes in personality and general decline in cognitive function. As noted above, amyloid plaques in AD are defined by accumulations of the A β peptide, which is derived from the amyloid precursor protein (APP), and can be detected in both insoluble fibrillar and soluble oligomeric forms [76]. In contrast, NFTs are intracellular structures composed of hyperphosphorylated tau and are found in nerve cell bodies and processes [97]. While it is currently debated which of the two types of inclusions is responsible for Alzheimer's pathology [98], the deposition of A β and the formation of NFTs contribute to neuronal dysfunction and generally correlate with the clinical progression of AD. The recent approval of Lecanemab and donanemab [99] as monoclonal antibodies targeting amyloid-beta plaques in the brain is promising, although drugs targeting NFTs should still be pursued in the event that these treatments are not effective in the long-term, and toxic side-effects have been noted [100, 101]. Unfortunately, the timing of treatment of AD is difficult, as it is most effective when administered extremely early in disease progression, long before patients become symptomatic.

In addition to plaques and tangles, AD is characterized by the loss of synapses, selective neuronal cell death, and the loss of certain neurotransmitters. Neurons in specific brain regions, such as the entorhinal cortex, hippocampus, and neocortex, are particularly vulnerable in AD [102, 103]. Dysfunction of cholinergic and noradrenergic neurons has been linked to attention and memory impairments in AD, and like the approved drugs noted above, drugs targeting these systems have shown only modest symptomatic improvements [104, 105]. The disruption of network connections between key brain regions within the limbic system and neocortex also contributes to cognitive dysfunction in AD, with the default mode network being one of the early affected networks. A β deposition shows a preference for brain regions within this network and may be related to its high baseline neuronal activity [106].

While amyloids are difficult to disaggregate in metazoans, which lack the AAA+ ATPase Hsp104 (discussed in later sections), they can still be degraded, albeit with low efficiency. A β levels are regulated through the action of various proteases in the extracellular space and the endomembrane system, including NEP, Cathepsin D, and the proteasome [107]. Because these proteases are working at near capacity to maintain physiological levels of A β , problems arise when excess A β begins to accumulate, consequently snowballing into the formation of amyloid plaques.

Currently, the genetic database for mutations associated with AD is predominated by three genes: PSEN1, PSEN2, and amyloid precursor protein (APP) [108]. PSEN1 and 2 are both involved in the cleavage of APP into A β via the activity of the gamma secretase complex. A hallmark of AD pathology is an elevated ratio of these APP cleavage products with an excess of the more aggregation prone A β 42 relative to the native A β 40 species [109]. Mutations in these proteins alter A β 42:40 ratio, either through overexpression of A β 42, reduction of A β 40, or a combination both [110, 111]. However, amyloid plaques are primarily cleared by autophagy, as

supported by the fact that defects in endosome trafficking, autophagosome clearance and lysosomal degradation all contribute to AD pathology [112, 113]. To date, there is no known mammalian disaggregase that fully dissolves amyloid plaques, with the most effective therapeutic treatments involving the recruitment of macrophages via antibody administration, as mentioned above. This has led to active investigations to identify drugs that activate autophagy [114].

1.2.3.1.2 Huntington's Disease

Huntington's disease is caused by autosomal dominantly-inherited mutations in huntingtin protein, where expansion of the poly-glutamine sequence drives aggregation [115]. Mutations result in the lengthening of the polyQ sequence beyond 36 residues, with longer expansions correlating with earlier disease onset. Similar expansions are observed in other disease-causing proteins, mainly members of the ataxin family, including SCA7 and SCA17, indicating that repeat expansion represents a common disease mechanism. Yet, the specific effects of polyQ expansions on huntingtin and the various consequences on cellular function are controversial and still not fully understood.

Extended polyQ repeats lead to the formation of amyloid-like fibrils, similar to those found in other neurodegenerative diseases [116], that are associated with neuronal toxicity [117, 118]. Additionally, mutant huntingtin can recruit and sequester normal huntingtin protein, potentially disrupting its normal function and contributing to the dominant phenotype. Aggregation also interferes with protein degradation machinery, such as the proteasome (see section 1.4.1 below), further affecting cellular homeostasis. Interestingly, mutant huntingtin can overwhelm the cell not only by aggregating but also indirectly through the disruption of the ER-associated degradation (ERAD) pathway via gp78 inhibition [119], interruption of substrate retrotranslocation via

VCP/p97 inhibition [120], or the formation of “rosettes” at the ER membrane surface which structurally and biochemically alter proteostasis [121].

While proteostasis is disrupted in individuals with Huntington’s disease [122, 123], *in vitro* and *in vivo* studies suggest that the Hsp40/70/110 chaperone complex in mammalian cells should be able to resolve huntingtin aggregates (see section 1.3.3.3). Specifically, substrate specificity granted by overexpression of the Hsp40 DNAJB1 reduced polyQ huntingtin aggregation in cultured cells [124]. It is somewhat of a paradox, then, that aggregated huntingtin disrupts proteostasis machinery that would otherwise be competent to resolve aggregates. Regardless, the toxicity of aggregated huntingtin may arise from a combination of gain-of-toxic-function effects, sequestration of normal huntingtin, and disruption of cellular processes involved in protein degradation. Yet, further research is needed to fully elucidate the mechanisms underlying the relationship between protein aggregation and dysfunction in specific neurons in Huntington's disease.

1.2.3.1.3 Parkinson’s Disease

α -Synuclein is a small (140 amino acids), intrinsically disordered protein encoded by the SNCA (synuclein) gene predominantly expressed in the CNS. Mutant α -synuclein is genetically and pathologically associated with Parkinson’s Disease [125]. α -Synuclein is a member of the synuclein protein family, which also includes gamma and beta synucleins [126], with approximately 1% of the total proteins in neuronal cytosol consisting of α -synuclein [127]. The N-terminus of α -synuclein is amphipathic and contains seven imperfect sequence repeats of 11 residues, potentially forming an alpha helix that facilitates lipid binding, whereas the C-terminal domain, known as the non-amyloid component, facilitates calcium binding and inhibits protein aggregation [128].

The structural characteristics of α -synuclein predispose the protein for aggregation, especially in the presence of mutations. For instance, the NMR structure of human α -synuclein revealed that residues 3-37 and 45-97 form alpha-helices which are connected by a linker region in an unprecedented anti-parallel manner and the C-terminal region of α -synuclein (residues 98-140) exhibits high mobility [129]. This well-organized helical structure suggests a distinct association with the lipid bilayer, indicating its potential role in modulating protein conformation. Specific point mutations in α -synuclein correlate with autosomal dominant forms of Parkinson's Disease (PD). These mutations, such as A53E, A53T, A30P, E46K, H50Q, and G51D, all reside in the same hairpin involved in tetramer formation, markedly affecting protein conformation and the type of aggregates formed [130]. For instance, the A53 mutation in α -synuclein shows reduced aggregation in comparison to wild-type, which alleviates its burden on proteostasis [131]. Moreover, α -synuclein has been found to form dimers, with different mutations promoting dimerization and influencing distinct aggregation pathways [132].

The physiological function of α -synuclein remains elusive, but it is believed to be involved in several cellular processes, e.g., dopamine release, vesicular trafficking, and oxidative stress [133]. In animal models, the deletion of the α -synuclein gene led to the loss of dopaminergic neurons, reduction of striatal dopamine levels, and the absence of dopamine-induced locomotive responses mediated by the dopamine transporter (DAT) [134] which are also features of Huntington's Disease. In addition to PD, α -synuclein has been implicated in other synucleinopathies, including multiple system atrophy and dementia with Lewy bodies [135]. The presence of α -synuclein inclusions, often hyperphosphorylated at various sites, has been observed in these diseases [136]. Mutant α -synuclein proteins associated with familial PD also exhibit structural defects in membrane binding (see above), altering the protein's binding properties.

While α -synuclein is the aggregated protein in PD pathology, leading causes of disease are often the result of mutations in proteins that regulate α -synuclein processing or clearance, such as LRRK2, PARK2/7, and PNK1, among others. Of great importance is LRRK2 [137], a kinase whose dysfunction can influence PD pathology in three ways: aberrant phosphorylation of downstream targets (gain of function) [138], direct interactions with α -synuclein [139], and regulation of the neuroinflammatory response (loss of function) [140]. Interestingly, the E3 ubiquitin ligase PARK2, or “parkin”, has several loss-of-function mutations associated with PD pathology but does not directly interact with α -synuclein. Instead, it is suggested that mutant parkin is unable to properly ubiquitinate two substrates, namely AIMP2 and FBP-1, whose accumulation contributes to neurodegeneration [141].

Clearance of aggregated AS is inefficient in affected cells, but both the ubiquitin proteasome system and the autophagy pathway, as noted for AD above, make efforts to ameliorate its effects. Only small oligomers of α -synuclein are susceptible to degradation by the proteasome, and autophagy easily becomes overwhelmed after the lysosomes are loaded with α -synuclein aggregates [142]. Current therapies focus on symptom relief via dopaminergic medications and L-DOPA [143], however leading the field are prospective treatments to enhance the activity of proteostasis machinery [144].

1.2.3.1.4 Prion-related Diseases

Prion diseases, also known as transmissible spongiform encephalopathies, are fatal neurodegenerative diseases caused by misfolded and aggregated forms of the prion protein (PrP^c) [145]. A misfolded prion protein, called PrP^{Sc}, is uniquely associated with prion disease pathology as the cause of epidemics both within and between species, and is responsible for profound neurodegeneration. Normally, PrP^C is a glycosylphosphatidylinositol (GPI)-anchored protein

primarily present in mammalian neuronal cells [146]. It consists of a structured C-terminal domain (CTD) and an unstructured N-terminal region (NTR). The conformational conversion of PrPC into the misfolded and aggregated form (PrPSc) is associated with prion disease pathology. The structural details of PrPC have been extensively studied, while the exact biological function of PrPC remains unclear. Studies have suggested that PrPC may have multiple functions, including copper homeostasis, protection against apoptosis, signal transduction, and immunoregulation [147-149].

The disease that most strongly correlates with prion protein aggregation is Creutzfeldt–Jakob Disease (CJD), which is most often caused by sporadic prion propagation. Mutations in the PRNP gene cause only a small subset of CJD (~10-15% of cases), and while misfolding of prion protein remains a major element in the disease pathology, indirect cellular effects of PRNP mutations require further study. Prion aggregation is unique amongst proteinopathies in that pathological isoforms of PrP induce templated conformational changes in native PrP, initiating a chain reaction of oligomer formation [15, 150]. These oligomers are profoundly protease resistant in mammalian cells and can only be remodeled in the presence of powerful yeast/bacteria AAA+ ATPases [151] (see section 1.3.2).

As a review, I have summarized the aggregation-prone proteins involved in the proteinopathies discussed in Section 1.2.3.1 as well as the proteases involved in their cleavage.

Table 2 Major aggregation-prone proteins and their related proteases* pT α , Opsin-degron, and Pkd1 Δ N are artificial substrates

Substrate*	Protease	Major Findings	Refs
TDP-43	Caspase-3,4,7	Cleavage of monomer likely seeds further aggregates	[152, 153]
A β	α,β,γ -secretase	β to γ -secretase pathway generates aggregation prone A β from APP	[154]
α -synuclein	Calpain-1, Cathepsin D, Neurosin	Degradation via cleavage differs in each cellular compartment, can lead to clearance or seeding of further aggregates.	[155, 156]
Rhodopsin P23H	Unknown	Partially cleared by ERAD, ER-phagy, and ribosome quality control	[157]
pT α	RHBDL4	Cleavage via RHBDL4 contributes to ERAD of single spanning membrane protein.	[158]
Opsin-degron		Cleavage via RHBDL4 contributes to ERAD of polytopic membrane protein with unstable TMs	
Pkd1 Δ N			

1.3 Protein Disaggregation

1.3.1 Mechanism

Protein disaggregation is the method by which protein aggregates are separated into individual components either by mechanical force or chaperone-based remodeling of fibrils/condensates. Overall, the process of chaperone-mediated repair of misfolded species is much less ATP-consuming compared to the alternative of degrading and resynthesizing the proteins. Several organisms, including yeast and bacteria, utilize ATP-dependent disaggregation, driven by ATPases associated with diverse activities (AAA+), to resolve protein aggregates, therefore maintaining proteostasis and alleviating the burden of aggregate buildup. Heat-shock protein 104 (Hsp104) and its bacterial counterpart, ClpB, are two molecular chaperones that play

a crucial role in dissolving aggregated proteins. Below, I will highlight the major disaggregases or disaggregase-like complexes currently identified in the field.

1.3.2 Bacterial and Yeast Disaggregases

1.3.2.1 ClpB

Caseinolytic peptidase B (ClpB) is an ATP-dependent molecular chaperone found in *E. coli*. It belongs to the Clp/heat-shock protein (Hsp)100 family and the AAA+ superfamily. Its main function is to improve protein quality control by using ATP hydrolysis to disaggregate proteins in collaboration with the Hsp70/40/NEF chaperone system DnaKJE [159]. The importance of ClpB in protein disaggregation is evident from studies on clpB-null bacteria, which show increased sensitivity to heat shock and extreme stress [160]. As discussed above, protein aggregation and inclusion body formation are associated with various neurodegenerative diseases, making it crucial to understand how ClpB and similar enzymes might be able to rescue proteins from forming aggregates and lead to potential therapeutic applications.

The ClpB structure includes an N-terminal domain, AAA+ domain 1 (D1), AAA+ domain 2 (D2), and a unique coiled-coil M-domain in D1 [161]. ClpB, along with ClpA and Hsp104 (see below), contains two ATP-binding and hydrolysis sites per monomer, placing them in the class 1 Hsp100/Clp enzyme category. While it is known that ClpB forms hexameric rings like other class 1 Hsp100/Clp enzymes, the specific molecular mechanism by which these rings catalyze protein disaggregation remains unclear. Unlike ClpA, which interacts with the ClpP protease, ClpB does not interact with any known protease [162]. This has made it challenging to determine if ClpB processively translocates or employs alternative mechanisms to drive protein disaggregation [163, 164].

The Hsp100/ClpB-Hsp70/DnaK system exhibits both unfoldase and disaggregase activity. DnaK acts as an activator of ClpB and as a possible ATP-fueled unfolding machine, completing the unfolding of partially disentangled polypeptides [165]. Interestingly, ClpA and ClpX, which are highly homologous to ClpB, associate with the ClpP protease and function as cylindrical unfolding enzymes, actively degrading misfolded proteins in an ATP-dependent manner [166]. However, ClpB does not associate with ClpP and instead works with DnaK to disaggregate, unfold, and refold misfolded proteins into native forms. This unfolding mechanism was predicted by Rothman & Kornberg, who suggested that cells have unfolding enzymes associated with proteases: Some enzymes lose their proteolytic activity but still recognize incorrectly folded proteins and provide them a chance to refold properly [167]. In fact, it is considerably less energetically expensive to attempt to refold these protein aggregates instead of degrading them and rebuilding the polypeptide [168].

1.3.2.2 Hsp104

The yeast Hsp104 shares many of the structural and functional qualities of its homolog ClpB. It also belongs to the AAA⁺ superfamily and forms a two-ring ATPase engine that feeds polypeptide chains through its central pore. As opposed to other chaperones, such as Hsp90 (see section 1.1.2), Hsp104, in collaboration with Hsp70 and Hsp40, is able to actively disaggregate biologically inactive oligomers in an ATP-dependent manner [169]. This ability of the chaperone system to act on pre-aggregated oligomers was demonstrated in various experiments using heat denatured and aggregated luciferase as well as other proteins [170].

The Hsp104-Hsp70 complex can solubilize various fibrils expressed in yeast, including amyloid fibrils associated with diseases like Alzheimer's and Parkinson's, and like ClpB, translocates them through the central pore, and releases them as a single polypeptide for refolding

or degradation [171]. More specifically, the power stroke model is a common mechanism used by Hsp100s disaggregases, like Hsp104 and ClpB. ATPase activity translocates the peptide through the central pore, leading to the extraction and unfolding of amyloid aggregates. In fact, recent structural data shows that to generate the force necessary to move a polypeptide through the Hsp104 “barrel”, each subunit switches between an extended state and a closed state via ATP hydrolysis. In this fashion, each subunit “steps” by about two amino acids above its neighbor in the hexamer to “walk” along the substrate polypeptide [31]. Furthermore, each chaperone in an Hsp104 complex plays a unique role: Hsp70 and Hsp40 engage substrates via ATP hydrolysis-induced conformational changes, recruiting the Hsp104 hexamer for disaggregation. The Hsp70-Hsp40 complex loads the substrates onto Hsp104, and a conformational change triggered by a NEF releases the substrate inside the disaggregase complex [172]. As noted above, ATP binding and hydrolysis in Hsp104 initiate a power stroke, resulting in the translocation of the substrate through the central pore and ultimately disaggregating the oligomer.

The Brownian ratchet model is another proposed mechanism for protein translocation and disaggregation by Hsp100s [173]. This model suggests that a polypeptide within the amyloid aggregate randomly slides back and forth in the central pore due to collisions and fluctuations. Hsp70 prevents the backward movement and sliding of the substrate into the disaggregation complex while binding to the unfolded polypeptide. ATP hydrolysis-induced conformational changes allow repeated binding and release of the substrate to Hsp70, generating a pulling force that threads the entire amyloid aggregate through the central pore [174]. Unlike the power stroke model, the Brownian ratchet model emphasizes the role of Hsp70 in preventing substrate movement and relies on repeated binding to exert the pulling force for translocation and

disaggregation. However, current hypotheses using cryo-EM structure of Hsp104 confirm that the power stroke model is the most accurate description of AAA+ ATPase function (see above).

1.3.3 Mammalian disaggregases

While bacteria and yeast are equipped with dedicated machinery to handle the formation of low-energy aggregates, such as prions and amyloids, mammalian cells instead rely on a less powerful but perhaps sufficient combination of heat shock proteins to drive protein disaggregation.

1.3.3.1 Hsp70

As noted briefly above in section 1.1.2, Hsp70 family proteins are ATP-dependent chaperones. They are also abundant, conserved, and reside in any cellular compartments that contains ATP, utilizing their ATPase activity to power protein substrate binding and refolding [175]. In addition, Hsp70 itself is a weak ATPase in that it requires the assistance of Hsp40 co-chaperones and NEFs to efficiently cycle between closed and open conformations [176]. As a result, Hsp70 and its co-chaperones participate in a cycle of nucleotide exchange, substrate binding, and substrate release that progressively assists unfolded protein to reach a natively folded state. Their structure commonly consists of an N-terminal nucleotide binding domain, a flexible middle linker region, and a C-terminal substrate binding domain [177]. Importantly, Hsp70 proteins --whose specificity is modulated by binding co-chaperones such as Hsp40s (also see section 1.1.2 above) as well as those that contain an EEVD motif, such as cytoplasmic Hsp70s and Hsp90s-- allows for such modulation. Based on the ability of Hsp70s to recognize hydrophobic motifs, along with their co-chaperone partners (also see below), they can engage a wide variety of substrates.

1.3.3.2 Hsp40

Hsp40 family proteins, or J-domain proteins, are integral to the specificity and potency of Hsp70-centered protein refolding. They bind candidate substrates with exposed hydrophobic patches via their substrate binding domain (SBD) and stimulate the hydrolysis of ATP upon binding Hsp70 and delivering their cargo [178]. Not to be overlooked, a crucial element of Hsp40 family proteins is their ability to modulate not only Hsp70 specificity but the refolding and even disaggregation potential of the Hsp40-Hsp70-Hsp110 complex [33, 34](see section 1.3.3.3, below). *In vitro* studies have shown that beyond the specificity assigned to individual J-domain proteins, even their ratios in solution can drastically change the ability of metazoan disaggregation machinery to resolve inclusions. For example, synergistic effects on disaggregation via Hsp104 have been observed by mixing A and B class J-proteins in reconstituted yeast systems [179]. The A and B classes are in turn defined by unique structural motifs which determine their specificity. Both classes share the N-terminal J-domain which stimulates Hsp70 ATPase activity, followed by a glycine-rich region and two C-terminal domains responsible for client binding and dimerization. They differ in that Class A have a zinc binding domain near the first C-terminal domain while Class B have a binding site for the EEVD peptide motif shared by Hsp70s. While once thought to interact 1:1 with Hsp70 in order to direct substrate binding [180], it is now evident that more complex stoichiometry of these J-proteins in mammalian cells have evolved to finely tune proteostasis [35, 181].

1.3.3.3 Hsp70-40-110 complex

The Hsp70-Hsp40-Hsp110 chaperone machinery plays a crucial role in preventing the formation of toxic protein aggregates in animal cells. Unlike other organisms, like plants and yeast, animal cells lack the Hsp100/ClpB orthologs and instead rely on this machine for efficient

disaggregation of misfolded proteins. Hsp110 is closely related to Hsp70, but contains an extended substrate binding domain, and acts as an ATP-fueled Hsp40-regulated chaperone that also aids in substrate capture. Both Hsp70 and Hsp110 can induce the release of unfolded inactive proteins from each other and work together as functional partners to disaggregate and unfold misfolded polypeptides.

The cytosolic Hsp70-Hsp40-Hsp110 machinery can prevent the formation of early misfolded and aggregated conformers, which, as outlined above, can lead to synucleinopathies and tauopathies. For example, biochemical reconstitution experiments showed that a combination of human Hsp70, Hsp110, and Hsp40, along with ATP, can efficiently break apart stable α -synuclein fibrils in a manner comparable to bacterial chaperones and sonication [169]. Additionally, treating α -synuclein fibrils with these chaperones reduced the amount of misfolded β -sheets and inhibited the spontaneous formation of insoluble α -synuclein fibrils [182]. In a nematode model, cooperation between Class A and B J-proteins (see section 1.3.3.2), as well as with Hsp70, respond to stress-induced aggregate formation and clear post-stress aggregates (in the case of Hsc70) [183]. While the Hsp70/40/110 disaggregation complex is powerful enough to resolve some harmful protein aggregates, evidence in *C. elegans* also suggests that fragmentation of α -synuclein by the complex further seeds new aggregate formation [184].

In contrast to animal cells, the cytoplasm of plants, yeast, and fungi contains both Hsp100/ClpB as well as the Hsp70/DnaK, Hsp40/DnaJ, and GrpE disaggregating machineries, suggesting different specificities toward various aggregates [185]. The deficiency of the human cytoplasm, which lacks the Hsp104/ClpB-based disaggregating machinery present in yeast and plants, may contribute to the higher sensitivity of aging mammalian cells to toxic protein aggregates. However, the expression of Hsp100 class proteins is both energetically expensive for

the cell—a problem in aging neurons—and perhaps more difficult to regulate [186]. It is hypothesized that one of the reasons for the loss of Hsp104 in mammalian cells was the need for protective aggregates that otherwise could not form in the presence of such a powerful disaggregase. Still, experiments in transgenic mice [187] and flies [188] show that metazoan cells tolerate Hsp104 expression and effectively resolve harmful aggregates.

In sum, various molecular chaperones can act as unfolding catalysts, converting metastable misfolded polypeptides into low-affinity products that spontaneously refold into native proteins. Other unfolding mechanisms, exemplified by the GroEL and related Chaperonin Containing TCP-1 (CCT) chaperones [189] in higher cells—might also contribute to this phenomenon. The ability to unfold stable misfolded proteins into partially unfolded, natively refoldable, or protease-degradable proteins appears to be a common functional feature of molecular chaperones. Therefore, the term "chaperone" is described above in section 1.1.2. may need to be re-evaluated, as it implies only a passive binding function that prevents protein aggregation. Instead, many of these proteins, acting in complex with one another, appear to play active roles in unfolding and rehabilitating misfolded proteins.

1.3.3.4 sHsps

Indeed, a whole class of chaperone proteins called small heat shock proteins (sHsps) act as true “chaperones,” modulating the disaggregation machines described above through passive “holdase” activity [28]. The defining feature of sHsps is a central α -crystallin domain with a disordered N-terminal domain for substrate binding [190]. Prevalent aromatic residues in the N-terminal domain allow sHsps to preserve nascent polypeptides before they seriously misfold in the cytosol [191]. Some sHsps are responsible for keeping large inclusions divided into smaller, easier-to-handle “sequestromes” that also serve as an example of cytoprotective aggregates [192] (see

section 1.2.2). In fact, oligomeric inclusions of sHsps and unfolded proteins are thought to be uniquely accessible by Hsp70-Hsp100 complexes while preventing access by cellular machinery such as proteases [193]. Overall, sHsps represent an ATP-independent way the cell may finely tune protein folding concerning the powerful disaggregation machines outlined above.

1.4 Protein Quality Control

Protein quality control is the umbrella term for managing misfolded, aggregated, and accumulated protein. The cytoplasm can be defined by two major categories: temporal and spatial quality control. Key elements of these events are described below.

1.4.1 Ubiquitin Proteasome System

For the cell to properly dispose of excess or misfolded protein requires a dedicated degradation machine. In the cytosol, this machine is called the proteasome. The proteasome is an approximately 2.5 mDa complex that selectively identifies and degrades protein substrates [194]. Thus, the proteasome maintains proteostasis (“protein homeostasis”) as the endpoint for several quality control pathways. Structurally, the proteasome consists of the 20S core particle and one or two 19S regulatory particles, forming the full 26S proteasome [195]. In the 20S core particle, a system of inner and outer rings, formed by α and β subunits, respectively, creates a channel for unfolded protein substrates to access the degradation site. Specifically, the β 1,2, and 5 subunits are responsible for caspase-, trypsin-, and chymotrypsin-like activity, respectively [196]. While the 20S subunit is responsible for proteolytic activity, the 19S subunit regulates access to the

proteasome by forming a selective lid and base structure [197]. Rpt1-6 forms an AAA+ ATPase-rich base connected by a linker subunit, Rpn10, to the non-ATPase containing lid. Ultimately, Rpn1, Rpn10, and Rpn13 select substrates for degradation based upon an appended polyubiquitin, a post-translational modification that can identify misfolded proteins and other substrates for proteasome-dependent degradation [198].

The process that leads to polyubiquitination is initiated by the priming of ubiquitin by an E1 ubiquitin-activating enzyme, UBA1 [199]. E1 enzymes then activate and charge ubiquitin-conjugating enzymes, E2s, with ubiquitin, which is then brought to misfolded protein substrates with the help of ubiquitin ligases [200]. These ligases, called E3s, are ultimately responsible for identifying and attaching the ubiquitin tags to the misfolded protein in a complex with the E2 [201]. Ubiquitin itself can be appended in multiple different chain types specified by the internal lysine residue at which they branch. K48-linked polyubiquitin is the most commonly associated residue that forms the isopeptide polyubiquitin moiety and proteasome degradation [202]. In contrast, other isopeptide linkages, such as K63, are involved in endocytosis, autophagy, and histone modification [203].

The specificity of the ubiquitination machinery for a substrate increases as ubiquitin transitions from E1 to E2 to E3. That is to say that there are only a few E1 enzymes, with UBA1 activating about 99% of all ubiquitin in the cell [204]. E2 enzymes are more common, with human cells expressing around 40 involved in the transfer of ubiquitin or even ubiquitin-like proteins, some of which are also required for proteostasis, such as SUMO and NEDD8 [200]. Impressively, at least 600 E3 ligases exist in the human genome [201]. Because E3 ligases help specify substrates, this large number is due to not only the wide variety of proteins in different cellular compartments and in different developmental stages that need to be ubiquitinated but also for

processes ranging from protein degradation to the regulation of transcription and immune system function.

1.4.2 Cytoplasmic Quality Control

As RNA is translated into a nascent polypeptide, temporal protein quality control involves *de novo* folding, folding/refolding by molecular chaperones, the targeting of a nascent polypeptide to the cytosol or an intracellular compartment (such as the ER or the mitochondria), and the degradation of terminally misfolded proteins by proteases [205]. For cytosolic proteins, failure of temporal quality control can result in the accumulation of protein oligomers, which may go on to seed insoluble inclusions or aggregates (see section 1.2.3.1). Once advanced to this state, spatial quality control takes over, organizing inclusions into specific cellular compartments for bulk degradation by the autophagy pathway or at least to mitigate any toxic effects on the cell [206]. One such dynamic inclusion, which can also be relatively transient, is called a Q-body, which forms upon heat stress and rapidly dissociates upon return to native temperature [207]. Q-bodies can form at the ER but eventually come together under prolonged stress to form inclusions at/near the nucleus. These later inclusions are known as internal nuclear quality control (INQ) bodies or juxtannuclear quality control (JUNQ) bodies [207, 208]. If the misfolded proteins have aggregated, they can reside at or near the vacuole/lysosome and are known as an insoluble protein deposit (IPOD) [208, 209]. INQ/JUNQ bodies result from terminal misfolding of proteins sorted into Q-bodies while IPODs are terminal protein deposits that form independently of Q-bodies. Once the aberrant proteins have been sequestered and concentrated, they can more easily be refolded or cleared by the ubiquitin-proteasome system or endomembrane-lysosomal/autophagic degradation, as seen for IPODs.

1.4.3 Unfolded Protein Response

Approximately one-third of all proteins in eukaryotes are targeted to the ER, which serves as a rich source of protein folding, post-translational modification, and export machinery. The ER also acts as a quality control checkpoint before secreted and membrane proteins travel to the cell surface or other secretory pathway compartments or for some soluble proteins if they are released to the extracellular environment [210]. The ER is also responsible for triggering the unfolded protein response (UPR), which is a cascade of signaling pathways that responds to the buildup of aberrant protein in the ER by both increasing the amount of ER as well as the folding machinery that occupies it [211]. A specialized ER-associated degradation system and the autophagy pathway are also induced as quality control methods alongside the UPR. In higher cells, the activation of three distinct branches of the UPR is partially redundant but allows for a finely tuned-stress response [212]. Each branch utilizes a similar but unique signaling mechanism to transduce unfolded protein abundance into a stress relief response or, if stress cannot be rectified, into an apoptotic response [213].

The ATF6 branch initiates transcription through regulated proteolytic cleavage of the ATF6 transmembrane protein, ATF6 [214]. Upon recognition of an unfolded protein burden, ATF6 traffics to the Golgi via the secretory pathway, and site-specific proteases result in the release of ATF6(N), a transcription factor capable of upregulating a suite of UPR target genes. This includes BiP, protein disulfide isomerase (PDI), and an ER luminal GRP94 [215, 216]. The second branch is mediated by PERK, a tyrosine kinase that, like ATF6, also resides in the ER membrane. PERK dimerizes and is autophosphorylated in response to ER stress, whereby it also phosphorylates eIF2 α , a translation initiation factor [217]. This inactivates eIF2 and broadly limits the translation of most mRNAs, reducing the ER's protein load. Inactivation of eIF2 also leads to

the upregulation of a transcription factor, ATF4, and therefore target genes, such as CHOP and GADD34, responsible for apoptosis and growth arrest [218]. Consequently, the PERK branch can be modulated via eIF2 α phosphorylation to control subtle ER stress levels or initiate protective cell death in cases of extreme stress [219]. Finally, IRE1 is the third and most well-studied branch of the UPR, as it is also conserved in yeast and is a kinase capable of autophosphorylation [220]. IRE1 similarly oligomerizes in the ER membrane in response to stress, like PERK. Still, it leads not to downstream phosphorylation but to the site-specific cleavage of an mRNA encoding a transcription factor, XBP1 [221]. Only the spliced version of the mRNA corresponding to XBP1 is translated into an active transcription factor, with the resulting protein upregulating the synthesis of lipids to expand the ER [222]. ER-associated degradation, or ERAD, is also activated to turn over misfolded proteins in the ER (see below).

1.4.4 Endoplasmic Reticulum Associated Degradation

Since one-third of all proteins are translated and translocated into the ER, a large portion of cellular protein folding occurs in this compartment. Similar to the situation in the cytosol, systems are in place to prevent misfolded protein aggregation. In this case, the transport of misfolded proteins to other locations in the cell or the extracellular space. One such system is known as ERAD [223]. ERAD consists of four main steps: substrate recognition, ubiquitin ligation, protein retrotranslocation, and degradation [224]. ER luminal, membrane, or cytosolic chaperones are responsible for recognizing a misfolded protein, which is then marked for degradation by ubiquitination machinery. As outlined above in section 1.4.1, E1 enzymes activate ubiquitin, which is conjugated and brought to the protein substrate by E2 enzymes, which then work with E3s to ligate ubiquitin to the substrate. Once polyubiquitinated, the substrate protein is

mechanically extracted from the ER and into the cytosol by the AAA+ ATPase, p97, in a process dubbed retrotranslocation [225]. Finally, ubiquitinated proteins that have accessed the cytosol are delivered to the 26S proteasome, where the resulting amino acids and ubiquitin molecules are recycled for future use [226]. Below, each of the steps in the ERAD is better defined, and how they are tailored to maintain proteostasis is highlighted.

1.4.4.1 Substrate Recognition

ERAD was first established as a clearance mechanism for misfolded proteins; however, it can also target properly folded proteins—especially ER-associated enzymes—whose abundance must be tightly regulated [227]. To recognize misfolded proteins, the ER relies on resident chaperones sensitive to exposed hydrophobic stretches of amino acids. One particular Hsp70, BiP, is intimately linked to ERAD substrate selection [54]. In a repeated process of substrate binding and release via ATP binding/hydrolysis (see section 1.3.3.1), BiP works with Hsp40 binding partners and NEFs to guide substrates to an adequately folded state. BiP can also direct nascent proteins to fold/refolding chaperones, such as protein disulfide isomerases (PDIs), which catalyze the oxidation and formation/rearrangement of disulfide bonds between cysteine residues to stabilize the folded state [24, 228]. While this folding pathway applies to polypeptides in general, glycoproteins follow a distinct pathway that features a cycle of addition and then trimming of N-linked glycans, which are added to most proteins as they enter the ER. The glycan cycle serves as the signal and timer for export to the Golgi, or if the polypeptide is folding-compromised, to the ERAD pathway [229]. In brief, two out of three of the glucose on newly synthesized glycoproteins are trimmed by glucosidase I and II to prepare them for binding to one of two calcium-binding lectin-like chaperones in the ER, calreticulin or calnexin [230]. Cleavage of the last glucose moiety frees the substrate from calreticulin or calnexin, which represents the completion of the first round

of protein folding. If the protein is not folded correctly at this checkpoint, the glucosyltransferase UGGT adds back a single glucose to allow for re-binding to the lectins and restart the cycle [231]. In addition, function-specific chaperones, like ERp57, are protein disulfide isomerases [232], while another, like cyclophilin B, is a peptidyl-prolyl *cis-trans* isomerase which further promotes protein folding [233]. However, suppose unfolded proteins are retained too long in the ER via the glucose trimming/re-addition cycle noted above. In that case, the substrates become marked via the eventual removal of terminal mannose residues on the N-glycan chain via EDEM1 or EDEM3, which decreases the affinity of the glycoprotein for UGGT-dependent recycling [234]. It is currently thought that the lectins OS-9 and XTP3-B, which exhibit partially redundant functions, recognize these trimmed oligosaccharides and bridge the calnexin/calreticulin cycle and ERAD [235]. Both BiP and the Hsp90 homolog that resides in the ER in higher cells, Grp94, can bind OS-9 and shuttle misfolded proteins to the ubiquitination and retrotranslocation machinery [235].

1.4.4.2 Ubiquitination

Mammalian ERAD incorporates potentially one or several of the ~20 ER-associated E3 ligases based on the topologies of the different misfolded protein substrates, specific recognition motifs, and other currently unknown factors [236]. However, two RING domain ubiquitin ligases, HRD1 (in cooperation with another E3, gp78) and MARCH6, appear to be the significant enzymes used and are conserved in yeast. Both HRD1 and MARCH 6 are polytopic membrane proteins containing cytosol-facing RING domains. The main distinction between the two E3 ligases is that HRD1 is primarily responsible for the processing of luminal ERAD substrates (i.e., ERAD-L substrates) as well as ERAD substrates with misfolded lesions in the membrane (i.e., ERAD-M substrates) [237]. At the same time, MARCH6 primarily handles ERAD substrates with large cytosolic domains (i.e., ERAD-C substrates) [238]. HRD1 is also hypothesized to function as the

tunnel for the retrotranslocation of ERAD substrates out of the ER (see below) [239]. Furthermore, HRD1 is thought to collaborate with other ubiquitin ligases to encompass and screen/modify a more extensive variety of misfolded ER-resident substrates [240]. Interestingly, cycles of autoubiquitination and deubiquitination at several lysines in its RING finger domain have also been shown to regulate the retrotranslocation activity of HRD1 [241].

1.4.4.3 Retrotranslocation

For misfolded soluble proteins in the ER to access the proteasome machinery in the cytosol, they must be able to leave or retrotranslocate, through the ER membrane. While it is still not entirely clear how all ERAD substrates retrotranslocate across the membrane, it is becoming more apparent that the yeast homologs of an HRD1 ubiquitin ligase complex can function as a “retrotranslocon” for luminal substrates, as noted above [239]. According to models created from cryo-EM analysis and molecular dynamics simulations of the retrotranslocon, the most likely model involves yeast Hrd1 and a co-factor Der1, as forming a complex through which substrates access the cytosol via a putative aqueous interface that is created at the juncture of Hrd1 and Der1 [242, 243]. Der1, and the homologs in higher cells, are members of the rhomboid protease superfamily, which are traditionally viewed as being responsible for the cleavage of membrane proteins (see section 2.3); however they are proteolytically inactive [244].

The knockout of Der1 in yeast leads to an accumulation of ubiquitinated proteins [245]. In yeast, another protein, known as Dfm1, also appears to act as a retrotranslocon for some ERAD substrates [246]. The Hrd1 complex also appears to contribute to retrotranslocation through thinning the membrane surrounding the complex; this might favor the retrotranslocation of ERAD-M substrates, whose continued ER residence might be energetically unfavorable [247]. For ERAD-L substrates, the polypeptide is hypothesized to enter into a groove in Hrd1, which interfaces with

the hydrophilic cavity formed with Der1, permitting the passage of the misfolded polypeptide into the cytosol [243]. Much like ion channels, it is possible that specific amino acids are positioned within the cavity to engage the substrate protein as it moves through the membrane, but the current resolution of the structure and the lack of a structure of an ERAD substrate within the retrotranslocon preclude the identification of these residues. Because of the large spectrum of E3 ligases in mammalian cells which lack channel-like activities, it is also possible that a more universal retrotranslocon exists, such as DERL1 in higher cells. Moreover, DERL1 exhibits the potential for oligomerization into a pore for retrotranslocation.

While these potential retrotransposons may provide a route for ER exit, what must also be explained is the motive force for polypeptide transit from the ER. To this end, the ERAD machinery requires the cooperation of a AAA+ ATPase, p97 (or Cdc48 in yeast) in the cytosol, as noted in section 1.4.2. Much like other members of the AAA+ ATPase family, p97 consists of six subunits arranged in a helical structure through which protein substrates are mechanically translocated [248]. As discussed prior with Hsp104, p97 is thought to produce the mechanical force needed to move proteins through its central pore via “stepping” of subunits onto one another concomitant with ATP hydrolysis of each of the subunits sequentially. In this manner, a retrotranslocating polypeptide not only can overcome the energetic barrier that otherwise prevents them from moving across the ER membrane, but the substrate’s partially folded state is also disrupted as it transits through p97, which facilitates subsequent degradation by the proteasome [249].

Because p97 is a cytosolic protein, it must be recruited to the ER at or near the site of retrotranslocation, i.e., the HRD1 complex. To this end, the yeast Hrd1 has been shown to complex with co-factors that contain ubiquitin regulatory x (Ubx) domains, which are known to associate

with p97/Cdc48 and can regulate both its residence and temporal activity in the cell [250]. Some members of the Ubx protein family also have a ubiquitin-like domain (Uba), which allows for interaction with ERAD-targeted ubiquitinated substrates [251]. This dual motif creates a bridge between ubiquitinated substrates and the p97/Cdc48 “engine” at the site of retrotranslocation [252]. Because of its ability to bind protein substrates, p97/Cdc48 has also been hypothesized to maintain the solubility of retrotranslocated polypeptides in the cytosol before they can access the proteasome for degradation. Indeed, it is hypothesized that yeast Cdc48 acts as a “retrochaperone” since yeast lack a cytosolic holdase, such as the Bag6-SGTA-Trc35 complex, which has been shown to maintain the solubility of retrotranslocated substrates in higher cells [253].

1.4.4.4 Degradation

ERAD concludes with the arrival of the misfolded protein substrate at the proteasome, which selectively and efficiently break down proteins into amino acid, and short peptides that can be further hydrolyzed and then recycled back into nascent polypeptides or used as an energy source. Because the activity of the proteasome is potentially high, its activity must be tightly regulated so that it does not wreak havoc on the cell’s many protein-based operations. To accomplish this, ubiquitin receptors, namely Rpn1, Rpn10, and Rpn13, are placed near the entrance to the proteasome aperture through which substrates first engage the catalytic core of the proteasome and are then further threaded [196]. In fact, these receptors are about the length of a tetraubiquitin motif away from the aperture (a tetraubiquitin chain is required for efficient degradation), and they bind more avidly to K48 linked chains over other types, which again biases their recognition toward ERAD and cytosolic substrates [254]. In order to recycle ubiquitin and allow for chain editing, it also follows that the proteasome is equipped with deubiquitinating enzymes (DUBs). To recycle ubiquitin and allow easier substrate access through the aperture,

Rpn11 is the predominant DUB associated with the proteasome and is thus essential for proteasome function [255]. Rpn11 sits at the opening of the AAA+ motor and resides in close proximity to Rpn10 (one of the ubiquitin receptors) so it can deubiquitinate substrates after they dock with the proteasome but before they make their way to the internal sites at which degradation occurs.

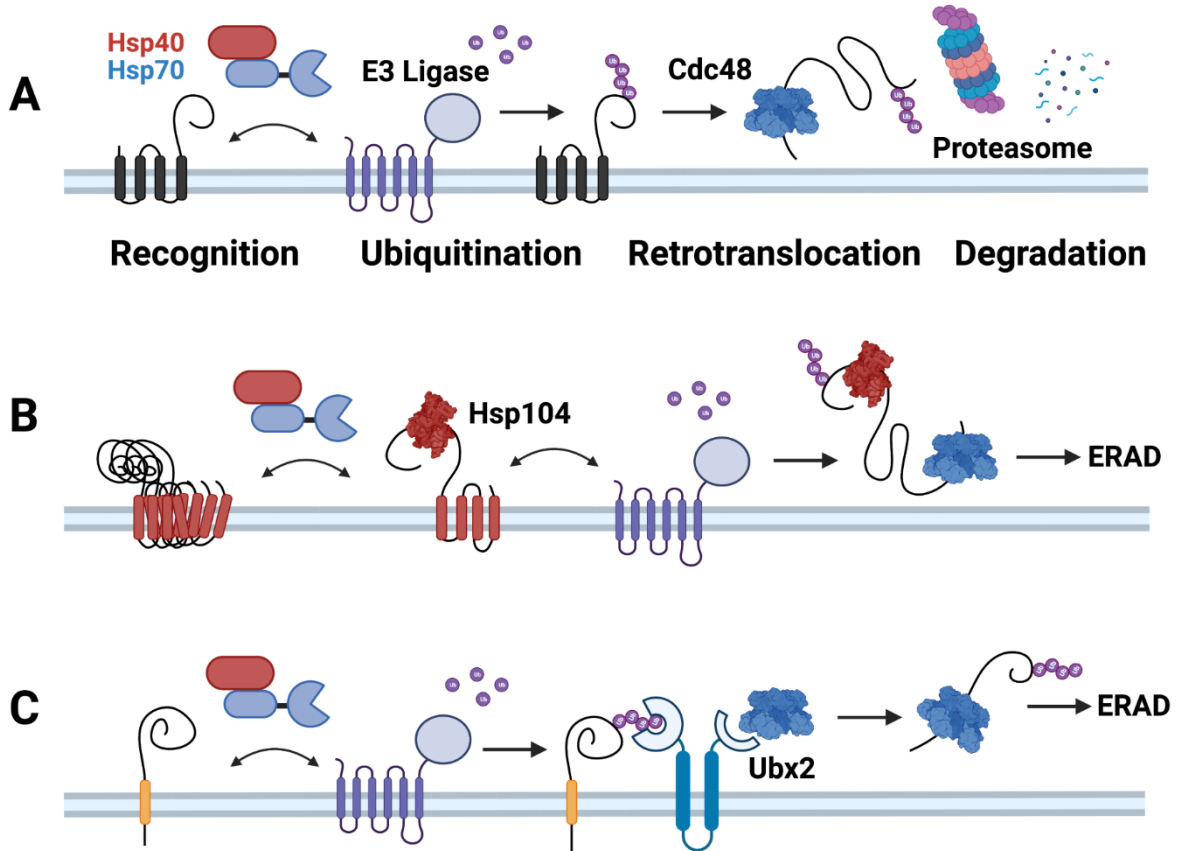


Figure 1 Summary of ERAD with respect to several types of substrate proteins. The ERAD of a misfolded protein substrate is shown with four steps highlighted. (A) Depicted is a substrate with a cytosolic facing legion, however luminal and intramembrane legions are detected and processed by ERAD as well. (B). Aggregation-prone proteins in bacteria and yeast are disaggregated by the AAA+ ATPase ClpB and Hsp104, respectively, before retrotranslocation and degradation by the proteasome. (C). Ubx domain proteins recruit p97 into proximity of substrates, such as the single-pass protein depicted here, in order to facilitate their retrotranslocation.

1.4.5 Decision between ER retention and ERAD vs. ER exit

ERAD is by no means the only way that the burden of misfolded or accumulated proteins within the ER can be resolved. There are myriad situations in which the cell employs other quality

control pathways. For example, post-ER quality control processes, like ER-phagy [256] or Golgi Quality Control (GQC) [257, 258], capture protein substrates in the ER that overwhelm the ERAD machinery and/or aggregate, which can trigger the unfolded protein response (UPR). Some misfolded proteins in the ER simply escape the ER, and in select cases the GQC machinery along with ER retrieval factors return them to the ER for ERAD [259, 260]. While strong degradation signals, or degrons, may predispose misfolded substrates for this form of proteasome-dependent GQC, proteins with more subtle lesions in the luminal or transmembrane domains, as well as those with strong ER exit sequences can be targeted to lysosome/vacuole-dependent GQC [257]. In some cases, it is the misfolded substrates with luminal lesions that may advance to the Golgi before returning to the ER for degradation, whereas substrates with cytosolic lesions are often retained, never leaving the ER until they are degraded [261].

In contrast to ERAD, GQC utilizes a different suite of E3 ligases and chaperones but ultimately shares broad similarities with ERAD: misfolded protein targets are ubiquitinated and shuttled to an end point for degradation. In the Golgi, Tull1 and Rsp5 are among the most prominent E3 ubiquitin ligases which tag substrates for vacuole-dependent degradation in yeast [262, 263]. However, for these misfolded proteins in the Golgi that must reach the vacuole/lysosome, they require transport via the multivesicular body (MVB) pathway [264]. By way of the ESCRT complex, substrates are packaged into endosomal vesicles that then merge with the vacuole/lysosome to deliver their protein cargo via this MVB pathway [265]. In Table 3, I have summarized a select group of ERAD substrates based upon their trends in degradation, solubility and ER retention.

Table 3 Degradation fates of chimeric ERAD substrates in yeast.

‡ lysosome dependent degradation seen in transient expression system at 37°C

Substrate	Degradation	Solubility	ER Exit	Cleavage Fragments	Refs
CPY*	ERAD-L	Only aggregates without functional Kar2, otherwise quickly degraded	Retained	None	[266, 267]
ChiA*	ERAD-C	Only select C-terminal truncations are insoluble	Retained	None	[268, 269]
KWW	ERAD-L	Not aggregation prone	Some is retained, while some returns to the ER from the Golgi	None	[261]
KSS	ERAD-C		Retained		
KWS	ERAD-C		Retained		
SZ*	ERAD-C, Vacuole	Insoluble at elevated temperature	Retained under conditions of overexpression or aggregation	None	[270, 271]
GD*	ERAD-C	Insoluble at elevated temperature	Retained‡	Yes, C-terminal	[269], this study

Another type of post-ER quality control is typified by ER-phagy, a subset of autophagy that selectively degrades excess or damaged ER all at once through fusion with an autophagosome [272]. The receptors responsible for signaling such an event include the membrane proteins FAM134B, SEC62, and RTN3 amongst others. When ER stress surpasses the capacity for ERAD or the unfolded protein response, FAM134B activates ER-phagy through both remodeling of the ER membrane by virtue of its reticulon-like domain, as well as recruitment of autophagic vesicles via LC3 interaction domains facing the cytosol [273, 274]. While FAM134B signals ER-phagy concomitant with a stress response, SEC62, a member of the translocation complex, has a similar LC3 interaction domain that activates after termination of ER stress as a sort of “clean-up” signal

for excess ER [275]. RTN3 functions much like FAM134B in ER fragmentation and autophagosome recruitment, but resides exclusively in ER tubules, whereas FAM134B is found in ER sheets [276].

One example of a protein substrate that requires both general autophagy and ER-phagy for clearance is a mutant form of α 1-anti-trypsin, AT-Z. Experiments in mouse and other mammalian cell models have shown a deficiency in clearance of AT-Z in autophagy gene knockouts as well as a concentration of AT-Z in autophagosomes [277-279]. Termed ERLAD (ER to Lysosome associated degradation pathway), the process for AT-Z degradation involves calnexin activating FAM134B to remodel the ER and prepare for disposal. At this point, ER is not captured within autophagosomes but instead endolysosomes, which are delivered to lysosomes for degradation [280]. While there are a multitude of examples describing substrates that are degraded by ERAD, ER-phagy, and quality control mechanisms throughout the cytosol and Golgi, more work must be done to define the rules that govern which pathway is utilized for any given condition.

1.5 Summary of Goals and Discoveries

Proteostasis is a complex process that requires the participation of signaling cascades, protein chaperones, and quality control machinery to protect the cell from toxic stress. In this Introduction, I have outlined how the UPR, ERAD, and general protein chaperones work together to maintain proteostasis through the maintenance of misfolded proteins. While a great deal is known about how these pathways function independently as well as communicate between each other, much work remains to understand how decisions are made based upon the wide variety of protein substrates encountered in the cell. In the following chapter, I provide evidence of an

aggregation-prone ERAD substrate with a unique proteolytic fate. Specifically, I show that generation of proteolytic fragments in substrate degradation can be used as evidence for the involvement of retrotranslocation machinery and proteases working prior to end point degradation by the proteasome.

My findings here also present a pipeline for the characterization and cataloguing of degradation-prone and/or aggregation prone substrates in mammalian cell systems. Using this standardized approach to substrate construction and investigation, hopefully we as scientists may better understand the complex role that chaperones and proteases play in not only the degradation of misfolded proteins, but also how they are remodeled in preparation for retrotranslocation.

2.0 Differential handling of an aggregation-prone integral membrane ERAD substrate in yeast and a human cell line

2.1 Introduction

Protein homeostasis, or proteostasis, is defined as the maintenance of the cellular proteome and plays a critical role in cellular and organismal health [281, 282]. Although errors during transcription, protein translation, and protein folding may result in damaged proteins and compromise proteostasis, inherited or spontaneous/somatic mutations in the genome more prominently result in the production of transiently misfolded or aberrantly processed proteins. Not surprisingly, myriad diseases are linked to these events, and drugs that modulate various nodes in the proteostasis pathway are under development [283, 284]. Because cells must also rapidly and dynamically adjust to environmental changes, the efficacy of inducible stress response pathways that maintain proteostasis under stressful conditions is also critical for cell and organismal health [285-287], and drugs that modulate these pathways are also under development. One class of downstream effectors of stress response pathways is molecular chaperones, which help ensure that proteins achieve their native structures [175, 288].

Proteostasis plays a particularly critical role in the secretory pathway. As a polypeptide destined for the secretory pathway is translated and exits the ribosome, N-terminal (for soluble) or in some cases internal (for membrane proteins) hydrophobic signal sequences ultimately engage the Sec61 translocon and are either delivered into the lumen of the endoplasmic reticulum (ER) or are integrated into the ER membrane [26]. To assist protein folding, specific molecular chaperones, such as the luminal heat shock protein-70 (Hsp70) homolog, BiP, associate with and retain nascent

polypeptides in a folding-competent state [21, 23, 54]. By virtue of its ability to bind and hydrolyze ATP, BiP traps these species, but it also requires the assistance of Hsp40 homologs to identify nascent misfolded proteins, activate ATP hydrolysis, and anchor BiP to the ER membrane [228]. The release of polypeptides from Hsp70-Hsp40 cycles then requires the participation of nucleotide exchange factors (NEFs), such as GRP170 in the ER, which also bind substrates that display hydrophobic runs of amino acids and—by virtue of their nucleotide exchange activity—restore Hsp70 to the ATP-bound state [289-291]. Concomitant with this cycle, polypeptides in the ER are post-translationally modified, which facilitates protein folding and oligomeric protein assembly [292, 293].

If protein folding is delayed and misfolded proteins accumulate, an ER stress response—the unfolded protein response (UPR)—is induced, which as noted above helps maintain proteostasis [285-287]. More specifically, UPR targets induce the expression of molecular chaperones, slow translation, and increase ER volume, which may rectify the potentially toxic effects of misfolded proteins; yet another protein quality control pathway is also induced: ER associated degradation (ERAD) [224, 294-296]. During ERAD, misfolded proteins are selected, removed (or “retrotranslocated”) from the ER, ubiquitinated, and delivered to the cytosolic proteasome for degradation. While the majority of ERAD substrates represent misfolded or aberrantly processed proteins, the ERAD pathway is also co-opted to manage levels of active ER-resident proteins [227]. How the ERAD pathway recognizes and handles its substrates compared to the vast number of nascent proteins that pass through the ER is poorly defined.

To date, our understanding of the ERAD pathway has employed both endogenous (and often disease-causing) substrates that harbor mutations, as well as artificial substrates. In one

example, ERAD substrates may consist of a naturally occurring transmembrane domain (TMD) fused to a “degron”, a peptide sequence that signals degradation [297]. Degrons used experimentally are either embedded within cellular proteins or have been obtained in yeast screens (see e.g., [298-300]), and degrons derived from native, disease-associated substrates can even be aggregation-prone [269]. In this case, the ERAD pathway must somehow disaggregate the polypeptide, as the presence of aggregates might impede retrotranslocation and/or proteasome access. In a yeast model, we previously showed that integral membrane substrates with an aggregation-prone cytosolic domain require the Hsp104 molecular chaperone [269, 301], a AAA-ATPase that disaggregates and threads proteins through its central cavity [302]. The yeast homolog of p97 (Cdc48), which is also a AAA-ATPase, might additionally contribute to this process, particularly since p97 can retrotranslocate and hold some ERAD substrates in solution prior to proteasome degradation [253, 303]. Alternatively, the cytosolic Hsp70-Hsp40-NEF disaggregase complex might facilitate the ERAD of aggregation-prone substrates, particularly since the complex resolves pre-formed cytosolic aggregates in higher eukaryotic cells [35]. This process can generate species competent for refolding or degradation, or in principle folding intermediates that seed aggregate formation [304, 305]. To date, the resolution of ER-associated aggregates prior to delivery to the ERAD pathway is largely uncharacterized in mammalian cells.

Another impediment to protein retrotranslocation from the ER, at least for membrane proteins, is TMD hydrophobicity [249, 268]. Because TMD-containing proteins are energetically lodged in the membrane—and may be combined with aggregation-prone domains—the trimming or clipping of TMDs by ER-resident proteases provides another route to kickstart retrotranslocation and degradation [306]. Through cleavage near transmembrane domains [307], TMD-containing ERAD substrates have been shown to be clipped by the signal peptide peptidase

(SPP) prior to retrotranslocation, perhaps to ease the burden on AAA-ATPases like p97 that drive extraction [308, 309] and/or to facilitate disaggregation [310]. Another protease that plays a similar role is RHBDL4 [311, 312]. RHBDL4 recognizes hydrophilic and positively charged residues that normally flank a transmembrane domain as well as the ubiquitin chains attached to them by E3 ligases. Only select RHBDL4 substrates have been identified, though the regulated cleavage of the OST complex by RHBDL4 was recently reported [313]. It is likely that additional ERAD substrates will ultimately be identified as substrates for RHBDL4, SPP, and other ER resident proteases [314].

In contrast to ERAD, problematic aggregation-prone soluble proteins within the ER can alternatively be delivered for ER-phagy [315-317], and misfolded ER proteins can even escape the ER in COPII vesicles that are then targeted for lysosome/vacuole-dependent degradation [318]. By using a substrate that toggles between ERAD and post-ER quality control via the multivesicular body (MVB) pathway, we showed that the ER retention and ERAD of membrane proteins in yeast correlates with both substrate aggregation [270] and ubiquitination, thanks to the participation of an ER resident ubiquitin binding protein [271]. Nevertheless, the rules that oversee the fate of non-native membrane proteins in the ER are generally mysterious, especially in mammalian cells.

To these ends, we expressed a model substrate, known as TM-Ubc9ts, in HEK293 cells. In yeast, TM-Ubc9ts requires Hsp104 prior to ERAD-targeting. In human cell lines, we now report that TM-Ubc9ts turnover relies on both the proteasome and lysosomal proteases, but at higher temperature proteasome-dependent degradation predominates. Also in contrast to yeast, proteasome inhibition stabilizes two clipped TM-Ubc9ts products, but inhibition of p97 primarily stabilizes only the first product, consistent with a p97-requirement for partial extraction and

proteasome delivery. Even though the ERAD mechanism in yeast and higher cells is generally conserved [224, 294-296]—and analyses of disease-causing proteins in yeast are commonly recapitulated in higher cells [319]—our study highlights distinct mechanisms required for the turnover of a more problematic model ERAD substrate and suggests a pipeline to investigate the mechanisms required for other aggregation-prone substrates in human cells.

2.2 Results

2.2.1 TM-Ubc9ts undergoes ERAD in mammalian cells, as in yeast

To determine how an aggregation-prone ERAD substrate, TM-Ubc9ts, which requires the Hsp104 disaggregase in yeast [269], might be handled in higher cells, we mapped the degradation pathway for this integral membrane protein. The logic underlying our project is that human cells lack Hsp104 [174, 302], so we reasoned that TM-Ubc9ts might require distinct disaggregases, might be routed to a different degradation pathway (e.g., ER-phagy), or might even be stable and toxic. TM-Ubc9ts was constructed by appending the first two TMDs of Ste6, a yeast mating factor transporter [320], to a temperature-sensitive mutant form of Ubc9 [208], a SUMO conjugating enzyme (**Fig. 2**). When expressed in the yeast cytosol, the Ubc9ts moiety (lacking the TMD) was sequestered into puncta dubbed “Q-bodies” after heat shock [207]. We then showed that when Ubc9ts was tethered to the ER membrane, the protein formed ER puncta, particularly after heat shock, and required Hsp104 activity for maximal proteasome-dependent degradation [269].

To elucidate the TM-Ubc9ts degradation pathway in higher cells, we first transiently transfected HEK293 cells with an expression plasmid encoding TM-Ubc9ts and conducted cycloheximide chase assays to measure protein stability. We also performed detergent solubility assays to determine aggregation propensity. Each assay was conducted at 37°C or after a shift to 42°C for 1 hr to investigate whether elevated temperature influences stability and/or detergent solubility, as observed in yeast. These conditions reflect an accepted method to induce temperature sensitive protein aggregation [321].

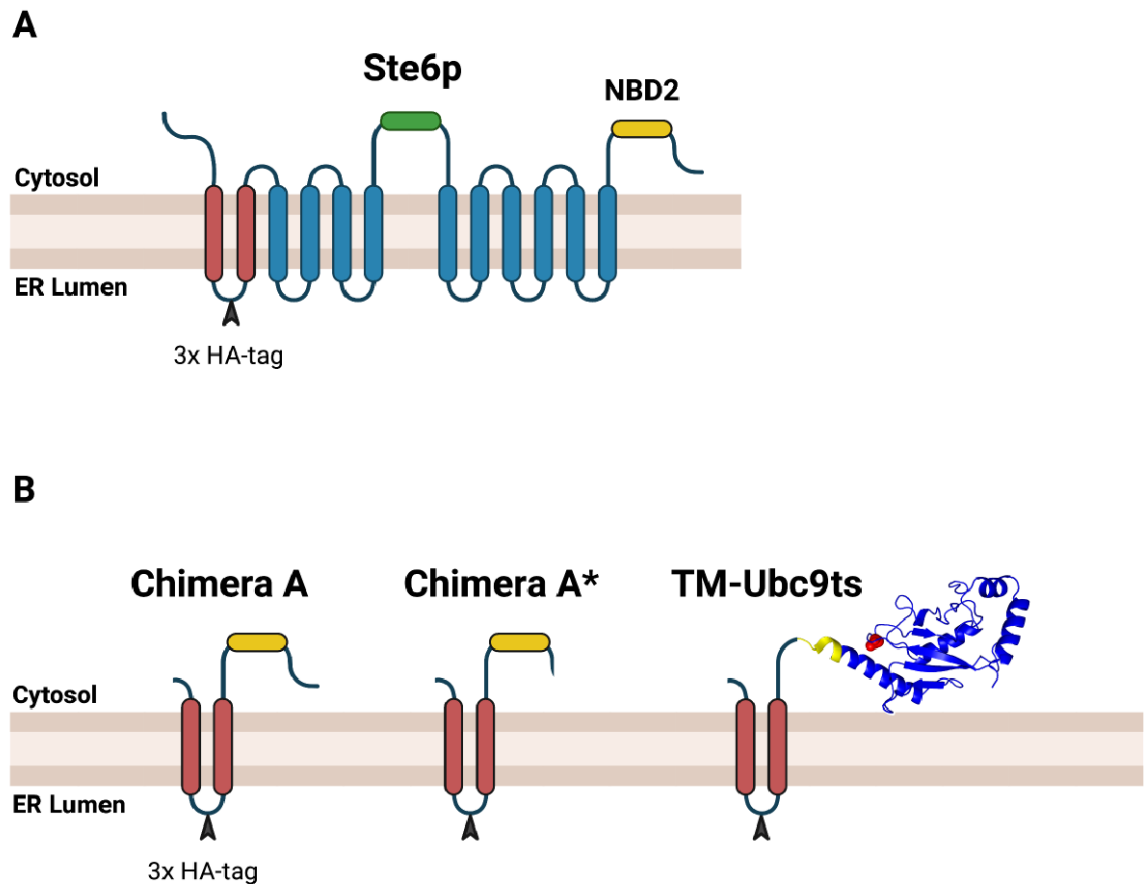


Figure 2 TM-Ubc9ts is a model aggregation-prone ERAD substrate.(A) A cartoon showing the membrane-spanning domains and the first and second nucleotide binding domain (in green and yellow, respectively) of Ste6p, a mating factor transporter in yeast. (B) A cartoon of the previously studied Chimera A and Chimera A* proteins,

which contain a modified version of the first two membrane-spanning domains of Ste6, as well as TM-Ubc9ts, which also contains the first two transmembrane regions of Ste6p but is followed by a temperature sensitive mutant form (Y68L) of the cytosolic yeast SUMO-conjugating enzyme Ubc9. The location of Y68L in Ubc9 is depicted in red and the 3x HA tag is marked with the black arrowhead.

Initially, we confirmed that TM-Ubc9ts-expressing cells exhibited robust growth, suggesting the substrate was not toxic. In fact, the substrate was efficiently degraded (**Fig. 3**), and in line with trends previously observed in yeast, TM-Ubc9ts was stabilized by the addition of MG132, a proteasome inhibitor [322], even though at later times the substrate was fully degraded, at least at 37°C (**Fig. 3A**). However, proteasome-dependent degradation was significantly stronger when cells were shifted to 42°C (**Fig. 3B**). Moreover, at both temperatures, we observed the appearance of proteolytic fragments generated from the full-length protein (“Band 1”). This was especially apparent in the presence of MG132 (note the appearance of the “Band 2” and “Band 3” fragments), suggesting that other proteases contribute to degradation—as outlined in the Introduction—and that the proteasome might then be responsible for their degradation. Because TM-Ubc9ts clipping was absent in yeast [269], these results indicate a distinct difference between how this substrate is recognized for ERAD in yeast versus human cell lines.

To determine if lysosome activity was required for TM-Ubc9ts turnover, especially since MG132 stabilization was incomplete at 37°C, we conducted chases in the presence of chloroquine (**Fig. 3C,D**). Yet, at both temperatures, little substrate stabilization was apparent compared to the vehicle control. Therefore, the lack of more robust stabilization with MG132 at 37°C likely reflects the impact of an alternate protease. Nevertheless, these data indicate, as shown before in yeast

[269], that the protein is primarily targeted for ERAD, but in cell culture partial proteolysis aids substrate turnover.

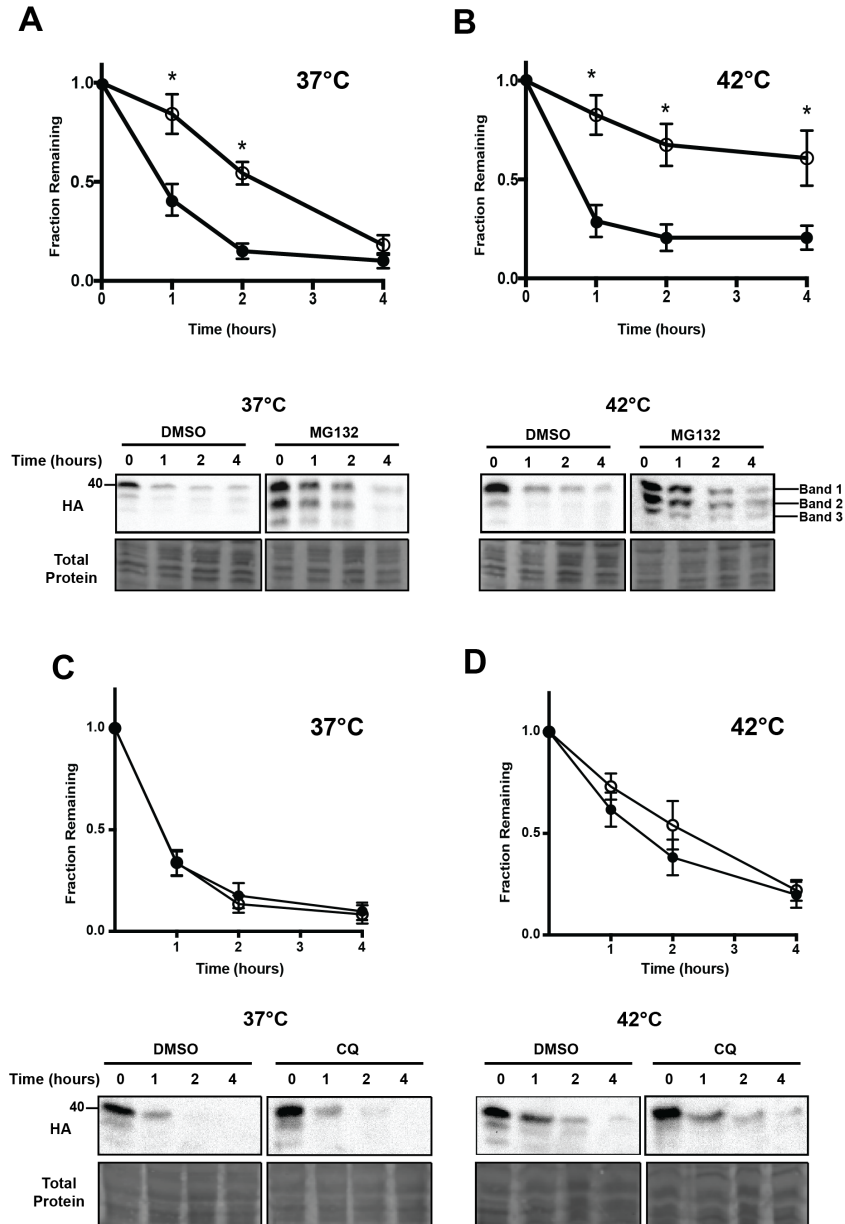


Figure 3 The ERAD of TM-Ubc9ts is magnified at elevated temperatures.

The stability of TM-Ubc9ts was determined by cycloheximide chase analyses at 37°C and 42°C over 4 hrs. (A,B) Cells were treated with either DMSO (closed circle) or 100 μ M MG132 (open circle) for the duration of the chase. (C,D) Cells were treated with either DMSO (closed circle) or 50 μ M chloroquine (open circle) for 2 hrs prior to the

chase and then throughout the chase. Western blots were visualized with anti-HA antibody. In all panels, n = 3 independent experiments +/- SEM; *P < 0.05. Gels are cropped from the full image.

2.2.2 TM-Ubc9ts is both more insoluble and clipped at higher temperatures

Our prior work linked ERAD propensity to the acquisition of detergent-insolubility for select membrane proteins [269, 301]. Therefore, we hypothesized that TM-Ubc9ts would become partially insoluble at 42°C, coincident with more efficient ERAD targeting and with previous observations that cytosolic Ubc9ts aggregates after a heat shock [207, 208]. Consequently, we measured TM-Ubc9ts solubility in HEK293 cells transiently transfected with the TM-Ubc9ts expression plasmid in the presence or absence of the proteasome inhibitor. For this analysis, NP-40 was used to liberate and solubilize membrane-bound proteins, based on prior work [323]. The resulting pellet was then treated with an SDS/sodium deoxycholate buffer to isolate and quantify the amount of insoluble substrate. As a control for this assay, we also examined the behavior of the F508del Cystic Fibrosis Transmembrane Conductance Regulator (CFTR), which becomes aggregation-prone at elevated temperatures [324]. As shown in **Fig. 4**, wild-type CFTR was more soluble than F508del CFTR at 42°C.

Next, as anticipated, TM-Ubc9ts solubility decreased in response to higher temperature incubation, especially when the proteasome was inhibited (**Fig. 5A**). More notable was that treatment with MG132 again stabilized the three distinct TM-Ubc9ts fragments, recapitulating results from the cycloheximide chase analyses (see above). Interestingly, the fragments primarily resided in the pellet fraction (**Fig. 5B**) and became more insoluble at 42°C after MG132 treatment, which stabilized Band 2 and Band 3 (**Fig. 5C**). Due to the nature of detection via an HA-tag between TM1 and TM2 facing the ER lumen (**Fig. 2**), bands 1/2/3 are likely to include the 2

transmembrane domains as most degradation products of the C-terminus could not be monitored. It is also noteworthy that fragments generated from select soluble proteins, e.g., α -synuclein [64, 65], myoglobin [66], and the cell cycle protein Cks1 [67], are also more aggregation-prone after cleavage. Our data suggest that a related phenomenon may be relevant during the ERAD of an aggregation-prone protein.

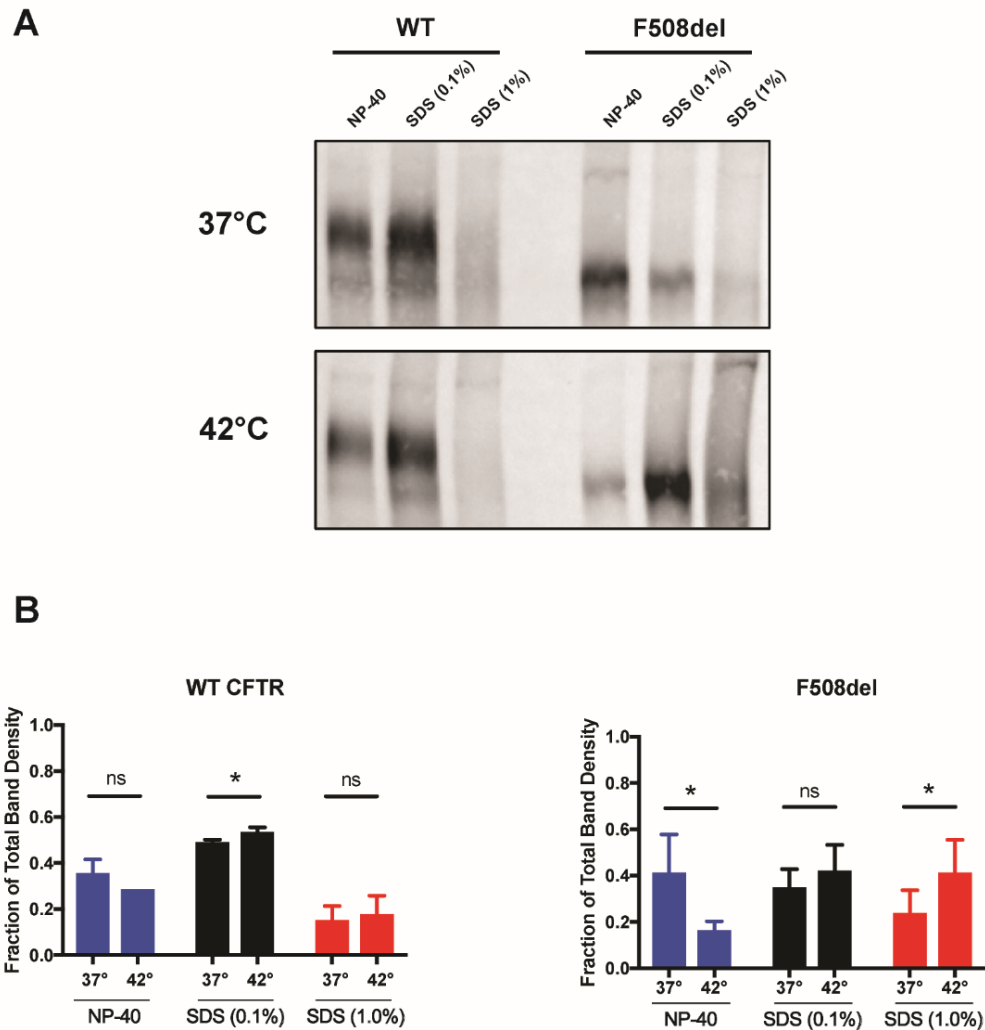


Figure 4. F508del CFTR is less soluble than WT at elevated temperatures

(A) HEK293 cells expressing either wild type or F508del CFTR at 37°C or after a 1 hour shift to 42°C were sequentially lysed and pelleted in the labeled detergents. (B) Quantification of the data in panel A; n=4, * = p<0.05

fraction. Western blots were visualized with anti-HA antibody (B) Solubility of TM-Ubc9ts was measured by comparing protein levels in the pellet fraction between DMSO and MG132 conditions at 42°C. All measurements were normalized to their respective band in the 42°C pellet. (C) Quantification of relative band density compared to full length TM-Ubc9ts at 37°C; all measurements normalized to Band 1 in each respective condition, n = 3 independent experiments +/- SEM; *P < 0.05, relative to the DMSO control. Gels are cropped from the full image.

2.2.3 TM-Ubc9ts degradation is consistent between transient and stable expression systems

Because transient transfection can induce secondary stress responses and lacks the ability to regulate expression, I created stable HEK293 lines that express TM-Ubc9ts under the control of a tetracycline inducible promoter. After selecting for and isolating the inducible stable lines (see Materials and Methods), I performed an expression time course after addition of 1 mg/ml tetracycline. TM-Ubc9ts expression was evident at 4 hrs and remained relatively consistent over 24 hrs (**Figure 6**). I chose a 16 hr time point for all future experiments since it ensured expression was robust, was at a level comparable to that after transient transfection, and permitted subsequent analyses. During this time course, cell growth was unchanged regardless of whether TM-Ubc9ts was expressed (data not shown). When I then performed stability assays (**Fig. 7**), the same overall trends as noted in the transient transfection system were again observed in the presence or absence of MG132, i.e. proteasome-dependent degradation was magnified at 42°C compared to the results at 37°C. However, at 37°C there was now both lysosome- and proteasome-dependent degradation, but at 42°C ERAD again predominated. The distinction between the relative degree of ERAD targeting might reflect the secondary stresses triggered by transient transfection. Regardless, once again, TM-Ubc9ts-generated fragments were stabilized by MG132 treatment (see below). Coupled with data in the transient expression system, these data confirm that the degradation pathway for TM-Ubc9ts increasingly relies on the ERAD pathway at elevated temperatures.

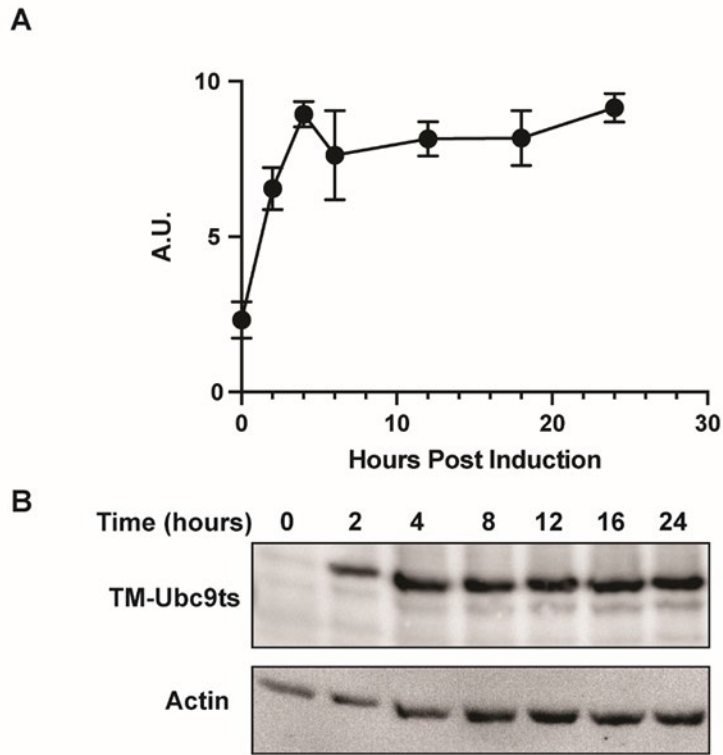


Figure 6. Time dependent induction of TM-Ubc9ts in a tetracycline-inducible expression system

A total of 1 $\mu\text{g/ml}$ tetracycline was added for the designated time prior to cell lysis and western blot. (A) Protein levels were normalized to actin; $n = 3$, \pm SEM. (B) A representative western blot of the time course is shown

The results presented in Fig. 7 are also consistent with data in the transient expression system that TM-Ubc9ts—and particularly the generated fragments—become detergent-insoluble. Therefore, I again performed detergent solubility assays in the stable lines expressing TM-Ubc9ts (Fig. 8). Although protein in the insoluble (pellet) fractions was negligible after the shift to 42°C (Fig. 8A, top, compare relative amounts in the “S” and “P” fractions at 37° and 42°C), the aforementioned TM-Ubc9ts fragments (and to a modest extent, the full-length protein) were not

only stabilized by MG132 but there was less soluble material under these conditions (Fig. 8A, bottom panels, and Fig. 8B).

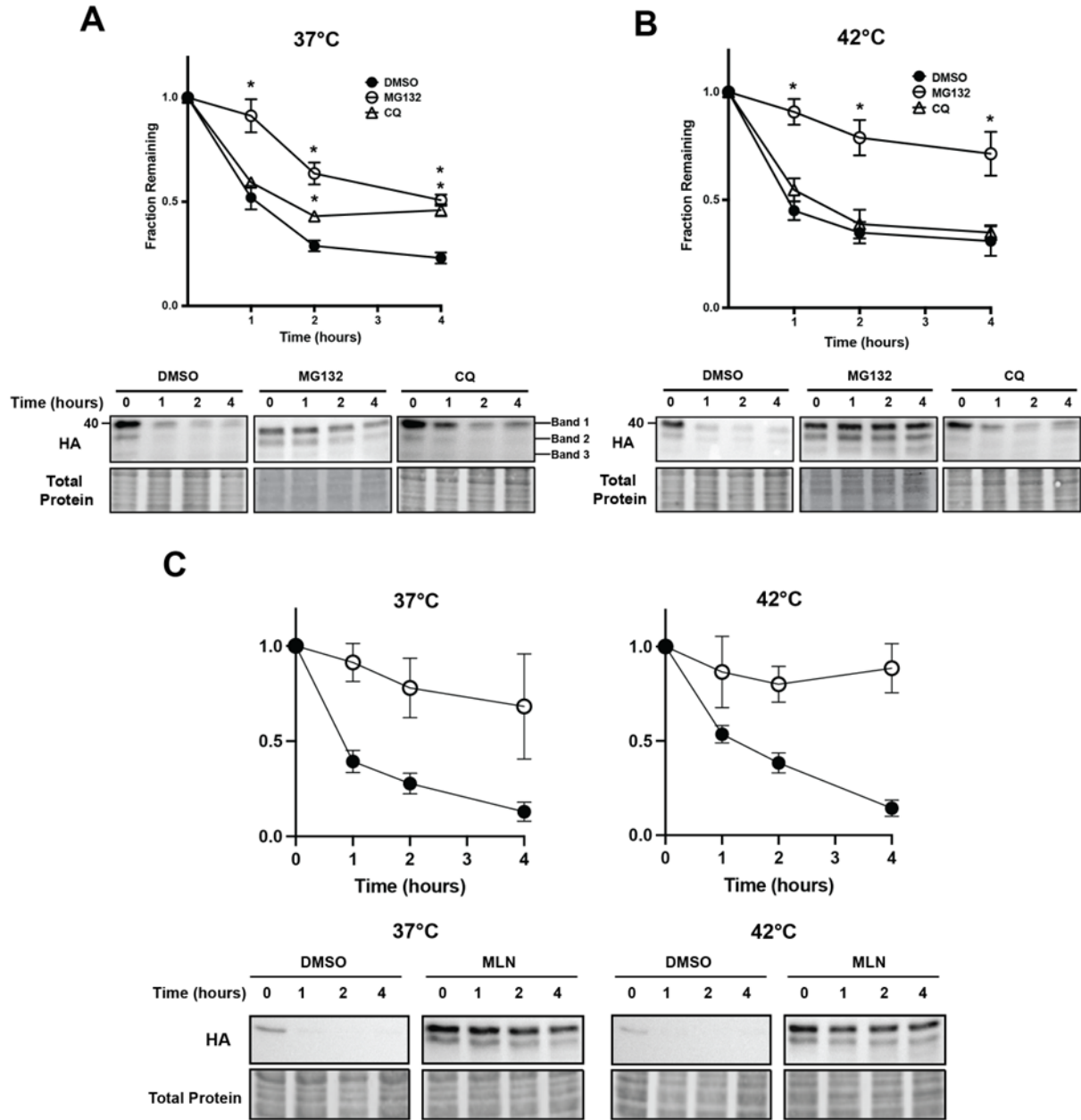


Figure 7 ERAD-dependent processing of TM-Ubc9ts is also temperature dependent in stable cells.

The stability of TM-Ubc9ts was determined by cycloheximide chase analyses at (A) 37°C and (B) 42°C over 4 hrs. Expression was induced with 1ug/ml tetracycline 16 hrs prior to the chase. Cells were treated with either DMSO (closed circle), 100 μ M MG132 (open circle) or 50 μ M chloroquine (open triangle) for 2 hrs prior to chase and then throughout the chase. (C) The degradation requirement for ubiquitination was determined by similar chases as shown in parts (A) and (B) in which cells were treated with either DMSO (closed circle) or 5 μ M of the E1 ubiquitin activating

enzyme inhibitor, MLN7243 (open circle; “MLN”). Western blots were visualized with anti-HA antibody to detect TM-Ubc9ts. In all panels, n = 3 independent biological experiments +/- SEM; *P < 0.05, relative to the DMSO control. Gels are cropped from the full image. TM-Ubc9ts fragments require p97 for retrotranslocation and degradation

p97 is a core component of the ATP-dependent retrotranslocation “engine” [248], and acts on polyubiquitinated and partially trimmed ubiquitinated species at the ER membrane [325, 326]. To examine if p97 also plays a role in TM-Ubc9ts degradation, I conducted another series of cycloheximide chase assays at both 37°C and 42°C in the presence or absence of CB-5083, a p97 inhibitor that entered clinical trials [327, 328]. As shown in **Fig. 9A,B**, TM-Ubc9ts was stabilized by CB-5083, and at least at initial time points, stronger stabilization was evident at 42°C, perhaps consistent with the magnified effect of ERAD (**Fig. 7**). Notably, I could detect the first clipped version of TM-Ubc9ts (“Band 2”), yet unlike the effect that was observed with MG132, Band 3 was present at significantly lower levels (**Fig. 9C**). In contrast to the observed changes in the fragments after proteasome inhibition, p97 inhibition only impacted Band 2 stability with little to no effect on solubility (compare relative Band 2 amounts in “P” fractions, **Fig. 8C,D**). These data support a model in which proteasome-independent clipping at the ER membrane precedes a p97-dependent step that allows for subsequent proteasome processing (see Discussion). Assuming that p97 is required for retrotranslocation, these data are also in-line with results from other investigations on the action of ER proteases [329-331]. In our case, a protease facilitates the conversion of a full-length product into a fragment, Band 2, which is then acted upon by the proteasome.

We next sought to better characterize the two lower molecular weight species (Band 2 and Band 3) that were stabilized after MG132 treatment and migrated at apparent molecular masses of ~36 kDa and ~33 kDa respectively. Consequently, samples from experiments under control

(DMSO) conditions or after treatment with MG132 or CB-5083 were treated with endoglycosidase H (endoH), which removes the N-glycan core from Asn-X-Ser/Thr-containing proteins in the lumen of the ER [332]. In the absence of endoH, vehicle-treated cells express full-length TM-Ubc9ts at a molecular mass of 39 kDa, which by virtue of a single N-linked glycosylation site (**Fig. 2**) is trimmed to a ~36 kDa product by endoH (**Fig. 9C**). The two processed fragments at 36 kDa and 33 kDa, which are stabilized by MG132, appear to be differentially acted upon by the enzyme: based on the strong increase in the magnitude of the species denoted Band 3, I surmise that only Band 3 is unaffected by endoH (since no product ~3 kDa lighter than this is seen), yet Band 1 and Band 2 are each acted upon by this enzyme. This modestly increases the 36 kDa species and strongly increases the levels of Band 3.

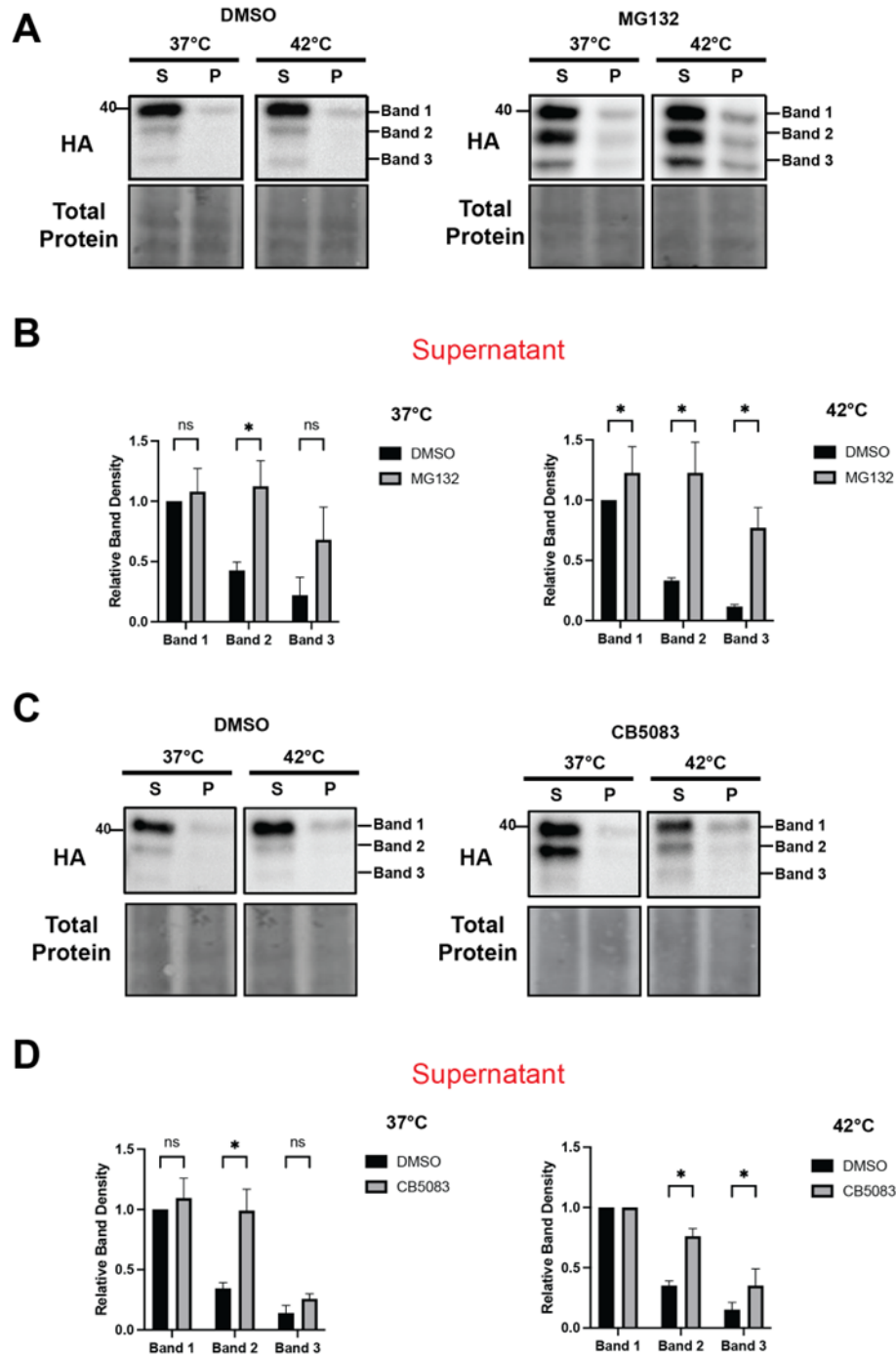


Figure 8. TM-Ubc9ts solubility and clipping in a stable expression system reflect the results after transient transfection

Protein solubility of TM-Ubc9ts was determined in stable HEK293H cells as in Figure 3. (A,C) Levels of protein were analyzed via western blot after centrifugation to isolate a supernatant (S) and pellet (P) fraction. Cells were treated with 100 μ M MG132 (A) or 50 μ M CB-5083 (C) for 3 hours prior to lysis. Western blots were visualized with anti-

HA antibody and chemiluminescence. Quantification of relative band density normalized to Band 1 in each respective condition: n = 3 independent experiments +/- SEM; *P < 0.05 relative to the DMSO control. Gels are cropped from full the image.

To further characterize the fragments, I treated lysates with sodium carbonate and then resolved membrane (i.e., the pellet fraction) versus soluble (i.e., the supernatant fraction) proteins after centrifugation. As depicted in **Fig. 9D**, Band 3, when stabilized by MG132 treatment, was almost entirely soluble, suggesting that it was freed from the ER prior to degradation. In contrast, after treatment with MG132 or CB-5083, Band 2 remained mostly membrane integrated (pellet) but a fraction resided in the supernatant. As a control for fractionation, the behavior of Hsp70, which is largely cytosolic, was also followed and resided primarily in the supernatant fraction. Combined with the data from experiments with endoH (**Fig. 9C**), I hypothesize that Band 2 is retrotranslocated by p97 after being clipped. The presence of a minor population of Band 2 in the supernatant, even after p97 was inhibited (**Fig. 8C, CB-5083, "S"**), suggests that the proteasome retrotranslocates Band 2 [266, 333, 334], albeit inefficiently. When combined with the data on the relative effects of MG132 and CB-5083, I present a model for the TM-Ubc9ts degradation pathway in the Discussion, below.

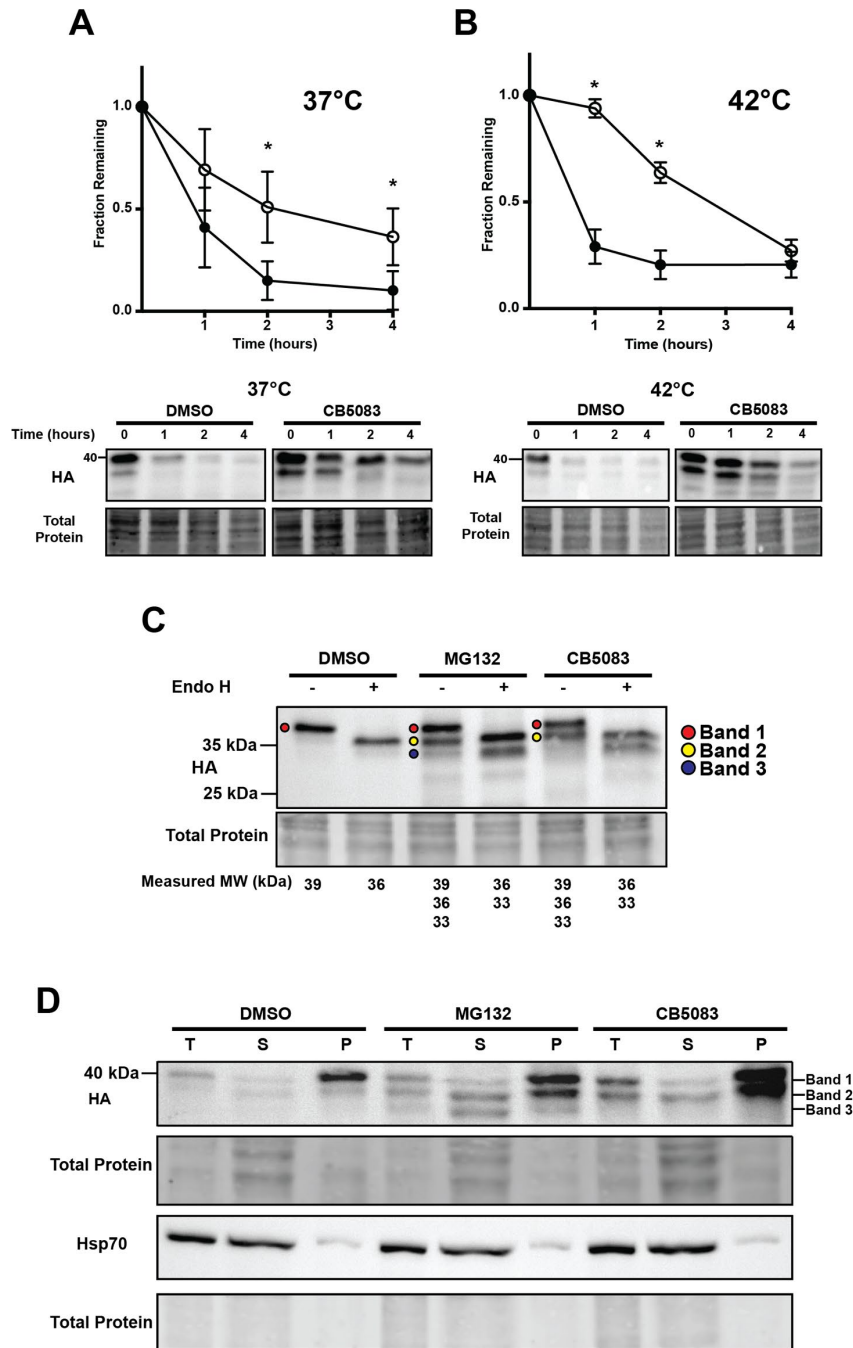


Figure 9 p97 inhibition liberates a proteolytic TM-Ubc9ts product.

The degradation of TM-Ubc9ts expressed in stable HEK293H lines was determined by cycloheximide chase analyses at (A) 37°C and (B) 42°C over 4 hrs. Expression was induced with 1µg/ml tetracycline 16 hrs prior to chase. Cells were treated with either DMSO (closed circle) or 50µM CB-5083 (open circle) for 2 hrs prior to chase. Western blots were visualized with anti-HA antibody to detect TM-Ubc9ts. (C) Endo H digestion of TM-Ubc9ts after treatment with

DMSO, MG132, or CB5083. Molecular weights of the bands are listed below, rounded to two significant figures. Bands are denoted by symbols: Band 1 (red circles), Band 2 (yellow circles), Band 3 (black circles). (D) Carbonate extraction of TM-Ubc9ts after treatment with DMSO, MG132, or CB5083 for 3 hours prior to lysis. Each treatment consists of a 1% total lysate (T), and a sample of the supernatant (S) and pellet (P) fractions. In addition to the analysis of TM-Ubc9ts, cytosolic Hsp70 was examined as a control. In all panels, n = 3 independent biological experiments +/- SEM; *P < 0.05. Gels are cropped from the full image.

2.2.4 Intramembrane protease RHBDL4 does not cleave TM-Ubc9ts.

Because a TM-Ubc9ts-generated species (i.e., Band 2) is acted upon by p97 and the proteasome, we asked if an intramembrane protease, RHBDL4, which can clip select ERAD substrates and acts prior to retrotranslocation [45, 77], contributes to TM-Ubc9ts turnover. Therefore, we utilized a stable HEK293 cell line with tetracycline-inducible expression of an RHBDL4-directed shRNA. Real-time qPCR analysis of tetracycline- versus vehicle-treated cells and western blot analysis indicated that RHBDL4 message was depleted by ~90%, and the protein levels were similarly reduced such that <10% of the protein remained (**Fig. 10A**). When we then introduced TM-Ubc9ts into the treated versus untreated cells, the density of the three bands corresponding to TM-Ubc9ts was unchanged, regardless of whether RHBDL4 was knocked-down and whether MG132 was present (**Fig. 10A**). RHBDL4 knockdown was verified by RT-qPCR, and consistent with the immunoblot data in Fig. 7B, RHBDL4 mRNA was present at <10% in the knockdown condition compared to the scrambled shRNA control (**Fig. 10C**). As a control for this experiment, previous studies established that this level of RHBDL4 reduction was sufficient to stabilize a C-terminal fragment derived from a model ERAD substrate, known as MHC202 [45]. Therefore, we expressed MHC202 in the same system and observed the formation of an MG132-

stabilized cleaved fragment at ~15 kDa (**Fig. 10B**, see arrowhead, lane 2), consistent with previous studies. However, the fragment was absent when RHBDL4 was knocked-down (**Fig. 10B**, see lane 5). The lack of an effect of RHBDL4 on TM-Ubc9ts cleavage, as seen in our hands, is perhaps consistent with the fact that TM-Ubc9ts contains a misfolded domain that faces the cytosol. In contrast, established RHBDL4 substrates, such as pT α , Pkd1 Δ N, Opsin-degron, MPZ-L170R, TCR α are cleaved primarily in juxtamembrane and loop regions [77].

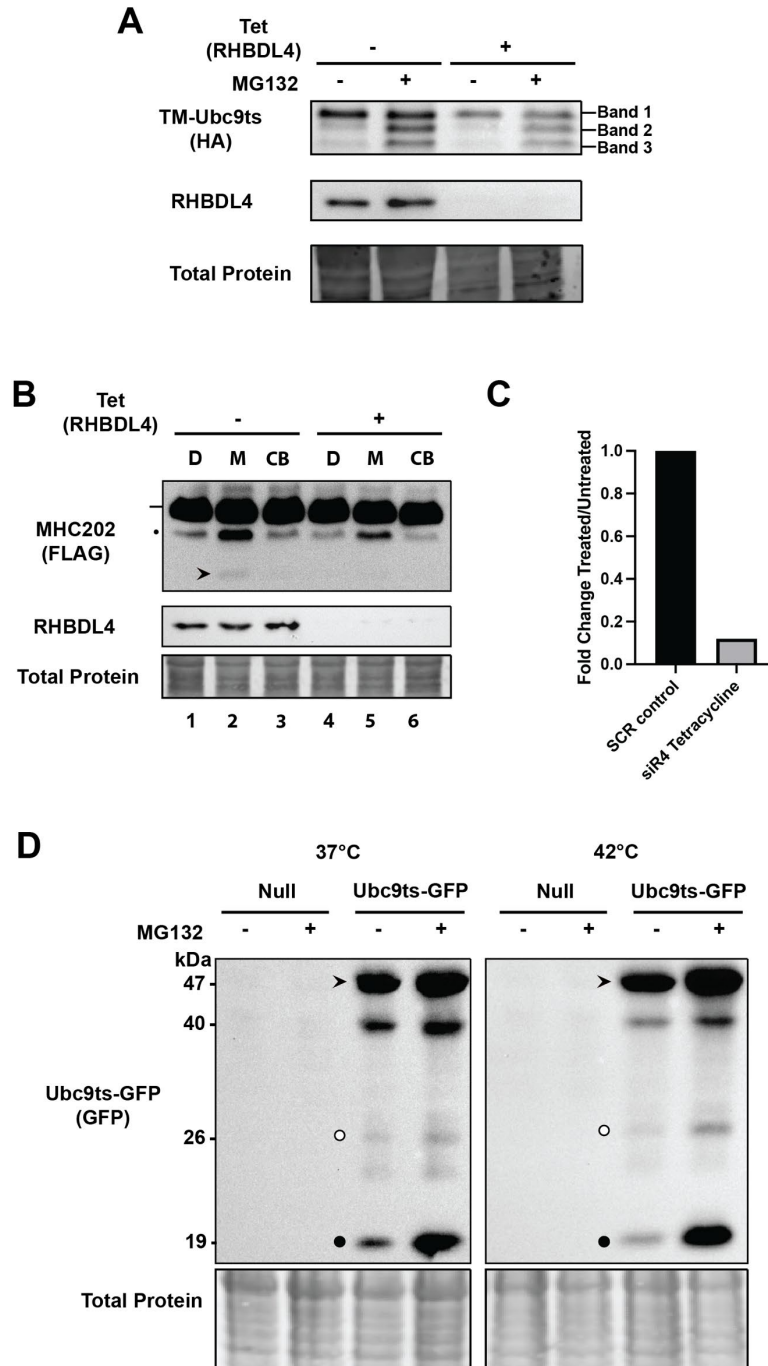


Figure 10. TM-Ubc9ts cleavage is RHBDL4 independent

(A) TM-Ubc9ts was transiently transfected into HEK293 cells 72 hrs after tetracycline induction of an shRNA to deplete RHBDL4. Under both DMSO and MG132 treated conditions, full-length substrate (Band 1) and TM-Ubc9ts fragment (Bands 2 and 3) abundance and ratio were unchanged between control and knockdown conditions. (B) MHC202 was transiently transfected into HEK293 cells 72hrs after tetracycline induction of an shRNA against

RHBDL4: “D”, DMSO; “M”, MG132; “CB”, CB-5083. Full-length MHC202 is indicated by a line, and deglycosylated MHC202 is denoted by a closed circle (•). Note that the cleaved fragment (arrowhead) stabilized by MG132 in lane 2 (-tet) was absent in lane 5 (+tet). (C) HEK293 cells transiently transfected with the cytosolic quality control substrate, Ubc9ts-GFP, were incubated at 37°C or were shifted to 42° and treated with DMSO or MG132 for 1 hr prior to harvesting and cell lysis. Full-length protein (arrowhead), GFP (open circle), and a cleaved fragment (closed circle) are indicated. Note the increase in the amount of the cleaved fragment in the presence of MG132 and at 42°C. Gels are cropped from the full image.

The data presented above, along with the residence of the Ubc9ts misfolded domain, suggest instead that cleavage requires a cytosolic (and not an ER resident) protease. To test this hypothesis, I examined a soluble form of TM-Ubc9ts that lacks the TMD. This cytosol quality control substrate, Ubc9ts-GFP [207], was then introduced into HEK293 cells. I also incubated the cells at the aforementioned temperatures (37°C or 42°C for 1 hr prior to lysis) and in the presence of DMSO or MG132. As shown in **Fig. 10C**, the full-length protein (~47 kDa, arrowhead), GFP (~26 kDa, open circle), as well as several fragments (see, for example, the closed circle at ~19 kDa) were each observed. Interestingly, MG132 treatment strongly suggested that ~26 and 19 kDa fragments are turned over by the proteasome, especially at 42°C, given their increase in intensity. Because both TM-Ubc9ts and Ubc9ts-GFP share the same temperature sensitive Ubc9 domain, these data suggest that a cytosolic protease cleaves both model substrates.

2.3 Discussion

While substantial work from many labs has revealed how misfolded proteins are targeted and processed by ERAD, significant details of how TMD-containing aggregation-prone substrates are degraded are lacking. Our results show that one such substrate, TM-Ubc9ts, is clipped in HEK293 cells after being transiently and inducibly expressed, and that the resulting fragments can aggregate, especially if stabilized by proteasome inhibition and if cells are incubated at higher temperatures. In other words, a human cell line overcomes the lack of the Hsp104 disaggregase by clipping an aggregation-prone protein in the ER membrane. In addition, while the larger generated fragment, Band 2, retains the N-linked glycan, Band 3 lacks this post-translational modification. In contrast, only the glycosylated and truncated species, Band 2, is primarily stabilized when p97 is inhibited. Consistent with the established function of the p97 complex [248, 249], Band 2 is mostly membrane-integrated (**Fig. 9D**). Based on these data, I present a model for the degradation pathway of TM-Ubc9ts in human cells (**Fig. 11**).

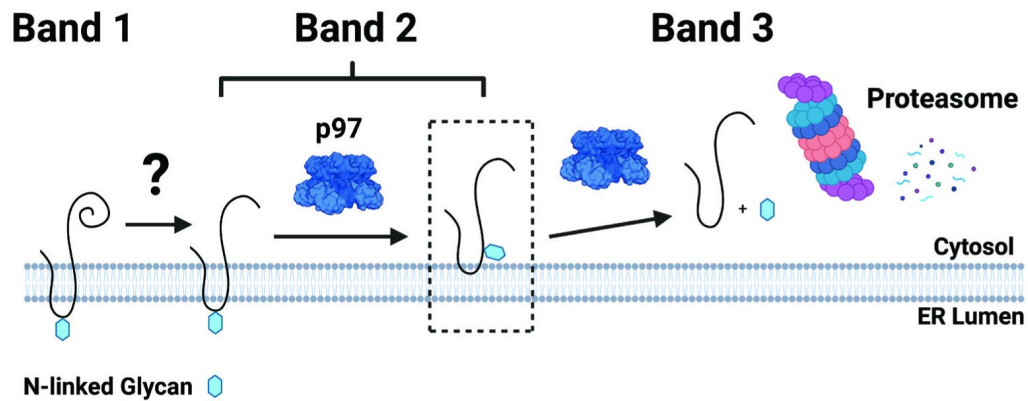


Figure 11 Proposed model for TM-Ubc9ts clipping during ERAD.

TM-Ubc9ts is shown as a solid black line in the ER membrane with its sole N-linked glycan depicted as a hexagon. As TM-Ubc9ts is processed by ERAD, it adopts three states, labeled in this figure as Band 1 (full length), Band 2 (clipped and glycosylated), and Band 3 (clipped and deglycosylated). Full-length TM-Ubc9ts is clipped prior to retrotranslocation by an unidentified protease in the transition from Band 1 to Band 2. Clipped TM-Ubc9ts is then extracted from the ER membrane by p97 in preparation for degradation. It is during this step that two populations of Band 2 can be observed via carbonate extraction, with the majority residing in the ER membrane as well as a small pool in the cytosol en route to the proteasome. Band 3 represents clipped TM-Ubc9ts that has been deglycosylated by glycosidases in the cytosol before ultimately being degraded by the proteasome.

A growing number of ER-associated proteases appear to contribute to the ERAD pathway [331, 335-337]. While a comprehensive analysis of the contributions of each protease, which may even act redundantly, is beyond the scope of the current study, I could rule out the possibility that the intramembrane protease RHBDL4 generates these fragments. Yet, it is noteworthy that other proteases act more specifically on substrates based on the frequency and composition of TMDs or based on the site of lesions or recognition motifs. For example, presenilin, which is part of the gamma-secretase complex, and several members of the rhomboid protease family have been

shown to initiate biological pathways through the clipping of substrates such as amyloid precursor protein (APP), the Notch receptor, and receptor tyrosine kinases [330, 338, 339]. More specifically, gamma secretase cleaves Notch receptors as well as distinct receptor tyrosine kinases, whereas APP is cleaved by both alpha and gamma secretase during non-amyloidogenic processing [154, 340, 341]. While these substrates lack homology, they all possess cleavage sites close to the membrane. After cleavage, functional motifs bound for cellular compartments, such as the nucleus or the extracellular environment, are liberated. In contrast, RHBDL4 primarily acts on ubiquitinated proteins at the ER that must be prepared for retrotranslocation and delivery to the proteasome.

To better dissect the requirements for the ERAD of TM-Ubc9ts in human cells, future experiments will identify partners—and ideally the contributing protease—through the use of activated crosslinking (“proximity labeling”) methods, such as BioID [342, 343]. A translationally encoded tetra-ubiquitin at the N-terminus could also be added to TM-Ubc9ts to compare how the protein interactome changes between the native and constitutively ubiquitinated substrate. Because RHBDL4 has both a substrate and ubiquitin-interacting domain [312], it stands to reason that other intramembrane proteases might only cleave proteins marked for degradation by a polyubiquitin moiety. Regardless, because the cytosolic Ubc9ts-GFP substrate is also cleaved, and the fragments are stabilized when cells are incubated with a proteasome inhibitor, I suggest that a cytosolic protease is responsible for TM-Ubc9ts clipping. Mapping the precise cleavage site after fragment purification by mass spectroscopy—along with the use of programs that predict protease dependence [344]—highlights another route to identify the protease.

One potential limitation of a comparison between the behavior of TM-Ubc9ts in yeast and HEK293 cells is that experiments were performed at 30° and 37° in yeast, but 37° and 42° in HEK293 cells. Thus, formally, substrate clipping in yeast might have only arisen at the higher temperature of 42°C. Nevertheless, an examination of TM-Ubc9ts has uncovered a previously overlooked step in the quality control of an ERAD substrate containing an aggregation-prone domain in the cytosol.

Although I have focused on a single model substrate in this study, it is likely that mutated versions of naturally occurring substrates that exhibit similar features as Ubc9ts meet the same fate. Other aggregation-prone and likely misfolded ER membrane proteins have been reported in the literature. Rhodopsin mutants, some of which are aggregation-prone in model systems (e.g., P23H), were variably targeted for ERAD or an ER-phagy-like pathway when overexpressed [345-347]. P23H rhodopsin aggregation causes retinitis pigmentosa and retinal degeneration, while wild-type rhodopsin is readily degraded by ERAD. During rhodopsin processing, I hypothesize that clipping via an intermembrane protease, such as RHBDL4, could facilitate retrotranslocation and proteasome-dependent degradation. Intriguingly, P23H rhodopsin was clipped after it was expressed in a *Xenopus laevis* model for retinitis pigmentosa [348]. In the future, introducing wild-type versus the P23H mutant rhodopsin into a higher cell system in which RHBDL4 and other putative proteases could be silenced, and then examining detergent solubility and the generation of fragments, might allow one to group TM-Ubc9ts with this substrate.

Another example is provided by a mutant aquaporin, AQP2-T126M, which is CHAPS-resistant in CHO cells and retained in the ER in transfected cells and in mice, but the substrate can

also be targeted for ERAD [349-351]. In turn, I previously showed that the N1303K cystic fibrosis transmembrane conductance regulator (CFTR) mutant is polyubiquitinated ~3x more than wild-type CFTR in a reconstituted system, yet in transfected cells the protein was detergent soluble, appeared to be ERAD-resistant, and was destroyed via an autophagy-like mechanism [352]. Other work reported that N1303K and different CFTR mutants reside in cytoplasmic aggresomes, which can be turned over by autophagy [353]. Considering the plethora of substrates and proteases yet to be characterized, our analysis of TM-Ubc9ts quality control provides the groundwork for significant continued work and contributes to our understanding of how aggregation prone proteins in the ER might be handled in higher cells.

2.4 Materials and Methods

2.4.1 Molecular Methods

The expression of the TM-Ubc9ts substrate was first reported by Preston et al. [269], and contains a temperature sensitive mutant form of the SUMO-conjugating enzyme Ubc9, which results in a temperature sensitive folding defect [208], fused to the sequences encoding the first two transmembrane (TM) domains of the yeast ABC transporter Ste6. A triple HA tag was also inserted between the first and second transmembrane domain, which resides within the ER lumen after the protein inserts in the ER membrane [268] (see **Fig. 4**). The resulting fusion protein was then inserted into pcDNA3.1 at the EcoRI and XhoI sites and amplified using 5- α Competent *E. coli* cells (NEB). The plasmid DNA sequence was confirmed by Plasmidsaurus and the insert was confirmed by primer-directed sequencing (Genewiz).

2.4.2 Human cell culture protocols

HEK293H cells (hereafter referred to as HEK293 cells) were obtained from the Weisz lab at the University of Pittsburgh and authenticated by the University of Arizona Genetics Core. The cells were also determined to lack mycoplasma contamination using the Universal Mycoplasma Detection Kit (ATCC). The cells were grown in a 37°C humidified incubator supplemented with 5% CO₂ in DMEM containing 10% FBS as well as penicillin and streptomycin. All experiments were conducted with cells before passage four. HEK293 cells were transfected at 50% confluency with the indicated plasmids using Lipofectamine 2000 (Thermofisher). Total transfected DNA was constant for each experiment at 2 mg/well of a 6-well plate or 1 mg/well of a 12 well plate. Cells were harvested 24 hrs post transfection unless indicated otherwise. For all experiments, cell pellets were collected by pipetting in the well to resuspend followed by centrifugation of the total media to obtain a cell pellet. The media was then aspirated, and the pellet was retained.

To isolate stable, tetracycline-inducible HEK293 cells expressing TM-Ubc9ts, I used the T-Rex inducible protein expression system (Thermofisher). In brief, HEK293 cells were first transfected with plasmid pcDNA6/TR and then selected in blasticidin as per the manufacturer's specification. Lines selected for stable integration of pcDNA6/TR were next transfected with an inducible expression vector containing the TM-Ubc9ts insert and selected with zeocin. The final selection of single cells that induced substrate expression occurred via dilution after several 2-3 day intervals (2 weeks total) of media changes in the presence of zeocin.

2.4.3 siRNA-mediated knockdown and RT-qPCR

siRNA knockdown using oligonucleotides was conducted according to the manufacturer's protocols (Horizon; but also see below). Inhibition of the proteasome, p97, or lysosomal proteases was performed by the addition of MG132, CB-5083, or chloroquine (2 hrs, 2 hrs, and 4 hrs, respectively). DMSO was used as a vehicle control for all drug treatments, and apart from solubility analyses (see below), cell lysis was conducted in RIPA buffer (50 mM HEPES, pH 7.4, 150 mM NaCl, 0.1% sodium dodecyl sulfate, 0.5% sodium deoxycholate), after cells had been washed with PBS. Prior to analysis, the mixture was centrifuged for 10 min at 12,000 rcf (4°C) to remove insoluble material.

siRNA mediated knockdown of RHBDL4 was instead conducted in HEK293 Flp-In T-REx cells (Invitrogen) with inducible expression of an shRNA against RHBDL4 (a kind gift from the Lemberg Lab [158]). Cells were plated to 20% confluency and then cultured in media containing 1 µg/ml tetracycline for the indicated times, ranging from 3 to 5 days. Prior to collection at these times, cells were transfected with the pcDNA3.1 transient expression vector for TM-Ubc9ts for 16 hrs prior to harvesting.

To quantify the extent of siRHBDL4 knockdown by siRNA transfection or inducible expression of shRNA (see above), total cellular RNA was extracted from HEK293 cells using the RNeasy mini kit (Qiagen) at the indicated time point. Extraction included a DNaseI digestion step as per protocol. The qScript cDNA Superscript Mix (Quantabio) was used for subsequent cDNA synthesis and conducted under the following PCR conditions: 5 min at 25°C, 30 min at 42°C, and 5 min at 85°C, and then storage at 4°C until further analysis. Each real-time (RT) qPCR reaction contained 80 ng cDNA, forward and reverse primer (forward: 5'-GGGTCGAACTTGTGGCTATT-3'; reverse: 5'-GAGGCCCTTGAGTGTACATTAG-3') mix,

and a SybrGreen I Mastermix (ThermoFisher Scientific). Each reaction was conducted using the Applied Biosystems 7300 RT PCR system at the following thermal cycling conditions: 10 min at 95°C, 40 cycles of three steps including 15 sec at 95°C, 1 min at 60°C, and 30 sec at 95°C. The C_T levels in each experiment were normalized to actin, and the $\Delta-C_T$ was calculated as $C_{T \text{ RHBDL4}} - C_{T \text{ actin}}$ for each time point and normalized to the 0 min time point.

2.4.4 Protein solubility assays

HEK293 cells were plated at ~50% confluency and grown for 24 hrs before transfection or TM-Ubc9ts induction. Transient transfection (2 μ g DNA per well) and tetracycline induction (1 μ g/mL) were both conducted 16 hrs prior to harvest. Cells were either kept at 37°C or shifted to 42°C for 1 hr to prior to harvesting. To harvest cells, they were dislodged from plates using a steady stream of media, harvested by centrifugation, and the supernatant was aspirated. The pellets were next resuspended in 150 μ l of ice-cold NP40 Buffer (50 mM HEPES, pH 7.4, 150 mM NaCl, 1% NP40) and incubated on ice for 30 min. The solution was then centrifuged for 10 min at 12,000 rcf (4°C) and the supernatant was aspirated and retained (i.e., the soluble NP40 fraction). The pellets were then resuspended in RIPA Buffer (50 mM HEPES, pH 7.4, 150 mM NaCl, 0.1% sodium dodecyl sulfate, 0.5% sodium deoxycholate), with 1 U/ml of benzonase added, and incubated end-over-end at 4°C for 1 hr or overnight, as indicated, to obtain the pellet (insoluble) fraction.

To analyze the extracted proteins via SDS-PAGE, 50 μ l of sample buffer with fresh 5% β -mercaptoethanol was added to 150 μ l of each sample. After incubation at 37°C for 30 min, 15 μ l of each sample was loaded onto 12.5% SDS polyacrylamide gels. Proteins were then transferred onto nitrocellulose membranes and stained with Revert 700 Total Protein Stain (Li-Cor) and

imaged at 700 nm. After reversing the Revert Total Protein stain and rinsing in double distilled water, the blots were blocked in 1% milk/TBST for 1 hr before incubation with anti-HA HRP antibody (Roche Diagnostics) overnight at 4°C. The blots were next washed in TBST prior to treatment with SuperSignal Femto Substrate (Thermofisher) and imaged using Bio-Rad Gel Doc equipment and software. Blots were quantified in ImageJ. Approximately equal sample loading was confirmed in all experiments via the analysis of the Revert Total Protein Stain, as shown.

2.4.5 Protein stability assays

HEK293 cells were grown to 50% confluency and then transfected with plasmids engineered to express TM-Ubc9ts or treated with 1µg/mL tetracycline to express TM-Ubc9ts in the stable lines (see above). After incubation for 24 hrs at 37°C for transfected cells or 16 hrs after induction in stable cells, 200 µg/ml of cycloheximide was added to each well. To measure proteasome-dependent degradation, MG132 at a final concentration of 50 µg/ml was added 2 hrs prior to the chase to half of the wells, and an equal volume of DMSO was added to the other (control) wells. To measure lysosome-dependent degradation, 50µM chloroquine (final concentration) or DMSO was added 2 hrs prior to chase. To inhibit substrate ubiquitination, 5 µM MLN7243 (Selleck Chemicals) or DMSO was added 2 hrs prior to chase. To inhibit p97, 10 µM CB-5083 (Selleck Chemicals) or DMSO was added 2 hrs prior to chase. Plates were incubated at either 37°C or 42°C, and samples were collected as above, except that a Protease Inhibitor Cocktail Tablet (Roche Diagnostics) was included during the resuspension of the samples prior to SDS-PAGE/western Blot analysis, as indicated above.

2.4.6 Carbonate Extraction

HEK293 cells were plated and grown to ~50% confluency before induction of TM-Ubc9ts expression 16 hrs before lysis (see above). As above, the cells were treated with DMSO, MG132, or CB-5083 for 3 hrs prior to lysis. Next, the HEK293 cells were harvested as above and pellets were collected by centrifugation at 800g for 10 min at 4°C followed by resuspension in 150µl cold 10mM Tris-HCl, pH 7.5, with protease inhibitors. Lysis was performed using needle passage before being centrifuged again as above. The supernatant was collected and then spun at 100,000g for 1 hr at 4°C to isolate a membrane pellet, which was resuspended in 150µl RIPA lysis buffer. Next, 15µl was set aside as the “total protein” while the remaining lysate was split and treated with either ice-cold 0.2 M sodium carbonate, pH 12, or 10 mM Tris-HCl, pH 7.5. Samples were incubated for 30 min on ice before another spin at 100,000g for 1 hr at 4°C. At this step, the supernatants were collected as the soluble fraction while pellets were resuspended as the membrane fraction. All samples were brought to pH 7.5 with acetic acid before adjusting samples to equal volumes and SDS-PAGE analysis.

2.4.7 Statistical methods

For all statistical analyses, a one tailed Student’s t-test with unequal variance was done with p value <0.05 for significance. All experiments were done with at least three biological replicates, as indicated in the figure legends. The equation used was:

$$t = \frac{x - \mu}{s / \sqrt{n}}$$

where x = mean, μ = population mean, s = standard deviation, n = sample size.

3.0 Conclusions & Future Directions

Misfolded proteins must be properly degraded by the cell before they persist long enough to aggregate and overwhelm protein homeostasis. To this end, I study the fate of model substrates in order to measure the impact that parameters such as protein solubility, stability, and structure have on processes like ERAD and autophagy. Despite the extensive number of both endogenous and chimeric substrates that have been catalogued in the past several years, our understanding of how cells handle protein aggregates, especially those involved in disease pathology, remains incomplete. In the following chapter I will address the current knowledge gap in the field of aggregation-prone protein degradation and how my work contributes to closing said gap. I will also hypothesize about future experiments to answer lingering questions about protein substrate processing and quality control.

3.1 A characterization pipeline for both endogenous and chimeric aggregation-prone ER membrane proteins

To better understand how aggregated proteins are resolved and degraded by ERAD, I characterized a model protein substrate, TM-Ubc9ts. Originally designed for expression in yeast systems, I translated the substrate to mammalian cell culture to answer the following questions: 1) Is TM-Ubc9ts an aggregation-prone ERAD substrate in mammalian cells? 2) Does substrate solubility correlate with stability in mammalian cells as it does in yeast? 3) What mammalian

proteases and/or disaggregases are involved in the processing of TM-Ubc9ts for degradation in the absence of the key yeast disaggregase Hsp104.

To this end, I first transiently transfected TM-Ubc9ts in HEK293H cells and assessed both its solubility and degradation through detergent fractionation and cycloheximide chase assays respectively. Observing that it became more insoluble at elevated temperatures and subjected to ERAD, I created a stable cell line expressing TM-Ubc9ts under a tetracycline-inducible promoter. I confirmed that my findings in the transient expression system remained consistent with the stable expression system while also observing robust generation of TM-Ubc9ts cleavage products during degradation. Then, I used a combination of drug treatments and siRNA knockdown to evaluate the role of the retrotranslocation engine p97 and the intramembrane protease RHBDL4 in the generation and degradation of both full-length TM-Ubc9ts and its cleavage fragments. While I found that RHBDL4 was not responsible for TM-Ubc9ts cleavage, I did confirm that soluble Ubc9ts undergoes a similar pattern of processing, suggesting that a cytosolic protease is responsible in both cases. The findings from this study are summarized in **Chapter 2**.

As discussed in Section 1.2.3.1, proteinopathies such as Alzheimer's Disease and Parkinson's Disease are caused by a disruption of proteostasis through the accumulation of misfolded protein. Often, these misfolded proteins result from the incorrect cleavage of membrane-bound signaling precursor proteins. For example, amyloid precursor protein (APP) is usually cleaved by α -secretase and γ -secretase to release p3 into the extracellular space as a signal molecule. In the amyloidogenic pathway, β -secretase cleaves APP before γ -secretase, generating amyloid-beta which aggregates and causes disease symptoms [154]. γ -secretase is just one of the intramembrane proteases integral to cell-cell signaling in the brain [354], which emphasizes the importance of understanding them and their substrates as they relate to proteopathic diseases.

Recent studies have used proteomic approaches to identify substrates of proteases such as ADAM10 and BACE1 [355, 356]. Once identified, these substrates must be experimentally categorized for their aggregation propensity and stability within the cell. Furthermore, chimeric substrates could then be designed based upon the identified endogenous substrates to interrogate the activity of understudied intramembrane proteases.

Because of the recent emphasis on targeting intramembrane proteases in neurodegenerative disease treatment, it is equally important to efficiently categorize their substrates and mechanisms of action. For example, BACE1 has long been known to cleave APP to form amyloid-beta, but its inhibition causes cognitive decline associated with its unidentified substrates [357]. Therefore, I suggest that the pipeline for aggregation-prone substrate characterization proposed in Section 2.3 could be applied to substrates of intramembrane proteases such as ADAM10 and BACE1 as identified by proteomic studies.

3.2 Manipulating substrate structure to answer questions of membrane insertion and topology

ERAD is the process responsible for recognizing and degrading a wide variety of misfolded proteins with legions in the cytosol, within the ER membrane, and in the ER lumen. Previous studies have leveraged the differences between how the cell degrades a substrate with a cytosolic or luminal facing legion in yeast [261]. Furthermore, location of a substrate's degron can determine whether it is processed by ERAD, ER-phagy, or the endomembrane/lysosome system [270, 358]. TM-Ubc9ts has a cytosolic-facing degron and has shown dependence both on the proteasome and autophagy for degradation. It is possible that by moving that degron into the lumen of the ER, the

ultimate degradation fate of TM-Ubc9ts or the generation of proteolytic fragments will be changed. By comparing this result to the data I presented in **Chapter 2**, I would be able to further refine the rules that define how the cell makes decisions about misfolded protein substrates.

There is precedent for manipulating the topology of an ER resident protein substrate to study decisions made about its degradation. One way to manipulate the insertion of a membrane protein is through the alteration of amino acids within the transmembrane domain itself [268]. While transmembrane domains in general are formed by hydrophobic residues to remain energetically favorable while embedded in the ER membrane, a score can be assigned to each amino acid in the domain to quantify the free energy of insertion [359]. In this fashion, point mutations can be made to the transmembrane sequence to make it energetically unfavorable when inside the membrane. By preventing the insertion of the second transmembrane domain of TM-Ubc9ts in this fashion, I would change its access to cytosolic chaperones and proteases, while exposing it those residing in the ER lumen. Comparing these two sets of data would allow me to make conclusions about which aspects of protein quality control are shared between them and which depend on the location of the degron itself.

3.3 Unbiased screening of the substrate “proximity proteome”

As discussed in section 1.3.3, mammalian cells have employed a suite of chaperones in a complex to compensate for the lack of a dedicated disaggregase such as Hsp104. The Hsp70-40-110 complex is capable of disaggregating loosely packed aggregates but struggles to resolve structures such as amyloids and prion oligomers. It is tempting to search for a true compensatory disaggregase, though it is more likely that many protein chaperones work in concert in response

to toxic aggregates. Therefore, I suggest a two-fold approach: assessment of putative chaperones with disaggregase activity via targeted knockdown and screening for chaperones that interact with aggregation prone substrates via proximity labeling. The first approach is useful in cases where evidence of disaggregation activity is observed based upon substrate binding, substrate refolding, or ATPase activity but can also be time consuming. Here, I will expand on the second approach which does not identify a disaggregase by its activity but instead by its proximity to an aggregation prone substrate.

Biotin ligation occurs in bacteria via the ligase BirA as a step in the processing of acetyl-CoA carboxylase in what is usually a specific reaction. However, a mutant BirA was discovered that promiscuously ligates biotin to any protein within a certain proximity. This BirA mutant has been leveraged in a technique dubbed BioID [360] where it is linked to a substrate of interest to label and isolate all proteins within close proximity, which are then identified by mass spectrometry. This technique has already been employed to make discoveries including substrate identification for RHBDL4 [361], protein interaction networks in neurodegenerative diseases [362], and dissecting the relationship between pathology, amyloid plaques, and tau tangles in Alzheimer's disease. [363]

I predict that the use of BioID with TM-Ubc9ts could identify a suite of cytosolic chaperones that interact with aggregation-prone ER resident proteins, some of which may be novel. I expect that a large portion of the labeled protein will be the known mammalian disaggregase machinery (Hsp70,40, and 110) however I also expect to find protein chaperones acting as holdases, unfoldases, or complex scaffolds amongst the proteins surrounding TM-Ubc9ts. An important element of labeling screens such as these is the elimination of background signal. To do this, samples of labeled protein can be collected under a variety of conditions including

temperature, proteasome inhibition, and p97 inhibition. Furthermore, several BirA fusions can be constructed either with only the two transmembrane domains of TM-Ubc9ts or various truncations to the C-terminus. In this manner, proteins common to each group can be subtracted, leaving only those unique to conditions in which the cell is responding to protein aggregation.

3.4 Limitations of this study

Though I was able to determine that a cytosolic protease is likely responsible for the generation of fragments in the degradation of TM-Ubc9ts, a handful of conditions limited the scope of the study. First, because TM-Ubc9ts was constructed from yeast protein and expressed in mammalian cells, issues with protein stability and solubility could arise from the organism of study independent of the protein's characteristics. Ubc9ts was shown to be temperature sensitive in yeast where normal growth occurs around 27°C and 37°C is a functionally elevated temperature. Mammalian cells grow normally at 37°C, which means it is likely that TM-Ubc9ts aggregates somewhat even before temperature is elevated to 42°C. I attempted to navigate around this issue by growing cells at lower temperatures (30°C) after transfection with TM-Ubc9ts, however no differences in stability or solubility were observed. Still, results at 42°C show somewhat decreased solubility which worked well enough for this study. Efforts were also made to reverse the temperature sensitive mutation in Ubc9ts to restore proper folding, however TM-Ubc9 exhibited little to no experimental difference from TM-Ubc9ts. Based upon these findings, I concluded that TM-Ubc9ts aggregation in mammalian cells resulted in a combination of foreign protein expression and temperature. As discussed in Appendix A, attempts were also made to construct substrates with mammalian protein, to avoid problems with interspecies expression.

Second, it is possible that the use of chloroquine to inhibit autophagy in section 2.2.1 does not fully account for all lysosome-related degradation. Chloroquine is an effective inhibitor of autophagosome fusion with the lysosome, which is ultimately responsible for degradation via autophagy [364]. Furthermore, it is FDA approved and used in current cancer treatments to slow tumor growth, which makes it an effective and attractive option for autophagy inhibition. Still, other drug alternatives interact with the autophagy pathway in different ways. Bafilomycin targets the proton pumps of the lysosome, which interferes with its ability to maintain a low pH [365]. Lysosomal inhibitor cocktails specifically target the contents of the lysosome and do not impact autophagosome-lysosome fusion [366]. To be thorough in my claim that degradation of substrates like TM-Ubc9ts does not rely on autophagy, future experiments should use either a combination of these drugs or a complementary set to fully block autophagy. In a similar manner, although the activity of the proteasome can be efficiently inhibited by MG132, it is far downstream from the previous steps of ERAD. To be sure that ubiquitination of a substrate targets it for degradation, an E1 inhibitor, TAK-243 [367], can be used as a complement to MG132.

Finally, I encountered difficulties in determining the precise cellular localization of TM-Ubc9ts aggregates. I imaged TM-Ubc9ts using indirect immunofluorescence with antibodies against both HA and KDEL to visualize the substrate and ER respectively. Results showed that there were accumulations of TM-Ubc9ts present, of which some co-localized with the ER. However, indirect immunofluorescence involves fixing cells and may distort localization results compared to live imaging with a fluorescent tag. Therefore, I suggest that future experiments employ a GFP fusion of TM-Ubc9ts to confirm whether it accumulates at the ER, in the cytoplasm, or somewhere along the endomembrane trafficking system. However, it would also need to be

verified that this addition to the substrate does not alter its solubility or stability before localization data can be taken into consideration.

3.5 Concluding remarks

Due to the complexity of the machinery within, the cell must strike a careful balance between protein production and degradation, all while maintaining homeostasis. Within this document I have provided a thorough documentation of proteostasis, from the chaperones and pathways that preserve it to the diseases that result from its disruption. Then, I presented a case where a previously identified aggregation prone ERAD substrate in yeast was translated into a mammalian cell system to answer questions concerning its retrotranslocation and degradation. My findings have not only established a pipeline for the characterization of putative aggregation-prone substrates in the future, but they have also emphasized the importance of substrate proteolysis in the retrotranslocation step of ERAD. By understanding the basic science behind protein degradation, my hope is to aid in the treatment and prevention of proteopathic diseases.

Appendix A Characterization of a pair of disease-relevant aggregation prone substrates:

Sec62-A β 42 and Sec62-A β 40

Appendix A.1 Introduction

As discussed in Chapter 2, aggregation-prone ERAD substrates can be used to interrogate checkpoints of mammalian protein quality control. However, one limitation of the substrate used in Chapter 2, TM-Ubc9ts, is that it is fully constructed from native yeast protein. Expressing yeast proteins in mammalian cells is known to cause stress independent of protein function due to codon usage bias [368]. In addition, the degron of this substrate, Ubc9ts, is a temperature sensitive mutant of a non-pathogenic protein. To address issues with native protein expression as well as disease relevance, I designed a pair of aggregation-prone substrates constructed entirely from mammalian proteins: Sec62-A β 40 and Sec62-A β 42. These two substrates share the full amino acid sequence of Sec62, a native ER-resident membrane protein; however, they differ in their C-terminal regions which are two different lengths of amyloid beta protein. Amyloid beta 40 is less aggregation prone than amyloid beta 42 due to the deletion of two C-terminal amino acids that stabilize aggregate structure [109]. In theory, Sec62-A β 40 is a powerful control for Sec62-A β 42 because it can function as a large background subtraction in proximity labeling and mass spectrometry experiments. I hypothesized that aggregation-prone substrates constructed from mammalian proteins would resolve issues with inter-species expression while reinforcing trends observed with TM-Ubc9ts degradation and solubility. To this end, I evaluated Sec62-A β 42 and Sec62-A β 40 degradation and solubility in HEK293H cells both in transiently transfected and stable expression systems.

Appendix A.2 Materials & Methods

Molecular methods, human cell culture protocols, protein solubility and stability assays, and statistical methods were conducted as described in **Section 2.4**.

Appendix A.3 Results and Discussion

Similar to the strategy employed in Section 2.2, I first assessed the degradation of Sec62-A β 42/40 in HEK293h in a transient transfection system. Cells were transfected with a plasmid expressing either Sec62-A β 42 or Sec62-A β 40 prior to conducting a cycloheximide chase assay at both 37°C and 42°C over 8 hrs to assess substrate stability. The rate of degradation was observed to be nearly identical independent of the substrate, though each substrate was slightly more stable at elevated temperatures. Both substrates were stabilized with the addition of MG132 to inhibit the proteasome. Nearly complete stabilization under MG132 treatment suggests that all degradation of both substrates is conducted by the proteasome. To assess substrate solubility, I also conducted detergent solubility assays in a similar transient transfection model. NP-40 was used to liberate and solubilize membrane-bound proteins before the pellet was treated with SDS buffer as done in Section 2.2.2. I observed little to no marked decrease in the solubility of either substrate under conditions of proteasome inhibition, p97 inhibition, or elevated temperature.

Despite the hypothesis that a substrate containing amyloid beta as a degron would be either robustly degraded or aggregation prone, I concluded that both Sec62-A β 42 and Sec62-A β 40 were not adequate candidates to interrogate mammalian proteostasis. Unlike TM-Ubc9ts, they exhibited no hallmarks of a “difficult to process” substrate such as the generation of proteolytic fragments

and no insult was able to decrease their solubility. This naturally leads to the question: Why would attaching amyloid-beta protein to a transmembrane domain prevent it from aggregating?

The first explanation is that anchoring amyloid-beta to the ER membrane reduces its ability to fit into the regulated structures required for aggregate formation. When expressed *in vivo*, amyloid-beta can freely move about the cytoplasm or extracellular space, which in turn allows it to sample many more orientations and configurations than when it is relatively fixed in place at the ER membrane. Therefore, despite the insults of increased temperature or inhibition of ERAD machinery, Sec62-A β 42 and Sec62-A β 40 may be unable to nucleate or propagate the formation of aggregates. Secondly, the results in Figure 11 show that there is about a 50/50 split between soluble and insoluble substrate populations. It is possible that under our experimental conditions, this level of aggregation is both the minimal and maximal amount, regardless of changes to cellular conditions. Finally, studies in human brain samples of individuals with advanced Alzheimer's disease show that distinct populations of aggregates form: those with A β 42 or A β 40 alone, and those with a combination of the two [369]. The ratio of A β 42/40 has become a marker for severity of the disease, with individuals showing increased ratios of A β 42 to A β 40 also showing advanced symptoms [370]. Therefore, in future experiments, it may be more important to express both sizes of amyloid beta protein together in different ratios to characterize heterologous aggregates as opposed to homologous. All together, this result highlights the importance of verifying assumptions made about how aggregation prone proteins behave in different cellular environments.

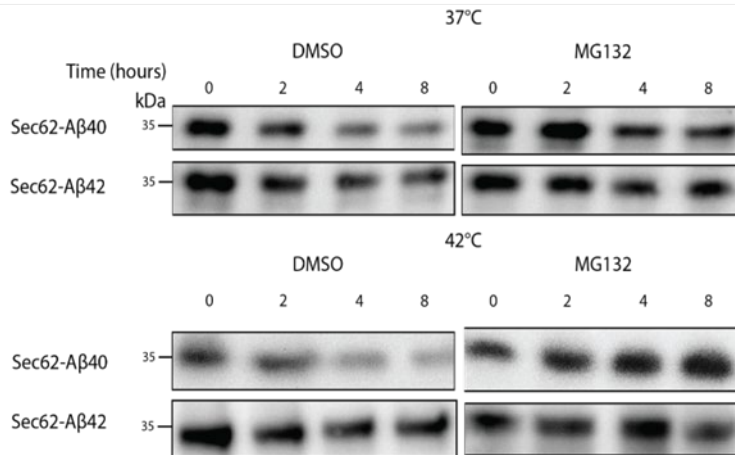
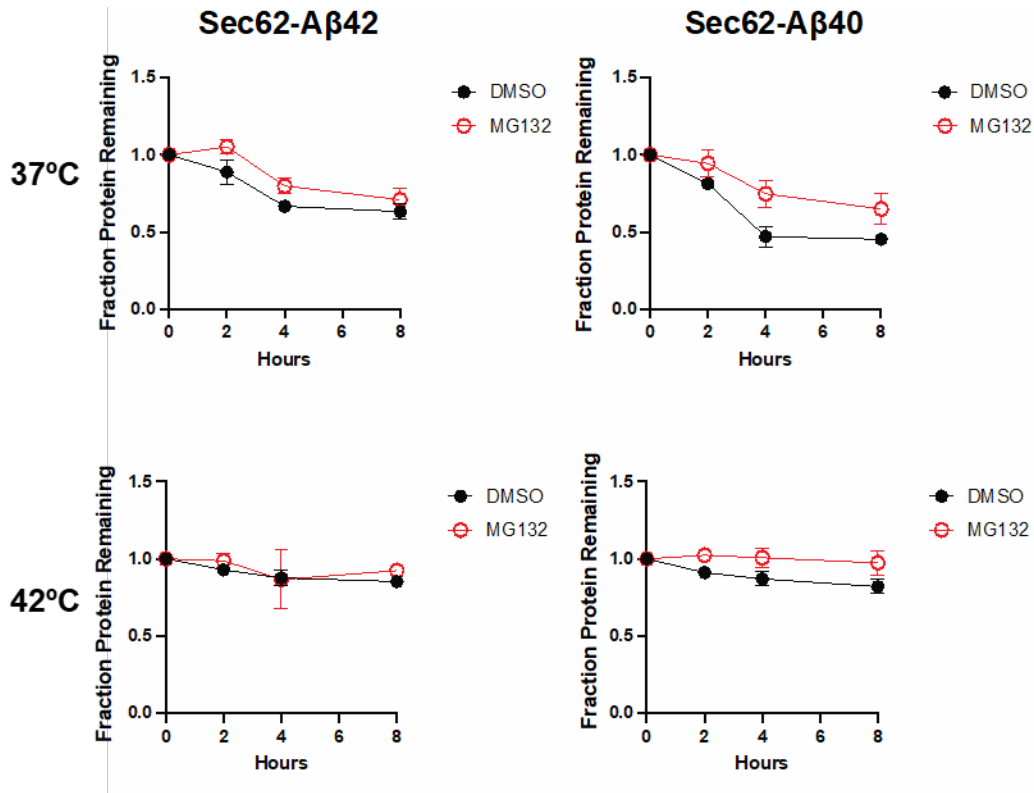


Figure 12 Sec62-Aβ42 and Sec62-Aβ40 undergo ERAD but are relatively stable

Sec62-Aβ42 and Sec62-Aβ40 stability were determined by cycloheximide chase at 37° and 42°C over 8 hours. Cells were treated with either DMSO or MG132 for the duration of the chase. In all panels, n = 3 independent experiments +/- SEM *p < 0.05.

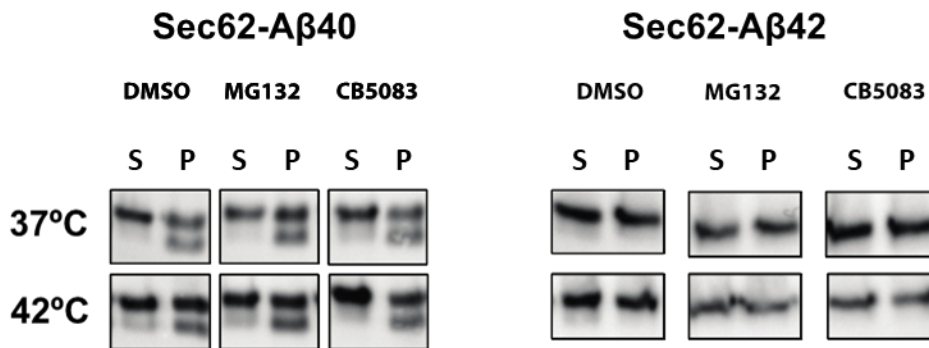
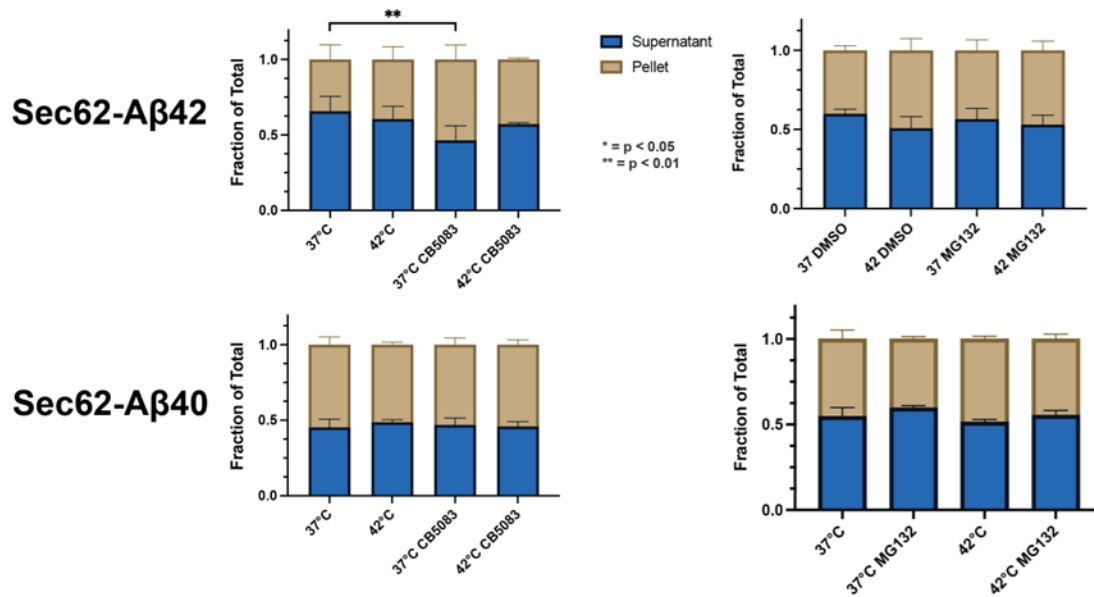


Figure 13. Sec62-Aβ42 and Sec62-Aβ40 solubility does not change under temperature or ERAD inhibition

Protein solubility of Sec62-Aβ42 and Sec62-Aβ40 were determined after treating with NP40 (soluble fraction) and RIPA (insoluble fraction). Protein levels were quantified via western blot as visualized with HA-antibody

Bibliography

1. Anfinsen, C.B., *Principles that govern the folding of protein chains*. Science, 1973. **181**(4096): p. 223-30.
2. Levinthal, C., *Are there pathways for protein folding?* Journal de chimie physique, 1968. **65**: p. 44-45.
3. Dill, K.A., *Dominant forces in protein folding*. Biochemistry, 1990. **29**(31): p. 7133-55.
4. Minor, D.L., Jr. and P.S. Kim, *Context-dependent secondary structure formation of a designed protein sequence*. Nature, 1996. **380**(6576): p. 730-4.
5. Dill, K.A. and H.S. Chan, *From Levinthal to pathways to funnels*. Nat Struct Biol, 1997. **4**(1): p. 10-9.
6. Creamer, T.P. and G.D. Rose, *Alpha-helix-forming propensities in peptides and proteins*. Proteins, 1994. **19**(2): p. 85-97.
7. Deechongkit, S., P.E. Dawson, and J.W. Kelly, *Toward assessing the position-dependent contributions of backbone hydrogen bonding to beta-sheet folding thermodynamics employing amide-to-ester perturbations*. J Am Chem Soc, 2004. **126**(51): p. 16762-71.
8. Drozdov, A.N., A. Grossfield, and R.V. Pappu, *Role of solvent in determining conformational preferences of alanine dipeptide in water*. J Am Chem Soc, 2004. **126**(8): p. 2574-81.
9. Nilsson, O.B., et al., *Cotranslational Protein Folding inside the Ribosome Exit Tunnel*. Cell Rep, 2015. **12**(10): p. 1533-40.
10. O'Brien, E.P., et al., *Understanding the influence of codon translation rates on cotranslational protein folding*. Acc Chem Res, 2014. **47**(5): p. 1536-44.
11. Etchells, S.A., et al., *The cotranslational contacts between ribosome-bound nascent polypeptides and the subunits of the hetero-oligomeric chaperonin TRiC probed by photocross-linking*. J Biol Chem, 2005. **280**(30): p. 28118-26.
12. Fang, Y., *Gibbs Free Energy Formula for Protein Folding*, in *Thermodynamics - Fundamentals and Its Application in Science*, M.-R. Ricardo, Editor. 2012, IntechOpen: Rijeka. p. Ch. 3.
13. Mallamace, F., et al., *Energy landscape in protein folding and unfolding*. Proc Natl Acad Sci U S A, 2016. **113**(12): p. 3159-63.
14. Biasini, E. and P. Faccioli, *Functional, pathogenic, and pharmacological roles of protein folding intermediates*. Proteins, 2023. **n/a**(n/a).
15. Sanz-Hernandez, M., et al., *Mechanism of misfolding of the human prion protein revealed by a pathological mutation*. Proc Natl Acad Sci U S A, 2021. **118**(12): p. e2019631118.
16. Apetri, A.C. and W.K. Surewicz, *Kinetic intermediate in the folding of human prion protein*. J Biol Chem, 2002. **277**(47): p. 44589-92.
17. Selkoe, D.J.H., J., *The amyloid hypothesis of Alzheimer's disease at 25 years*. EMBO Mol. Med., 2016. **8**: p. 595-608.
18. Laskey, R., et al., *Nucleosomes are assembled by an acidic protein which binds histones and transfers them to DNA*. Nature, 1978. **275**(5679): p. 416-420.
19. Ellis, J., *Proteins as molecular chaperones*. Nature, 1987. **328**(6129): p. 378-379.

20. Frydman, J., et al., *Folding of nascent polypeptide chains in a high molecular mass assembly with molecular chaperones*. Nature, 1994. **370**(6485): p. 111-7.
21. Haas, I.G. and M. Wabl, *Immunoglobulin heavy chain binding protein*. Nature, 1983. **306**(5941): p. 387-9.
22. Jakob, U., et al., *Small heat shock proteins are molecular chaperones*. J Biol Chem, 1993. **268**(3): p. 1517-20.
23. Skowronek, M.H., L.M. Hendershot, and I.G. Haas, *The variable domain of nonassembled Ig light chains determines both their half-life and binding to the chaperone BiP*. Proc Natl Acad Sci U S A, 1998. **95**(4): p. 1574-8.
24. Nishikawa, S.I., et al., *Molecular chaperones in the yeast endoplasmic reticulum maintain the solubility of proteins for retrotranslocation and degradation*. J Cell Biol, 2001. **153**(5): p. 1061-70.
25. Polier, S., et al., *Structural basis for the cooperation of Hsp70 and Hsp110 chaperones in protein folding*. Cell, 2008. **133**(6): p. 1068-79.
26. Rapoport, T.A., L. Li, and E. Park, *Structural and Mechanistic Insights into Protein Translocation*. Annu Rev Cell Dev Biol, 2017. **33**: p. 369-390.
27. Craig, E.A., *Hsp70 at the membrane: driving protein translocation*. BMC Biology, 2018. **16**(1): p. 11.
28. Haslbeck, M., S. Weinkauf, and J. Buchner, *Small heat shock proteins: Simplicity meets complexity*. J Biol Chem, 2019. **294**(6): p. 2121-2132.
29. Finn, T.E., et al., *Serum albumin prevents protein aggregation and amyloid formation and retains chaperone-like activity in the presence of physiological ligands*. J Biol Chem, 2012. **287**(25): p. 21530-40.
30. Mogk, A., B. Bukau, and H.H. Kampinga, *Cellular Handling of Protein Aggregates by Disaggregation Machines*. Mol Cell, 2018. **69**(2): p. 214-226.
31. Shorter, J. and D.R. Southworth, *Spiraling in Control: Structures and Mechanisms of the Hsp104 Disaggregase*. Cold Spring Harb Perspect Biol, 2019. **11**(8).
32. Fewell, S.W., et al., *Small molecule modulators of endogenous and co-chaperone-stimulated Hsp70 ATPase activity*. J Biol Chem, 2004. **279**(49): p. 51131-40.
33. Faust, O., et al., *HSP40 proteins use class-specific regulation to drive HSP70 functional diversity*. Nature, 2020. **587**(7834): p. 489-494.
34. Wyzkowski, H., et al., *Class-specific interactions between Sis1 J-domain protein and Hsp70 chaperone potentiate disaggregation of misfolded proteins*. Proc Natl Acad Sci U S A, 2021. **118**(49).
35. Nillegoda, N.B., et al., *Crucial HSP70 co-chaperone complex unlocks metazoan protein disaggregation*. Nature, 2015. **524**(7564): p. 247-51.
36. Joshi, S., et al., *Adapting to stress - chaperome networks in cancer*. Nat Rev Cancer, 2018. **18**(9): p. 562-575.
37. Kubota, S., H. Kubota, and K. Nagata, *Cytosolic chaperonin protects folding intermediates of G β from aggregation by recognizing hydrophobic β -strands*. Proceedings of the National Academy of Sciences, 2006. **103**(22): p. 8360-8365.
38. Kerner, M.J., et al., *Proteome-wide analysis of chaperonin-dependent protein folding in Escherichia coli*. Cell, 2005. **122**(2): p. 209-20.
39. Hohn, T., et al., *Isolation and characterization of the host protein groE involved in bacteriophage lambda assembly*. J Mol Biol, 1979. **129**(3): p. 359-73.

40. Tilly, K., H. Murialdo, and C. Georgopoulos, *Identification of a second Escherichia coli groE gene whose product is necessary for bacteriophage morphogenesis*. Proceedings of the National Academy of Sciences, 1981. **78**(3): p. 1629-1633.
41. Horwich, A.L., A.C. Apetri, and W.A. Fenton, *The GroEL/GroES cis cavity as a passive anti-aggregation device*. FEBS letters, 2009. **583**(16): p. 2654-2662.
42. Chakraborty, K., et al., *Chaperonin-catalyzed rescue of kinetically trapped states in protein folding*. Cell, 2010. **142**(1): p. 112-22.
43. Weaver, J., et al., *GroEL actively stimulates folding of the endogenous substrate protein PepQ*. Nature Communications, 2017. **8**(1): p. 15934.
44. Goloubinoff, P., A.A. Gatenby, and G.H. Lorimer, *GroE heat-shock proteins promote assembly of foreign prokaryotic ribulose biphosphate carboxylase oligomers in Escherichia coli*. Nature, 1989. **337**(6202): p. 44-7.
45. Tyagi, N.K., W.A. Fenton, and A.L. Horwich, *GroEL/GroES cycling: ATP binds to an open ring before substrate protein favoring protein binding and production of the native state*. Proceedings of the National Academy of Sciences, 2009. **106**(48): p. 20264-20269.
46. Chaudhuri, T.K., et al., *GroEL/GroES-mediated folding of a protein too large to be encapsulated*. Cell, 2001. **107**(2): p. 235-246.
47. Libich, D.S., V. Tugarinov, and G.M. Clore, *Intrinsic unfoldase/foldase activity of the chaperonin GroEL directly demonstrated using multinuclear relaxation-based NMR*. Proceedings of the National Academy of Sciences, 2015. **112**(29): p. 8817-8823.
48. Stan, G., G.H. Lorimer, and D. Thirumalai, *Friends in need: How chaperonins recognize and remodel proteins that require folding assistance*. Front Mol Biosci, 2022. **9**: p. 1071168.
49. Hoter, A., M.E. El-Sabban, and H.Y. Naim, *The HSP90 Family: Structure, Regulation, Function, and Implications in Health and Disease*. Int J Mol Sci, 2018. **19**(9).
50. Nathan, D.F., M.H. Vos, and S. Lindquist, *In vivo functions of the Saccharomyces cerevisiae Hsp90 chaperone*. Proceedings of the National Academy of Sciences, 1997. **94**(24): p. 12949-12956.
51. Biebl, M.M. and J. Buchner, *Structure, Function, and Regulation of the Hsp90 Machinery*. Cold Spring Harb Perspect Biol, 2019. **11**(9).
52. Rowlands, M., et al., *Detection of the ATPase activity of the molecular chaperones Hsp90 and Hsp72 using the transreener™ ADP assay kit*. Journal of biomolecular screening, 2010. **15**(3): p. 279-286.
53. Zuehlke, A. and J.L. Johnson, *Hsp90 and co-chaperones twist the functions of diverse client proteins*. Biopolymers, 2010. **93**(3): p. 211-7.
54. Gething, M.J., *Role and regulation of the ER chaperone BiP*. Semin Cell Dev Biol, 1999. **10**(5): p. 465-72.
55. Easton, D.P., Y. Kaneko, and J.R. Subjeck, *The hsp110 and Grp1 70 stress proteins: newly recognized relatives of the Hsp70s*. Cell Stress Chaperones, 2000. **5**(4): p. 276-90.
56. Leidhold, C., et al., *Structure and function of Hsp78, the mitochondrial ClpB homolog*. Journal of Structural Biology, 2006. **156**(1): p. 149-164.
57. Cupo, R.R. and J. Shorter, *Skd3 (human ClpB) is a potent mitochondrial protein disaggregase that is inactivated by 3-methylglutaconic aciduria-linked mutations*. eLife, 2020. **9**: p. e55279.
58. Payapilly, A. and S. High, *BAG6 regulates the quality control of a polytopic ERAD substrate*. J Cell Sci, 2014. **127**(Pt 13): p. 2898-909.

59. Claessen, J.H., S. Sanyal, and H.L. Ploegh, *The chaperone BAG6 captures dislocated glycoproteins in the cytosol*. PLoS One, 2014. **9**(3): p. e90204.
60. Zaarur, N., et al., *RuvbL1 and RuvbL2 enhance aggresome formation and disaggregate amyloid fibrils*. EMBO J, 2015. **34**(18): p. 2363-82.
61. Maji, S.K., et al., *Functional amyloids as natural storage of peptide hormones in pituitary secretory granules*. Science, 2009. **325**(5938): p. 328-332.
62. Jacob, R.S., et al., *Amyloid formation of growth hormone in presence of zinc: Relevance to its storage in secretory granules*. Scientific reports, 2016. **6**(1): p. 23370.
63. Saad, S., et al., *Reversible protein aggregation is a protective mechanism to ensure cell cycle restart after stress*. Nature Cell Biology, 2017. **19**(10): p. 1202-1213.
64. Audas, T.E., et al., *Adaptation to stressors by systemic protein amyloidogenesis*. Developmental cell, 2016. **39**(2): p. 155-168.
65. Auer, S., C.M. Dobson, and M. Vendruscolo, *Characterization of the nucleation barriers for protein aggregation and amyloid formation*. Hfsp j, 2007. **1**(2): p. 137-46.
66. March, D., V. Bianco, and G. Franzese, *Protein Unfolding and Aggregation near a Hydrophobic Interface*. Polymers (Basel), 2021. **13**(1).
67. Gsponer, J., U. Haberthür, and A. Caflisch, *The role of side-chain interactions in the early steps of aggregation: Molecular dynamics simulations of an amyloid-forming peptide from the yeast prion Sup35*. Proceedings of the National Academy of Sciences, 2003. **100**(9): p. 5154-5159.
68. Dindo, M., C. Conter, and B. Cellini, *Electrostatic interactions drive native-like aggregation of human alanine:glyoxylate aminotransferase*. Febs j, 2017. **284**(21): p. 3739-3764.
69. Tsemekhman, K., et al., *Cooperative hydrogen bonding in amyloid formation*. Protein Sci, 2007. **16**(4): p. 761-4.
70. Ellis, R.J., *Macromolecular crowding: an important but neglected aspect of the intracellular environment*. Current opinion in structural biology, 2001. **11**(1): p. 114-119.
71. Brown, G.C., *Total cell protein concentration as an evolutionary constraint on the metabolic control distribution in cells*. Journal of theoretical biology, 1991. **153**(2): p. 195-203.
72. Wang, W. and M.H. Hecht, *Rationally designed mutations convert de novo amyloid-like fibrils into monomeric β -sheet proteins*. Proceedings of the National Academy of Sciences, 2002. **99**(5): p. 2760-2765.
73. Sant'Anna, R., et al., *The importance of a gatekeeper residue on the aggregation of transthyretin: implications for transthyretin-related amyloidoses*. J Biol Chem, 2014. **289**(41): p. 28324-37.
74. Houben, B., et al., *Autonomous aggregation suppression by acidic residues explains why chaperones favour basic residues*. The EMBO Journal, 2020. **39**(11): p. e102864.
75. Friedreich, N. and A. Kekulé, *Zur amyloidfrage*. Archiv für pathologische Anatomie und Physiologie und für klinische Medizin, 1859. **16**(1-2): p. 50-65.
76. Thal, D.R., et al., *The development of amyloid beta protein deposits in the aged brain*. Sci Aging Knowledge Environ, 2006. **2006**(6): p. re1.
77. Li, J., et al., *The RIP1/RIP3 necrosome forms a functional amyloid signaling complex required for programmed necrosis*. Cell, 2012. **150**(2): p. 339-50.

78. Dean, D.N. and J.C. Lee, *pH-Dependent fibril maturation of a Pmel17 repeat domain isoform revealed by tryptophan fluorescence*. *Biochim Biophys Acta Proteins Proteom*, 2019. **1867**(10): p. 961-969.
79. Pfefferkorn, C.M., R.P. McGlinchey, and J.C. Lee, *Effects of pH on aggregation kinetics of the repeat domain of a functional amyloid, Pmel17*. *Proc Natl Acad Sci U S A*, 2010. **107**(50): p. 21447-52.
80. Rengifo-Gonzalez, J.C., et al., *The cooperative binding of TDP-43 to GU-rich RNA repeats antagonizes TDP-43 aggregation*. *eLife*, 2021. **10**: p. e67605.
81. Sopova, J.V., et al., *Amyloid conformers of the FXR1 protein prevent mRNA degradation in cortical neurons*. *bioRxiv*, 2019: p. 544650.
82. Fehilly, J., et al., *Condensate formation of the human RNA-binding protein SMAUG1 is controlled by its intrinsically disordered regions and interactions with 14-3-3 proteins*. *bioRxiv*, 2023: p. 2023.02.09.527857.
83. Wiedner, H.J. and J. Giudice, *It's not just a phase: function and characteristics of RNA-binding proteins in phase separation*. *Nat Struct Mol Biol*, 2021. **28**(6): p. 465-473.
84. Tauber, D., et al., *Modulation of RNA Condensation by the DEAD-Box Protein eIF4A*. *Cell*, 2020. **180**(3): p. 411-426.e16.
85. Prokopovich, D.V., et al., *Impact of Phosphorylation and Pseudophosphorylation on the Early Stages of Aggregation of the Microtubule-Associated Protein Tau*. *The Journal of Physical Chemistry B*, 2017. **121**(9): p. 2095-2103.
86. Schaffert, L.N. and W.G. Carter, *Do Post-Translational Modifications Influence Protein Aggregation in Neurodegenerative Diseases: A Systematic Review*. *Brain Sci*, 2020. **10**(4).
87. Ross, C.A. and M.A. Poirier, *Protein aggregation and neurodegenerative disease*. *Nat Med*, 2004. **10 Suppl**: p. S10-7.
88. Robinson, J.L., et al., *Neurodegenerative disease concomitant proteinopathies are prevalent, age-related and APOE4-associated*. *Brain*, 2018. **141**(7): p. 2181-2193.
89. Azam, S., et al., *The Ageing Brain: Molecular and Cellular Basis of Neurodegeneration*. *Frontiers in Cell and Developmental Biology*, 2021. **9**.
90. Bloom, G.S., *Amyloid- β and tau: the trigger and bullet in Alzheimer disease pathogenesis*. *JAMA Neurol*, 2014. **71**(4): p. 505-8.
91. Brundin, P., R. Melki, and R. Kopito, *Prion-like transmission of protein aggregates in neurodegenerative diseases*. *Nat Rev Mol Cell Biol*, 2010. **11**(4): p. 301-7.
92. Liu, S., et al., *Highly efficient intercellular spreading of protein misfolding mediated by viral ligand-receptor interactions*. *Nature Communications*, 2021. **12**(1): p. 5739.
93. Watts, J.C., et al., *Modulation of Creutzfeldt-Jakob disease prion propagation by the A224V mutation*. *Ann Neurol*, 2015. **78**(4): p. 540-53.
94. Lam, S., et al., *Transmission of amyloid-beta and tau pathologies is associated with cognitive impairments in a primate*. *Acta Neuropathologica Communications*, 2021. **9**(1): p. 165.
95. Rajmohan, R. and P.H. Reddy, *Amyloid-Beta and Phosphorylated Tau Accumulations Cause Abnormalities at Synapses of Alzheimer's disease Neurons*. *J Alzheimers Dis*, 2017. **57**(4): p. 975-999.
96. Abubakar, M.B., et al., *Alzheimer's Disease: An Update and Insights Into Pathophysiology*. *Front Aging Neurosci*, 2022. **14**: p. 742408.
97. Busche, M.A., et al., *Tau impairs neural circuits, dominating amyloid- β effects, in Alzheimer models in vivo*. *Nature neuroscience*, 2019. **22**(1): p. 57-64.

98. DeTure, M.A. and D.W. Dickson, *The neuropathological diagnosis of Alzheimer's disease*. *Molecular Neurodegeneration*, 2019. **14**(1): p. 32.
99. Ramanan, V.K. and G.S. Day, *Anti-amyloid therapies for Alzheimer disease: finally, good news for patients*. *Molecular Neurodegeneration*, 2023. **18**(1): p. 42.
100. Cummings, J., et al., *Lecanemab: Appropriate Use Recommendations*. *The Journal of Prevention of Alzheimer's Disease*, 2023. **10**(3): p. 362-377.
101. Gueorguieva, I., et al., *Donanemab exposure and efficacy relationship using modeling in Alzheimer's disease*. *Alzheimers Dement (N Y)*, 2023. **9**(2): p. e12404.
102. Zheng, H. and E.H. Koo, *Biology and pathophysiology of the amyloid precursor protein*. *Mol Neurodegener*, 2011. **6**(1): p. 27.
103. Twine, N.A., et al., *Whole transcriptome sequencing reveals gene expression and splicing differences in brain regions affected by Alzheimer's disease*. *PLoS One*, 2011. **6**(1): p. e16266.
104. Orlando, I.F., et al., *Noradrenergic and cholinergic systems take centre stage in neuropsychiatric diseases of ageing*. *Neuroscience & Biobehavioral Reviews*, 2023. **149**: p. 105167.
105. Ismaili, L., et al., *Multitarget compounds bearing tacrine- and donepezil-like structural and functional motifs for the potential treatment of Alzheimer's disease*. *Prog Neurobiol*, 2017. **151**: p. 4-34.
106. Greicius, M.D., et al., *Default-mode network activity distinguishes Alzheimer's disease from healthy aging: Evidence from functional MRI*. *Proceedings of the National Academy of Sciences*, 2004. **101**(13): p. 4637-4642.
107. Saido, T. and M.A. Leissring, *Proteolytic degradation of amyloid β -protein*. *Cold Spring Harb Perspect Med*, 2012. **2**(6): p. a006379.
108. Cruts, M. and C. Van Broeckhoven, *Data mining: applying the AD&FTD mutation database to progranulin*. *Progranulin: Methods and Protocols*, 2018: p. 81-92.
109. Yan, Y. and C. Wang, *Abeta42 is more rigid than Abeta40 at the C terminus: implications for Abeta aggregation and toxicity*. *J Mol Biol*, 2006. **364**(5): p. 853-62.
110. Gómez-Isla, T., et al., *The impact of different presenilin 1 and presenilin 2 mutations on amyloid deposition, neurofibrillary changes and neuronal loss in the familial Alzheimer's disease brain: evidence for other phenotype-modifying factors*. *Brain*, 1999. **122**(9): p. 1709-1719.
111. Pahrudin Arrozi, A., et al., *Evaluation of the Expression of Amyloid Precursor Protein and the Ratio of Secreted Amyloid Beta 42 to Amyloid Beta 40 in SH-SY5Y Cells Stably Transfected with Wild-Type, Single-Mutant and Double-Mutant Forms of the APP Gene for the Study of Alzheimer's Disease Pathology*. *Appl Biochem Biotechnol*, 2017. **183**(3): p. 853-866.
112. Nixon, R.A., *Amyloid precursor protein and endosomal-lysosomal dysfunction in Alzheimer's disease: inseparable partners in a multifactorial disease*. *The FASEB Journal*, 2017. **31**(7): p. 2729.
113. Dodson, S.E., et al., *Loss of LR11/SORLA enhances early pathology in a mouse model of amyloidosis: evidence for a proximal role in Alzheimer's disease*. *Journal of Neuroscience*, 2008. **28**(48): p. 12877-12886.
114. Eshraghi, M., et al., *Enhancing autophagy in Alzheimer's disease through drug repositioning*. *Pharmacol Ther*, 2022. **237**: p. 108171.

115. Schulte, J. and J.T. Littleton, *The biological function of the Huntingtin protein and its relevance to Huntington's Disease pathology*. *Curr Trends Neurol*, 2011. **5**: p. 65-78.
116. Khare, S.D., et al., *Molecular Origin of Polyglutamine Aggregation in Neurodegenerative Diseases*. *PLOS Computational Biology*, 2005. **1**(3): p. e30.
117. Igarashi, S., et al., *Inducible PC12 cell model of Huntington's disease shows toxicity and decreased histone acetylation*. *Neuroreport*, 2003. **14**(4): p. 565-568.
118. Ratovitski, T., et al., *N-terminal proteolysis of full-length mutant huntingtin in an inducible PC12 cell model of Huntington's disease*. *Cell Cycle*, 2007. **6**(23): p. 2970-81.
119. Yang, H., et al., *Huntingtin Interacts with the Cue Domain of gp78 and Inhibits gp78 Binding to Ubiquitin and p97/VCP*. *PLOS ONE*, 2010. **5**(1): p. e8905.
120. Fujita, K., et al., *A functional deficiency of TERA/VCP/p97 contributes to impaired DNA repair in multiple polyglutamine diseases*. *Nat Commun*, 2013. **4**: p. 1816.
121. Riguët, N., et al., *Nuclear and cytoplasmic huntingtin inclusions exhibit distinct biochemical composition, interactome and ultrastructural properties*. *Nature Communications*, 2021. **12**(1): p. 6579.
122. Kim, Y.E., et al., *Soluble oligomers of PolyQ-expanded huntingtin target a multiplicity of key cellular factors*. *Molecular cell*, 2016. **63**(6): p. 951-964.
123. Hipp, M.S., et al., *Indirect inhibition of 26S proteasome activity in a cellular model of Huntington's disease*. *Journal of Cell Biology*, 2012. **196**(5): p. 573-587.
124. Scior, A., et al., *Complete suppression of Htt fibrilization and disaggregation of Htt fibrils by a trimeric chaperone complex*. *The EMBO Journal*, 2018. **37**(2): p. 282-299.
125. Kruger, R., et al., *Epplen 1T, Schols L, Riess O. Ala30Pro mutation in the gene encoding alpha-synuclein in Parkinson's disease*. *Nat Genet*, 1998. **18**: p. 106-8.
126. George, J.M., *The synucleins*. *Genome Biol*, 2002. **3**(1): p. Reviews3002.
127. Stefanis, L., *α -Synuclein in Parkinson's disease*. *Cold Spring Harb Perspect Med*, 2012. **2**(2): p. a009399.
128. Meade, R.M., D.P. Fairlie, and J.M. Mason, *Alpha-synuclein structure and Parkinson's disease – lessons and emerging principles*. *Molecular Neurodegeneration*, 2019. **14**(1): p. 29.
129. Ulmer, T.S., et al., *Structure and Dynamics of Micelle-bound Human α -Synuclein* *^{*}*. *Journal of Biological Chemistry*, 2005. **280**(10): p. 9595-9603.
130. Kara, E., et al., *α -Synuclein mutations cluster around a putative protein loop*. *Neurosci Lett*, 2013. **546**: p. 67-70.
131. Lázaro, D.F., et al., *The effects of the novel A53E alpha-synuclein mutation on its oligomerization and aggregation*. *Acta Neuropathologica Communications*, 2016. **4**(1): p. 128.
132. Kyriukha, Y.A., et al., *α -Synuclein Dimers as Potent Inhibitors of Fibrillization*. *Journal of Medicinal Chemistry*, 2019. **62**(22): p. 10342-10351.
133. Sulzer, D. and R.H. Edwards, *The physiological role of α -synuclein and its relationship to Parkinson's Disease*. *Journal of Neurochemistry*, 2019. **150**(5): p. 475-486.
134. Butler, B., et al., *Dopamine Transporter Activity Is Modulated by α -Synuclein* ***. *Journal of Biological Chemistry*, 2015. **290**(49): p. 29542-29554.
135. Woerman, A.L., et al., *α -Synuclein: Multiple System Atrophy Prions*. *Cold Spring Harb Perspect Med*, 2018. **8**(7).
136. Kawahata, I., D.I. Finkelstein, and K. Fukunaga, *Pathogenic Impact of α -Synuclein Phosphorylation and Its Kinases in α -Synucleinopathies*. *Int J Mol Sci*, 2022. **23**(11).

137. Rui, Q., et al., *The Role of LRRK2 in Neurodegeneration of Parkinson Disease*. *Curr Neuropharmacol*, 2018. **16**(9): p. 1348-1357.
138. Ho, D.H., et al., *Phosphorylation of p53 by LRRK2 induces microglial tumor necrosis factor α -mediated neurotoxicity*. *Biochemical and biophysical research communications*, 2017. **482**(4): p. 1088-1094.
139. Carballo-Carbajal, I., et al., *Leucine-rich repeat kinase 2 induces α -synuclein expression via the extracellular signal-regulated kinase pathway*. *Cellular signalling*, 2010. **22**(5): p. 821-827.
140. Chen, C., et al., *(G2019S) LRRK2 activates MKK4-JNK pathway and causes degeneration of SN dopaminergic neurons in a transgenic mouse model of PD*. *Cell Death & Differentiation*, 2012. **19**(10): p. 1623-1633.
141. Dawson, T.M. and V.L. Dawson, *The role of parkin in familial and sporadic Parkinson's disease*. *Mov Disord*, 2010. **25 Suppl 1**(0 1): p. S32-9.
142. Fellner, L., et al., *Autophagy in α -Synucleinopathies—An Overstrained System*. *Cells*, 2021. **10**(11): p. 3143.
143. Dorszewska, J., et al., *Molecular Effects of L-dopa Therapy in Parkinson's Disease*. *Curr Genomics*, 2014. **15**(1): p. 11-7.
144. Lee, J., et al., *Targeted degradation of α -synuclein aggregates in Parkinson's disease using the AUTOTAC technology*. *Molecular Neurodegeneration*, 2023. **18**(1): p. 41.
145. Jankovska, N., et al., *Human Prion Disorders: Review of the Current Literature and a Twenty-Year Experience of the National Surveillance Center in the Czech Republic*. *Diagnostics (Basel)*, 2021. **11**(10).
146. Wille, H. and J.R. Requena, *The Structure of PrP(Sc) Prions*. *Pathogens*, 2018. **7**(1).
147. Legname, G., *Elucidating the function of the prion protein*. *PLOS Pathogens*, 2017. **13**(8): p. e1006458.
148. Salzano, G., G. Giachin, and G. Legname, *Structural Consequences of Copper Binding to the Prion Protein*. *Cells*, 2019. **8**(8).
149. Liang, J., et al., *Overexpression of PrPC and Its Antiapoptosis Function in Gastric Cancer*. *Tumor Biology*, 2006. **27**(2): p. 84-91.
150. Bernardi, L. and A.C. Bruni, *Mutations in Prion Protein Gene: Pathogenic Mechanisms in C-Terminal vs. N-Terminal Domain, a Review*. *Int J Mol Sci*, 2019. **20**(14).
151. Greene, L.E., et al., *Mechanisms for Curing Yeast Prions*. *Int J Mol Sci*, 2020. **21**(18).
152. Kumar, S.T., et al., *Seeding the aggregation of TDP-43 requires post-fibrillization proteolytic cleavage*. *Nature Neuroscience*, 2023. **26**(6): p. 983-996.
153. Li, Q., et al., *The cleavage pattern of TDP-43 determines its rate of clearance and cytotoxicity*. *Nature Communications*, 2015. **6**(1): p. 6183.
154. Chow, V.W., et al., *An overview of APP processing enzymes and products*. *Neuromolecular Med*, 2010. **12**(1): p. 1-12.
155. Magalhaes, P. and H.A. Lashuel, *Opportunities and challenges of alpha-synuclein as a potential biomarker for Parkinson's disease and other synucleinopathies*. *NPJ Parkinsons Dis*, 2022. **8**(1): p. 93.
156. Bluhm, A., et al., *Proteolytic α -Synuclein Cleavage in Health and Disease*. *Int J Mol Sci*, 2021. **22**(11).
157. Kim, K., et al., *Network biology analysis of P23H rhodopsin interactome identifies protein and mRNA quality control mechanisms*. *Scientific Reports*, 2022. **12**(1): p. 17405.

158. Fleig, L., et al., *Ubiquitin-dependent intramembrane rhomboid protease promotes ERAD of membrane proteins*. Mol Cell, 2012. **47**(4): p. 558-69.
159. Weibezahn, J., et al., *Thermotolerance requires refolding of aggregated proteins by substrate translocation through the central pore of ClpB*. Cell, 2004. **119**(5): p. 653-665.
160. Squires, C.L., et al., *ClpB is the Escherichia coli heat shock protein F84.1*. J Bacteriol, 1991. **173**(14): p. 4254-62.
161. Lee, S., et al., *The structure of ClpB: a molecular chaperone that rescues proteins from an aggregated state*. Cell, 2003. **115**(2): p. 229-240.
162. Duran, E.C., C.L. Weaver, and A.L. Lucius, *Comparative Analysis of the Structure and Function of AAA+ Motors ClpA, ClpB, and Hsp104: Common Threads and Disparate Functions*. Frontiers in Molecular Biosciences, 2017. **4**.
163. Rizo, A.N., et al., *Structural basis for substrate gripping and translocation by the ClpB AAA+ disaggregase*. Nat Commun, 2019. **10**(1): p. 2393.
164. Haslberger, T., et al., *Protein disaggregation by the AAA+ chaperone ClpB involves partial threading of looped polypeptide segments*. Nature structural & molecular biology, 2008. **15**(6): p. 641-650.
165. Doyle, S.M., et al., *Interplay between E. coli DnaK, ClpB and GrpE during protein disaggregation*. J Mol Biol, 2015. **427**(2): p. 312-27.
166. Gottesman, S., et al., *The ClpXP and ClpAP proteases degrade proteins with carboxy-terminal peptide tails added by the SsrA-tagging system*. Genes Dev, 1998. **12**(9): p. 1338-47.
167. Rothman, J.E. and R.D. Kornberg, *Cell biology: An unfolding story of protein translocation*. Nature, 1986. **322**(6076): p. 209-210.
168. Sharma, S.K., et al., *The kinetic parameters and energy cost of the Hsp70 chaperone as a polypeptide unfoldase*. Nature chemical biology, 2010. **6**(12): p. 914-920.
169. Shorter, J., *The mammalian disaggregase machinery: Hsp110 synergizes with Hsp70 and Hsp40 to catalyze protein disaggregation and reactivation in a cell-free system*. PLoS One, 2011. **6**(10): p. e26319.
170. Torrente, M.P., et al., *Mechanistic Insights into Hsp104 Potentiation*. J Biol Chem, 2016. **291**(10): p. 5101-15.
171. Gates, S.N., et al., *Ratchet-like polypeptide translocation mechanism of the AAA+ disaggregase Hsp104*. Science, 2017. **357**(6348): p. 273-279.
172. Ullrich, F., *Condensate dispersal by Hsp104–Hsp70–Hsp40*. Nature Structural & Molecular Biology, 2022. **29**(3): p. 189-189.
173. Mazal, H., et al., *Ultrafast pore-loop dynamics in a AAA+ machine point to a Brownian-ratchet mechanism for protein translocation*. Science Advances, 2021. **7**(36): p. eabg4674.
174. Lin, J., J. Shorter, and A.L. Lucius, *AAA+ proteins: one motor, multiple ways to work*. Biochem Soc Trans, 2022. **50**(2): p. 895-906.
175. Rosenzweig, R., et al., *The Hsp70 chaperone network*. Nat Rev Mol Cell Biol, 2019. **20**(11): p. 665-680.
176. Zuiderweg, E.R., L.E. Hightower, and J.E. Gestwicki, *The remarkable multivalency of the Hsp70 chaperones*. Cell Stress and Chaperones, 2017. **22**: p. 173-189.
177. Mayer, M.P. and L.M. Gierasch, *Recent advances in the structural and mechanistic aspects of Hsp70 molecular chaperones*. Journal of Biological Chemistry, 2019. **294**(6): p. 2085-2097.

178. Minami, Y., et al., *Regulation of the heat-shock protein 70 reaction cycle by the mammalian DnaJ homolog, Hsp40*. J Biol Chem, 1996. **271**(32): p. 19617-24.
179. Nillegoda, N.B., et al., *Evolution of an intricate J-protein network driving protein disaggregation in eukaryotes*. Elife, 2017. **6**.
180. Kampinga, H.H. and E.A. Craig, *The HSP70 chaperone machinery: J proteins as drivers of functional specificity*. Nature reviews Molecular cell biology, 2010. **11**(8): p. 579-592.
181. Craig, E.A. and J. Marszalek, *How do J-proteins get Hsp70 to do so many different things?* Trends in biochemical sciences, 2017. **42**(5): p. 355-368.
182. Gao, X., et al., *Human Hsp70 Disaggregase Reverses Parkinson's-Linked α -Synuclein Amyloid Fibrils*. Mol Cell, 2015. **59**(5): p. 781-93.
183. Kirstein, J., et al., *In vivo properties of the disaggregase function of J-proteins and Hsc70 in Caenorhabditis elegans stress and aging*. Aging Cell, 2017. **16**(6): p. 1414-1424.
184. Tittelmeier, J., et al., *The HSP110/HSP70 disaggregation system generates spreading-competent toxic alpha-synuclein species*. EMBO J, 2020. **39**(13): p. e103954.
185. Erives, A.J. and J.S. Fassler, *Metabolic and Chaperone Gene Loss Marks the Origin of Animals: Evidence for Hsp104 and Hsp78 Chaperones Sharing Mitochondrial Enzymes as Clients*. PLOS ONE, 2015. **10**(2): p. e0117192.
186. Lo Bianco, C., et al., *Lindquist S., Aebischer P.: Hsp104 antagonizes α -synuclein aggregation and reduces dopaminergic degeneration in a rat model of Parkinson disease*. J. Clin. Invest, 2008. **118**: p. 3087-3097.
187. Vacher, C., L. Garcia-Oroz, and D.C. Rubinsztein, *Overexpression of yeast hsp104 reduces polyglutamine aggregation and prolongs survival of a transgenic mouse model of Huntington's disease*. Human molecular genetics, 2005. **14**(22): p. 3425-3433.
188. Cushman-Nick, M., N.M. Bonini, and J. Shorter, *Hsp104 suppresses polyglutamine-induced degeneration post onset in a drosophila MJD/SCA3 model*. PLoS genetics, 2013. **9**(9): p. e1003781.
189. Grantham, J., *The Molecular Chaperone CCT/TRiC: An Essential Component of Proteostasis and a Potential Modulator of Protein Aggregation*. Frontiers in Genetics, 2020. **11**.
190. Yu, C., et al., *Structural basis of substrate recognition and thermal protection by a small heat shock protein*. Nature Communications, 2021. **12**(1): p. 3007.
191. Clouser, A.F., et al., *Interplay of disordered and ordered regions of a human small heat shock protein yields an ensemble of 'quasi-ordered' states*. Elife, 2019. **8**.
192. Shrivastava, A., et al., *The cytoprotective sequestration activity of small heat shock proteins is evolutionarily conserved*. J Cell Biol, 2022. **221**(10).
193. Źwirowski, S., et al., *Hsp70 displaces small heat shock proteins from aggregates to initiate protein refolding*. The EMBO journal, 2017. **36**(6): p. 783-796.
194. Baumeister, W., et al., *The proteasome: paradigm of a self-compartmentalizing protease*. Cell, 1998. **92**(3): p. 367-380.
195. Jung, T. and T. Grune, *Structure of the proteasome*. Prog Mol Biol Transl Sci, 2012. **109**: p. 1-39.
196. Groll, M. and T. Clausen, *Molecular shredders: how proteasomes fulfill their role*. Curr Opin Struct Biol, 2003. **13**(6): p. 665-73.
197. Liu, C.W. and A.D. Jacobson, *Functions of the 19S complex in proteasomal degradation*. Trends Biochem Sci, 2013. **38**(2): p. 103-10.

198. Tomita, T. and A. Matouschek, *Substrate selection by the proteasome through initiation regions*. Protein Sci, 2019. **28**(7): p. 1222-1232.
199. McGrath, J.P., S. Jentsch, and A. Varshavsky, *UBA 1: an essential yeast gene encoding ubiquitin-activating enzyme*. The EMBO journal, 1991. **10**(1): p. 227-236.
200. Stewart, M.D., et al., *E2 enzymes: more than just middle men*. Cell Research, 2016. **26**(4): p. 423-440.
201. Yang, Q., et al., *E3 ubiquitin ligases: styles, structures and functions*. Mol Biomed, 2021. **2**(1): p. 23.
202. Chau, V., et al., *A multiubiquitin chain is confined to specific lysine in a targeted short-lived protein*. Science, 1989. **243**(4898): p. 1576-1583.
203. Komander, D. and M. Rape, *The ubiquitin code*. Annual review of biochemistry, 2012. **81**: p. 203-229.
204. Borgo, C., et al., *Targeting the E1 ubiquitin-activating enzyme (UBA1) improves elexacaftor/tezacaftor/ivacaftor efficacy towards F508del and rare misfolded CFTR mutants*. Cellular and Molecular Life Sciences, 2022. **79**(4): p. 192.
205. Hartl, F.U. and M. Hayer-Hartl, *Converging concepts of protein folding in vitro and in vivo*. Nature structural & molecular biology, 2009. **16**(6): p. 574-581.
206. Schneider, K.L., T. Nyström, and P.O. Widlund, *Studying Spatial Protein Quality Control, Proteopathies, and Aging Using Different Model Misfolding Proteins in S. cerevisiae*. Front Mol Neurosci, 2018. **11**: p. 249.
207. Escusa-Toret, S., W.I. Vonk, and J. Frydman, *Spatial sequestration of misfolded proteins by a dynamic chaperone pathway enhances cellular fitness during stress*. Nat Cell Biol, 2013. **15**(10): p. 1231-43.
208. Kaganovich, D., R. Kopito, and J. Frydman, *Misfolded proteins partition between two distinct quality control compartments*. Nature, 2008. **454**(7208): p. 1088-95.
209. Tyedmers, J., et al., *Prion induction involves an ancient system for the sequestration of aggregated proteins and heritable changes in prion fragmentation*. Proceedings of the National Academy of Sciences, 2010. **107**(19): p. 8633-8638.
210. Braakman, I. and N.J. Bulleid, *Protein folding and modification in the mammalian endoplasmic reticulum*. Annual review of biochemistry, 2011. **80**: p. 71-99.
211. Gow, A. and R. Sharma, *The unfolded protein response in protein aggregating diseases*. Neuromolecular Med, 2003. **4**(1-2): p. 73-94.
212. Thibault, G., N. Ismail, and D.T.W. Ng, *The unfolded protein response supports cellular robustness as a broad-spectrum compensatory pathway*. Proceedings of the National Academy of Sciences, 2011. **108**(51): p. 20597-20602.
213. Karagöz, G.E., D. Acosta-Alvear, and P. Walter, *The unfolded protein response: detecting and responding to fluctuations in the protein-folding capacity of the endoplasmic reticulum*. Cold Spring Harbor Perspectives in Biology, 2019. **11**(9): p. a033886.
214. Hillary, R.F. and U. FitzGerald, *A lifetime of stress: ATF6 in development and homeostasis*. Journal of Biomedical Science, 2018. **25**(1): p. 48.
215. Haze, K., et al., *Mammalian transcription factor ATF6 is synthesized as a transmembrane protein and activated by proteolysis in response to endoplasmic reticulum stress*. Molecular biology of the cell, 1999. **10**(11): p. 3787-3799.
216. Shen, J., et al., *ER stress regulation of ATF6 localization by dissociation of BiP/GRP78 binding and unmasking of Golgi localization signals*. Developmental cell, 2002. **3**(1): p. 99-111.

217. Shi, Y., et al., *Identification and characterization of pancreatic eukaryotic initiation factor 2 α -subunit kinase, PEK, involved in translational control*. *Molecular and cellular biology*, 1998. **18**(12): p. 7499-7509.
218. Harding, H.P., et al., *Regulated translation initiation controls stress-induced gene expression in mammalian cells*. *Molecular cell*, 2000. **6**(5): p. 1099-1108.
219. Salaroglio, I.C., et al., *PERK induces resistance to cell death elicited by endoplasmic reticulum stress and chemotherapy*. *Molecular Cancer*, 2017. **16**(1): p. 91.
220. Chen, Y. and F. Brandizzi, *IRE1: ER stress sensor and cell fate executor*. *Trends Cell Biol*, 2013. **23**(11): p. 547-55.
221. Cabral-Miranda, F., et al., *Unfolded protein response IRE1/XBP1 signaling is required for healthy mammalian brain aging*. *EMBO J*, 2022. **41**(22): p. e111952.
222. Han, D., et al., *IRE1 α kinase activation modes control alternate endoribonuclease outputs to determine divergent cell fates*. *Cell*, 2009. **138**(3): p. 562-575.
223. McCracken, A.A. and J.L. Brodsky, *Assembly of ER-associated protein degradation in vitro: dependence on cytosol, calnexin, and ATP*. *J Cell Biol*, 1996. **132**(3): p. 291-8.
224. Krshnan, L., M.L. van de Weijer, and P. Carvalho, *Endoplasmic Reticulum-Associated Protein Degradation*. *Cold Spring Harb Perspect Biol*, 2022. **14**(12).
225. Nakatsukasa, K. and J.L. Brodsky, *The recognition and retrotranslocation of misfolded proteins from the endoplasmic reticulum*. *Traffic*, 2008. **9**(6): p. 861-70.
226. Mehrtash, A.B. and M. Hochstrasser, *Ubiquitin-dependent protein degradation at the endoplasmic reticulum and nuclear envelope*. *Semin Cell Dev Biol*, 2019. **93**: p. 111-124.
227. Kumari, D. and J.L. Brodsky, *The Targeting of Native Proteins to the Endoplasmic Reticulum-Associated Degradation (ERAD) Pathway: An Expanding Repertoire of Regulated Substrates*. *Biomolecules*, 2021. **11**(8).
228. Pobre, K.F.R., G.J. Poet, and L.M. Hendershot, *The endoplasmic reticulum (ER) chaperone BiP is a master regulator of ER functions: Getting by with a little help from ERdj friends*. *J Biol Chem*, 2019. **294**(6): p. 2098-2108.
229. Moremen, K.W. and M. Molinari, *N-linked glycan recognition and processing: the molecular basis of endoplasmic reticulum quality control*. *Current opinion in structural biology*, 2006. **16**(5): p. 592-599.
230. Kozlov, G. and K. Gehring, *Calnexin cycle - structural features of the ER chaperone system*. *Febs j*, 2020. **287**(20): p. 4322-4340.
231. Adams, B.M., et al., *Quantitative glycoproteomics reveals cellular substrate selectivity of the ER protein quality control sensors UGGT1 and UGGT2*. *eLife*, 2020. **9**: p. e63997.
232. Oliver, J.D., et al., *Interaction of the thiol-dependent reductase ERp57 with nascent glycoproteins*. *Science*, 1997. **275**(5296): p. 86-88.
233. Stocki, P., et al., *Depletion of Cyclophilins B and C Leads to Dysregulation of Endoplasmic Reticulum Redox Homeostasis**. *Journal of Biological Chemistry*, 2014. **289**(33): p. 23086-23096.
234. Hosokawa, N., et al., *EDEM1 accelerates the trimming of α 1,2-linked mannose on the C branch of N-glycans*. *Glycobiology*, 2010. **20**(5): p. 567-575.
235. van der Goot, A.T., et al., *Redundant and Antagonistic Roles of XTP3B and OS9 in Decoding Glycan and Non-glycan Degrons in ER-Associated Degradation*. *Mol Cell*, 2018. **70**(3): p. 516-530.e6.
236. Christianson, J.C., E. Jarosch, and T. Sommer, *Mechanisms of substrate processing during ER-associated protein degradation*. *Nat Rev Mol Cell Biol*, 2023.

237. Bays, N.W., et al., *Hrd1p/Der3p is a membrane-anchored ubiquitin ligase required for ER-associated degradation*. Nature cell biology, 2001. **3**(1): p. 24-29.
238. Stefanovic-Barrett, S., et al., *MARCH6 and TRC8 facilitate the quality control of cytosolic and tail-anchored proteins*. EMBO Rep, 2018. **19**(5).
239. Vasic, V., et al., *Hrd1 forms the retrotranslocation pore regulated by auto-ubiquitination and binding of misfolded proteins*. Nature Cell Biology, 2020. **22**(3): p. 274-281.
240. Zhang, T., et al., *gp78 functions downstream of Hrd1 to promote degradation of misfolded proteins of the endoplasmic reticulum*. Mol Biol Cell, 2015. **26**(24): p. 4438-50.
241. Peterson, B.G., et al., *Cycles of autoubiquitination and deubiquitination regulate the ERAD ubiquitin ligase Hrd1*. eLife, 2019. **8**: p. e50903.
242. Rao, B., et al., *The cryo-EM structure of an ERAD protein channel formed by tetrameric human Derlin-1*. Sci Adv, 2021. **7**(10).
243. Wu, X., et al., *Structural basis of ER-associated protein degradation mediated by the Hrd1 ubiquitin ligase complex*. Science, 2020. **368**(6489).
244. Kadowaki, H., et al., *Molecular mechanism of ER stress-induced pre-emptive quality control involving association of the translocon, Derlin-1, and HRD1*. Scientific Reports, 2018. **8**(1): p. 7317.
245. Knop, M., et al., *Der1, a novel protein specifically required for endoplasmic reticulum degradation in yeast*. Embo j, 1996. **15**(4): p. 753-63.
246. Neal, S., et al., *The Dfm1 Derlin Is Required for ERAD Retrotranslocation of Integral Membrane Proteins*. Mol Cell, 2018. **69**(2): p. 306-320.e4.
247. Wu, X. and T.A. Rapoport, *Translocation of Proteins through a Distorted Lipid Bilayer*. Trends Cell Biol, 2021. **31**(6): p. 473-484.
248. Ye, Y., H.H. Meyer, and T.A. Rapoport, *The AAA ATPase Cdc48/p97 and its partners transport proteins from the ER into the cytosol*. Nature, 2001. **414**(6864): p. 652-6.
249. Carlson, E.J., D. Pitonzo, and W.R. Skach, *p97 functions as an auxiliary factor to facilitate TM domain extraction during CFTR ER-associated degradation*. EMBO J, 2006. **25**(19): p. 4557-66.
250. Schubert, C. and A. Buchberger, *UBX domain proteins: major regulators of the AAA ATPase Cdc48/p97*. Cell Mol Life Sci, 2008. **65**(15): p. 2360-71.
251. McNEILL, H., et al., *A novel UBA and UBX domain protein that binds polyubiquitin and VCP and is a substrate for SAPKs*. Biochemical Journal, 2004. **384**(2): p. 391-400.
252. Blueggel, M., et al., *The UBX domain in UBXD1 organizes ubiquitin binding at the C-terminus of the VCP/p97 AAA-ATPase*. Nature Communications, 2023. **14**(1): p. 3258.
253. Neal, S., et al., *A Cdc48 "Retrochaperone" Function Is Required for the Solubility of Retrotranslocated, Integral Membrane Endoplasmic Reticulum-associated Degradation (ERAD-M) Substrates*. J Biol Chem, 2017. **292**(8): p. 3112-3128.
254. Grice, G.L. and J.A. Nathan, *The recognition of ubiquitinated proteins by the proteasome*. Cell Mol Life Sci, 2016. **73**(18): p. 3497-506.
255. Verma, R., et al., *Role of Rpn11 metalloprotease in deubiquitination and degradation by the 26 S proteasome*. Science, 2002. **298**(5593): p. 611-615.
256. Yang, M., et al., *ER-Phagy: A New Regulator of ER Homeostasis*. Frontiers in Cell and Developmental Biology, 2021. **9**.
257. Chang, H.Y. and W.Y. Yang, *Golgi quality control and autophagy*. IUBMB Life, 2022. **74**(4): p. 361-370.

258. Anelli, T. and R. Sitia, *Protein quality control in the early secretory pathway*. The EMBO Journal, 2008. **27**(2): p. 315-327.
259. Pan, S., X. Cheng, and R.N. Sifers, *Golgi-situated endoplasmic reticulum α -1, 2-mannosidase contributes to the retrieval of ERAD substrates through a direct interaction with γ -COP*. Molecular Biology of the Cell, 2013. **24**(8): p. 1111-1121.
260. Vashist, S., et al., *Distinct retrieval and retention mechanisms are required for the quality control of endoplasmic reticulum protein folding*. Journal of Cell Biology, 2001. **155**(3): p. 355-368.
261. Vashist, S. and D.T. Ng, *Misfolded proteins are sorted by a sequential checkpoint mechanism of ER quality control*. J Cell Biol, 2004. **165**(1): p. 41-52.
262. Tong, Z., et al., *Identification of Candidate Substrates for the Golgi Tull E3 Ligase Using Quantitative diGly Proteomics in Yeast**. Molecular & Cellular Proteomics, 2014. **13**(11): p. 2871-2882.
263. Hettema, E.H., J. Valdez-Taubas, and H.R. Pelham, *Bsd2 binds the ubiquitin ligase Rsp5 and mediates the ubiquitination of transmembrane proteins*. Embo j, 2004. **23**(6): p. 1279-88.
264. Wang, S., G. Thibault, and D.T.W. Ng, *Routing Misfolded Proteins through the Multivesicular Body (MVB) Pathway Protects against Proteotoxicity* *. Journal of Biological Chemistry, 2011. **286**(33): p. 29376-29387.
265. Babst, M., *MVB vesicle formation: ESCRT-dependent, ESCRT-independent and everything in between*. Curr Opin Cell Biol, 2011. **23**(4): p. 452-7.
266. Lipson, C., et al., *A proteasomal ATPase contributes to dislocation of endoplasmic reticulum-associated degradation (ERAD) substrates*. J Biol Chem, 2008. **283**(11): p. 7166-75.
267. Hiller, M.M., et al., *ER degradation of a misfolded luminal protein by the cytosolic ubiquitin-proteasome pathway*. Science, 1996. **273**(5282): p. 1725-1728.
268. Guerriero, C.J., et al., *Transmembrane helix hydrophobicity is an energetic barrier during the retrotranslocation of integral membrane ERAD substrates*. Mol Biol Cell, 2017. **28**(15): p. 2076-2090.
269. Preston, G.M., et al., *Substrate Insolubility Dictates Hsp104-Dependent Endoplasmic-Reticulum-Associated Degradation*. Mol Cell, 2018. **70**(2): p. 242-253 e6.
270. Sun, Z. and J.L. Brodsky, *The degradation pathway of a model misfolded protein is determined by aggregation propensity*. Mol Biol Cell, 2018. **29**(12): p. 1422-1434.
271. Sun, Z., C.J. Guerriero, and J.L. Brodsky, *Substrate ubiquitination retains misfolded membrane proteins in the endoplasmic reticulum for degradation*. Cell Rep, 2021. **36**(12): p. 109717.
272. Ferro-Novick, S., F. Reggiori, and J.L. Brodsky, *ER-Phagy, ER Homeostasis, and ER Quality Control: Implications for Disease*. Trends Biochem Sci, 2021. **46**(8): p. 630-639.
273. Chen, W., et al., *The pivotal role of FAM134B in selective ER-phagy and diseases*. Biochimica et Biophysica Acta (BBA) - Molecular Cell Research, 2022. **1869**(8): p. 119277.
274. Jiang, X., et al., *FAM134B oligomerization drives endoplasmic reticulum membrane scission for ER-phagy*. Embo j, 2020. **39**(5): p. e102608.
275. Fumagalli, F., et al., *Translocon component Sec62 acts in endoplasmic reticulum turnover during stress recovery*. Nat Cell Biol, 2016. **18**(11): p. 1173-1184.

276. Grumati, P., et al., *Full length RTN3 regulates turnover of tubular endoplasmic reticulum via selective autophagy*. eLife, 2017. **6**: p. e25555.
277. Pan, S., et al., *Single nucleotide polymorphism-mediated translational suppression of endoplasmic reticulum mannosidase I modifies the onset of end-stage liver disease in alpha1-antitrypsin deficiency*. Hepatology, 2009. **50**(1): p. 275-281.
278. Kamimoto, T., et al., *Intracellular inclusions containing mutant alpha1-antitrypsin Z are propagated in the absence of autophagic activity*. Journal of Biological Chemistry, 2006. **281**(7): p. 4467-4476.
279. Hidvegi, T., et al., *An autophagy-enhancing drug promotes degradation of mutant alpha1-antitrypsin Z and reduces hepatic fibrosis*. Science, 2010. **329**(5988): p. 229-232.
280. Gelling, C.L., et al., *The endosomal protein-sorting receptor sortilin has a role in trafficking [alpha]-1 antitrypsin*. Genetics (Austin), 2012. **192**(3): p. 889.
281. Balch, W.E., et al., *Adapting Proteostasis for Disease Intervention*. Science, 2008. **319**(5865): p. 916-919.
282. Labbadia, J. and R.I. Morimoto, *The biology of proteostasis in aging and disease*. Annu Rev Biochem, 2015. **84**: p. 435-64.
283. Kelly, J.W., *Pharmacologic Approaches for Adapting Proteostasis in the Secretory Pathway to Ameliorate Protein Conformational Diseases*. Cold Spring Harb Perspect Biol, 2020. **12**(5).
284. Kline, G.M., K. Nugroho, and J.W. Kelly, *Inverse Drug Discovery identifies weak electrophiles affording protein conjugates*. Curr Opin Chem Biol, 2022. **67**: p. 102113.
285. Walter, P. and D. Ron, *The Unfolded Protein Response: From Stress Pathway to Homeostatic Regulation*. Science, 2011. **334**(6059): p. 1081-1086.
286. Wiseman, R.L., J.S. Mesgarzadeh, and L.M. Hendershot, *Reshaping endoplasmic reticulum quality control through the unfolded protein response*. Molecular Cell, 2022. **82**(8): p. 1477-1491.
287. Hetz, C., K. Zhang, and R.J. Kaufman, *Mechanisms, regulation and functions of the unfolded protein response*. Nat Rev Mol Cell Biol, 2020. **21**(8): p. 421-438.
288. Kim, Y.E., et al., *Molecular chaperone functions in protein folding and proteostasis*. Annu Rev Biochem, 2013. **82**: p. 323-55.
289. Polier, S., et al., *Structural Basis for the Cooperation of Hsp70 and Hsp110 Chaperones in Protein Folding*. Cell, 2008. **133**(6): p. 1068-1079.
290. Yakubu, U.M. and K.A. Morano, *Roles of the nucleotide exchange factor and chaperone Hsp110 in cellular proteostasis and diseases of protein misfolding*. Biol Chem, 2018. **399**(10): p. 1215-1221.
291. Bracher, A. and J. Verghese, *Nucleotide Exchange Factors for Hsp70 Molecular Chaperones: GrpE, Hsp110/Grp170, HspBP1/Sil1, and BAG Domain Proteins*. Subcell Biochem, 2023. **101**: p. 1-39.
292. Ellgaard, L., et al., *Co- and Post-Translational Protein Folding in the ER*. Traffic, 2016. **17**(6): p. 615-38.
293. Braakman, I. and N.J. Balleid, *Protein folding and modification in the mammalian endoplasmic reticulum*. Annu Rev Biochem, 2011. **80**: p. 71-99.
294. Oikonomou, C. and L.M. Hendershot, *Disposing of misfolded ER proteins: A troubled substrate's way out of the ER*. Mol Cell Endocrinol, 2020. **500**: p. 110630.
295. Lemberg, M.K. and K. Strisovsky, *Maintenance of organellar protein homeostasis by ER-associated degradation and related mechanisms*. Mol Cell, 2021. **81**(12): p. 2507-2519.

296. Vembar, S.S. and J.L. Brodsky, *One step at a time: endoplasmic reticulum-associated degradation*. Nat Rev Mol Cell Biol, 2008. **9**(12): p. 944-57.
297. Dohmen, R.J., P. Wu, and A. Varshavsky, *Heat-inducible degron: a method for constructing temperature-sensitive mutants*. Science, 1994. **263**(5151): p. 1273-6.
298. Mashahreh, B., et al., *Conserved degronome features governing quality control associated proteolysis*. Nat Commun, 2022. **13**(1): p. 7588.
299. Abildgaard, A.B., et al., *HSP70-binding motifs function as protein quality control degrons*. Cell Mol Life Sci, 2023. **80**(1): p. 32.
300. Maurer, M.J., et al., *Degradation Signals for Ubiquitin-Proteasome Dependent Cytosolic Protein Quality Control (CytoQC) in Yeast*. G3 (Bethesda), 2016. **6**(7): p. 1853-66.
301. Doonan, L.M., et al., *Hsp104 facilitates the endoplasmic-reticulum-associated degradation of disease-associated and aggregation-prone substrates*. Protein Sci, 2019. **28**(7): p. 1290-1306.
302. Shorter, J. and D.R. Southworth, *Spiraling in Control: Structures and Mechanisms of the Hsp104 Disaggregase*. Cold Spring Harbor Perspectives in Biology, 2019. **11**(8).
303. Berner, N., K.R. Reutter, and D.H. Wolf, *Protein Quality Control of the Endoplasmic Reticulum and Ubiquitin-Proteasome-Triggered Degradation of Aberrant Proteins: Yeast Pioneers the Path*. Annu Rev Biochem, 2018. **87**: p. 751-782.
304. Nachman, E., et al., *Disassembly of Tau fibrils by the human Hsp70 disaggregation machinery generates small seeding-competent species*. Journal of Biological Chemistry, 2020. **295**(28): p. 9676-9690.
305. Tittelmeier, J., et al., *The HSP110/HSP70 disaggregation system generates spreading-competent toxic α -synuclein species*. The EMBO Journal, 2020. **39**(13): p. e103954.
306. Kühnle, N., V. Dederer, and M.K. Lemberg, *Intramembrane proteolysis at a glance: from signalling to protein degradation*. Journal of Cell Science, 2019. **132**(16).
307. Lemberg, M.K. and B. Martoglio, *Requirements for Signal Peptide Peptidase-Catalyzed Intramembrane Proteolysis*. Molecular Cell, 2002. **10**(4): p. 735-744.
308. Sun, L., X. Li, and Y. Shi, *Structural biology of intramembrane proteases: mechanistic insights from rhomboid and S2P to γ -secretase*. Current Opinion in Structural Biology, 2016. **37**: p. 97-107.
309. Avci, D., et al., *The yeast ER-intramembrane protease Ypf1 refines nutrient sensing by regulating transporter abundance*. Mol Cell, 2014. **56**(5): p. 630-40.
310. Avci, D., et al., *The intramembrane protease SPP impacts morphology of the endoplasmic reticulum by triggering degradation of morphogenic proteins*. J Biol Chem, 2019. **294**(8): p. 2786-2800.
311. Wunderle, L., et al., *Rhomboid intramembrane protease RHBDL4 triggers ER-export and non-canonical secretion of membrane-anchored TGF α* . Scientific reports, 2016. **6**(1): p. 1-15.
312. Bock, J., et al., *Rhomboid protease RHBDL4 promotes retrotranslocation of aggregation-prone proteins for degradation*. Cell Rep, 2022. **40**(6): p. 111175.
313. Knopf, J.D., et al., *Intramembrane protease RHBDL4 cleaves oligosaccharyltransferase subunits to target them for ER-associated degradation*. Journal of Cell Science, 2020. **133**(6).
314. Kandel, R.R. and S.E. Neal, *The role of rhomboid superfamily members in protein homeostasis: Mechanistic insight and physiological implications*. Biochim Biophys Acta Mol Cell Res, 2020. **1867**(10): p. 118793.

315. Fregno, I., et al., *ER-to-lysosome-associated degradation of proteasome-resistant ATZ polymers occurs via receptor-mediated vesicular transport*. EMBO J, 2018. **37**(17).
316. Cui, Y., et al., *A COPII subunit acts with an autophagy receptor to target endoplasmic reticulum for degradation*. Science, 2019. **365**(6448): p. 53-60.
317. Shrestha, N., et al., *Integration of ER protein quality control mechanisms defines β cell function and ER architecture*. J Clin Invest, 2023. **133**(1).
318. Haynes, C., S. Caldwell, and A. Cooper, *An HRD/DER-independent ER quality control mechanism involves Rsp5p-dependent ubiquitination and ER-Golgi transport*. The Journal of cell biology, 2002. **158**: p. 91-101.
319. Needham, P.G., C.J. Guerriero, and J.L. Brodsky, *Chaperoning Endoplasmic Reticulum-Associated Degradation (ERAD) and Protein Conformational Diseases*. Cold Spring Harb Perspect Biol, 2019. **11**(8).
320. Kuchler, K., H.G. Dohlman, and J. Thorner, *The a-factor transporter (STE6 gene product) and cell polarity in the yeast Saccharomyces cerevisiae*. J Cell Biol, 1993. **120**(5): p. 1203-15.
321. Xu, G., et al., *Vulnerability of newly synthesized proteins to proteostasis stress*. J Cell Sci, 2016. **129**(9): p. 1892-901.
322. Lee, D.H. and A.L. Goldberg, *Proteasome inhibitors: valuable new tools for cell biologists*. Trends in Cell Biology, 1998. **8**(10): p. 397-403.
323. Holden, P. and W.A. Horton, *Crude subcellular fractionation of cultured mammalian cell lines*. BMC Res Notes, 2009. **2**: p. 243.
324. Ward, C.L., S. Omura, and R.R. Kopito, *Degradation of CFTR by the ubiquitin-proteasome pathway*. Cell, 1995. **83**(1): p. 121-7.
325. Bodnar, N.O. and T.A. Rapoport, *Molecular Mechanism of Substrate Processing by the Cdc48 ATPase Complex*. Cell, 2017. **169**(4): p. 722-735 e9.
326. Ji, Z., et al., *Translocation of polyubiquitinated protein substrates by the hexameric Cdc48 ATPase*. Mol Cell, 2022. **82**(3): p. 570-584 e8.
327. Kilgas, S. and K. Ramadan, *Inhibitors of the ATPase p97/VCP: From basic research to clinical applications*. Cell Chem Biol, 2023. **30**(1): p. 3-21.
328. Wang, F., et al., *P97/VCP ATPase inhibitors can rescue p97 mutation-linked motor neuron degeneration*. Brain Commun, 2022. **4**(4): p. fcac176.
329. Knopf, J.D., et al., *Intramembrane protease RHBDL4 cleaves oligosaccharyltransferase subunits to target them for ER-associated degradation*. J Cell Sci, 2020. **133**(6).
330. Sun, L., X. Li, and Y. Shi, *Structural biology of intramembrane proteases: mechanistic insights from rhomboid and S2P to gamma-secretase*. Curr Opin Struct Biol, 2016. **37**: p. 97-107.
331. Kuhnle, N., V. Dederer, and M.K. Lemberg, *Intramembrane proteolysis at a glance: from signalling to protein degradation*. J Cell Sci, 2019. **132**(16).
332. Ellgaard, L., M. Molinari, and A. Helenius, *Setting the standards: quality control in the secretory pathway*. Science, 1999. **286**(5446): p. 1882-8.
333. Lee, R.J., et al., *Uncoupling retro-translocation and degradation in the ER-associated degradation of a soluble protein*. EMBO J, 2004. **23**(11): p. 2206-15.
334. Kaiser, M.L. and K. Romisch, *Proteasome 19S RP binding to the Sec61 channel plays a key role in ERAD*. PLoS One, 2015. **10**(2): p. e0117260.
335. Weihofen, A., et al., *Identification of signal peptide peptidase, a presenilin-type aspartic protease*. Science, 2002. **296**(5576): p. 2215-8.

336. Quigley, A., et al., *The structural basis of ZMPSTE24-dependent laminopathies*. Science, 2013. **339**(6127): p. 1604-7.
337. Manolaridis, I., et al., *Mechanism of farnesylated CAAX protein processing by the intramembrane protease Rce1*. Nature, 2013. **504**(7479): p. 301-5.
338. Marinko, J.T., et al., *Folding and Misfolding of Human Membrane Proteins in Health and Disease: From Single Molecules to Cellular Proteostasis*. Chem Rev, 2019. **119**(9): p. 5537-5606.
339. Dang, S., et al., *Cleavage of amyloid precursor protein by an archaeal presenilin homologue PSH*. Proc Natl Acad Sci U S A, 2015. **112**(11): p. 3344-9.
340. Merilahti, J.A.M. and K. Elenius, *Gamma-secretase-dependent signaling of receptor tyrosine kinases*. Oncogene, 2019. **38**(2): p. 151-163.
341. Yang, G., et al., *Structural basis of Notch recognition by human gamma-secretase*. Nature, 2019. **565**(7738): p. 192-197.
342. Zafra, F. and D. Piniella, *Proximity labeling methods for proteomic analysis of membrane proteins*. J Proteomics, 2022. **264**: p. 104620.
343. Zhou, Y. and P. Zou, *The evolving capabilities of enzyme-mediated proximity labeling*. Curr Opin Chem Biol, 2021. **60**: p. 30-38.
344. Li, F., et al., *Procleave: Predicting Protease-specific Substrate Cleavage Sites by Combining Sequence and Structural Information*. Genomics Proteomics Bioinformatics, 2020. **18**(1): p. 52-64.
345. Lee, E.J., et al., *ATF6 is required for efficient rhodopsin clearance and retinal homeostasis in the P23H rho retinitis pigmentosa mouse model*. Sci Rep, 2021. **11**(1): p. 16356.
346. Parfitt, D.A. and M.E. Cheetham, *Targeting the Proteostasis Network in Rhodopsin Retinitis Pigmentosa*. Adv Exp Med Biol, 2016. **854**: p. 479-84.
347. Kennedy, A., et al., *Lysosome docking to WIPI1 rings and ER-connected phagophores occurs during DNAJB12- and GABARAP-dependent selective autophagy of misfolded P23H-rhodopsin*. Mol Biol Cell, 2022. **33**(9): p. ar84.
348. Tam, B.M. and O.L. Moritz, *Dark rearing rescues P23H rhodopsin-induced retinal degeneration in a transgenic Xenopus laevis model of retinitis pigmentosa: a chromophore-dependent mechanism characterized by production of N-terminally truncated mutant rhodopsin*. J Neurosci, 2007. **27**(34): p. 9043-53.
349. Tamarappoo, B.K., B. Yang, and A.S. Verkman, *Misfolding of mutant aquaporin-2 water channels in nephrogenic diabetes insipidus*. J Biol Chem, 1999. **274**(49): p. 34825-31.
350. Yang, B., et al., *Neonatal mortality in an aquaporin-2 knock-in mouse model of recessive nephrogenic diabetes insipidus*. J Biol Chem, 2001. **276**(4): p. 2775-9.
351. Levin, M.H., et al., *Diffusion in the endoplasmic reticulum of an aquaporin-2 mutant causing human nephrogenic diabetes insipidus*. J Biol Chem, 2001. **276**(24): p. 21331-6.
352. Estabrooks, S.K. and J.L. Brodsky, *Ubiquitination of disease-causing CFTR variants in a microsome-based assay*. Anal Biochem, 2020. **604**: p. 113829.
353. He, L., et al., *DNAJB12 and Hsp70 triage arrested intermediates of N1303K-CFTR for endoplasmic reticulum-associated autophagy*. Mol Biol Cell, 2021. **32**(7): p. 538-553.
354. Müller, S.A., S.D. Scilabra, and S.F. Lichtenthaler, *Proteomic Substrate Identification for Membrane Proteases in the Brain*. Front Mol Neurosci, 2016. **9**: p. 96.
355. Guo, D., et al., *A Disintegrin and Metalloproteinase 10 (ADAM10) Is Essential for Oligodendrocyte Precursor Development and Myelination in the Mouse Brain*. Mol Neurobiol, 2023. **60**(3): p. 1675-1689.

356. Das, B., et al., *BACE1 controls synaptic function through modulating release of synaptic vesicles*. *Molecular Psychiatry*, 2021. **26**(11): p. 6394-6410.
357. Müller, S.A., et al., *The Alzheimer's disease-linked protease BACE1 modulates neuronal IL-6 signaling through shedding of the receptor gp130*. *Mol Neurodegener*, 2023. **18**(1): p. 13.
358. Houck, S.A., et al., *Quality control autophagy degrades soluble ERAD-resistant conformers of the misfolded membrane protein GnRHR*. *Mol Cell*, 2014. **54**(1): p. 166-179.
359. Guerriero, C.J., et al., *Harmonizing Experimental Data with Modeling to Predict Membrane Protein Insertion in Yeast*. *Biophys J*, 2019. **117**(4): p. 668-678.
360. Varnaite, R. and S.A. MacNeill, *Meet the neighbors: Mapping local protein interactomes by proximity-dependent labeling with BioID*. *Proteomics*, 2016. **16**(19): p. 2503-2518.
361. Hsiao, J.M., et al., *Putative Protein Interactome of the Rhomboid Protease RHBDL4*. *Biochemistry*, 2023. **62**(6): p. 1209-1218.
362. Calabrese, G., C. Molzahn, and T. Mayor, *Protein interaction networks in neurodegenerative diseases: From physiological function to aggregation*. *Journal of Biological Chemistry*, 2022. **298**(7).
363. Rayaprolu, S., et al., *Systems-based proteomics to resolve the biology of Alzheimer's disease beyond amyloid and tau*. *Neuropsychopharmacology*, 2021. **46**(1): p. 98-115.
364. Mauthe, M., et al., *Chloroquine inhibits autophagic flux by decreasing autophagosome-lysosome fusion*. *Autophagy*, 2018. **14**(8): p. 1435-1455.
365. Xie, Z., et al., *Bafilomycin A1 inhibits autophagy and induces apoptosis in MG63 osteosarcoma cells*. *Mol Med Rep*, 2014. **10**(2): p. 1103-1107.
366. Lee, S., Y. Sato, and R.A. Nixon, *Lysosomal proteolysis inhibition selectively disrupts axonal transport of degradative organelles and causes an Alzheimer's-like axonal dystrophy*. *J Neurosci*, 2011. **31**(21): p. 7817-30.
367. Zhuang, J., et al., *Ubiquitin-activating enzyme inhibition induces an unfolded protein response and overcomes drug resistance in myeloma*. *Blood*, 2019. **133**(14): p. 1572-1584.
368. Deng, Y., et al., *Hidden patterns of codon usage bias across kingdoms*. *Journal of The Royal Society Interface*, 2020. **17**(163): p. 20190819.
369. Gu, L. and Z. Guo, *Alzheimer's A β 42 and A β 40 peptides form interlaced amyloid fibrils*. *J Neurochem*, 2013. **126**(3): p. 305-11.
370. Huang, Y.-r. and R.-t. Liu, *The Toxicity and Polymorphism of β -Amyloid Oligomers*. *International Journal of Molecular Sciences*, 2020. **21**(12): p. 4477.